

---

# Establishing a novel diagnostic method to localize the epileptogenic zone in cryptogenic focal epilepsy

---

Joanna Goc

Munich, 4<sup>th</sup> November 2016



*Dissertation der  
Graduate School of Systemic Neurosciences der  
Ludwig-Maximilians-Universität München*



*Date of Oral Defense:*

Munich, 4<sup>th</sup> April 2017

*Supervisor:*

Dr. med. Dr. phil. Christian Vollmar

*Examination Committee:*

1<sup>st</sup> reviewer: Dr. med. Dr. phil. Christian Vollmar

2<sup>nd</sup> reviewer Dr. Afra Wohlschläger

External reviewer: Dr. Philipp Sämann

Dr. Thomas Stephan



*To my fiancé and family.*

## **ABSTRACT**

Epilepsy is one of the most common neurological disorder worldwide and about 30% of diagnosed patients are pharmaco-resistant. For some of these, the most efficient treatment is resective surgery, which surgically removes the epileptogenic zone (EZ). However, this surgery is challenging in patients with cryptogenic focal epilepsy (cFE), when conventional MRI fails to localize the EZ.

The purpose of this project was to establish a novel diagnostic method to localize the EZ in patients with pharmaco-resistant cFE using diffusion tensor imaging (DTI). The main hypothesis was that the short association fibers, called U-fibers, located directly at the grey and white matter junction are affected in epilepsy by a common pathology called focal cortical dysplasia, which is often not seen in conventional MRI.

This thesis entailed different steps in the development of the method, starting with a pilot version of the method where U-fiber track density images (ufTDI) were quantified for patients with cFE using a small number of healthy controls and default settings of the used software. The remaining part of the thesis involved optimizing and improving the method to increase the sensitivity and specificity.

This novel diagnostic method is now a valuable tool in patients considered for resective epilepsy surgery. It is already routinely used at the Epilepsy Centre at the University of Munich Hospital, as a guidance tool for implantation of the electrodes for invasive EEG recordings.

# TABLE OF CONTENTS

<b>Abstract.....</b>	<b>vi</b>
<b>Abbreviations .....</b>	<b>viii</b>
<b>Chapter 1. Introduction.....</b>	<b>1</b>
<b>1.1. Epilepsy .....</b>	<b>1</b>
1.1.1. Six Cortical Zones in Focal Epilepsy.....	2
1.1.2. Pathology.....	5
1.1.3. Pre-surgical Evaluation .....	7
1.1.4. Cryptogenic Focal Epilepsy .....	10
<b>1.2. Diffusion MRI.....</b>	<b>11</b>
1.2.1. Diffusion Tensor Imaging.....	11
1.2.2. Tractography .....	12
1.2.3. DTI in Epilepsy .....	13
<b>1.3. Aims of the Thesis.....</b>	<b>15</b>
<b>Chapter 2. From FA to U-Fibers .....</b>	<b>16</b>
<b>2.1. Contributions.....</b>	<b>16</b>
<b>Chapter 3. On The Clinical Side.....</b>	<b>39</b>
<b>3.1. Contributions.....</b>	<b>39</b>
<b>Chapter 4. Effects of Pre-processing.....</b>	<b>70</b>
<b>4.1. Contributions.....</b>	<b>70</b>
<b>Chapter 5. Gender and Controls .....</b>	<b>91</b>
<b>5.1. Contributions.....</b>	<b>91</b>
<b>Chapter 6. General Discussion .....</b>	<b>110</b>
<b>6.1. Overview .....</b>	<b>110</b>
<b>6.2. Clinical Application .....</b>	<b>115</b>
<b>Summary Points.....</b>	<b>116</b>
<b>References.....</b>	<b>117</b>
<b>Acknowledgments.....</b>	<b>123</b>
<b>Curriculum Vitae .....</b>	<b>124</b>
<b>List of Publications.....</b>	<b>126</b>
<b>Affidavit.....</b>	<b>127</b>
<b>Declaration of Author Contributions .....</b>	<b>128</b>

## **ABBREVIATIONS**

ADC: Apparent Diffusion Coefficient

AEDs: Antiepileptic Drugs

ANTs: Advanced Normalization Tools

cFE: cryptogenic Focal Epilepsy

DTI: Diffusion Tensor Imaging

DWI: Diffusion Weighted Images

EZ: Epileptogenic Zone

FA: Fractional Anisotropy

FCD: Focal Cortical Dysplasia

FLAIR: Fluid-Attenuated Inversion Recovery

fMRI: functional MRI

MCD: Malformatations of Cortical Development

MD: Mean Diffusivity

mMCD: mild Malformation of Cortical Development

MRI: Magnetic Resonance Imaging

PET: Positron Emission Tomography

SPECT: Single-Photon Emission Computed Tomography

SPM: Statistical Parametric Mapping

SPMd: SPM default

SPMo: SPM optimised

TDI: Track Density Images

## **CHAPTER 1. INTRODUCTION**

### **1.1. EPILEPSY**

Epilepsy, characterized by recurrent seizures, is one of the most common neurological disorder affecting ~1% of population worldwide. It can be treated with antiepileptic drugs (AEDs), but ~30% of patients have pharmaco-resistant epilepsy, which is diagnosed after a failure of at least two AEDs treatments. In many of these cases, resective surgery is an alternative treatment, where the source of the focal epilepsy is removed.

The success of resective surgery, measured by seizure freedom, depends on different prognostic factors e.g. presence of detectable lesions, scope of the resection, underlying pathology, the localization of the epileptogenic zone (EZ) and the surrounding brain structures (McIntosh et al., 2012; Ramey et al., 2013). However, seizure freedom is achieved in only 49.8% of extratemporal lobe epilepsy (Ramey et al., 2013), possibly due to partial resection or incorrect estimation of the extent of the EZ.

Epilepsy can be secondary to various detectable lesions, such as tumors, vascular malformation, ischemic changes or cortical dysplasia. Therefore, pre-surgical evaluation and planning of the resection is greatly dependent on neuroimaging techniques (McIntosh et al., 2012). However, up to 50% of patients with focal epilepsy do not have a visible lesion in a conventional MRI and therefore are diagnosed with cryptogenic focal epilepsy (cFE). This makes the surgical outcome harder to predict due to limited pre-surgical outlining of the region that needs to be resected (Ramey et al., 2013).

### 1.1.1. SIX CORTICAL ZONES IN FOCAL EPILEPSY

Apart from the epileptogenic lesion, six cortical zones are defined to aid in the pre-surgical evaluation (Lüders, 2008): seizure onset zone, irritative zone, symptomatogenic zone, epileptogenic zone, functional deficit zone and eloquent cortex. The spatial extent of the zones varies. They can be regional, lateralized, non-lateralized, bilateral or bilateral with asymmetrical seizure evolution. This can have a great impact on the surgery planning and its outcome.

The *epileptogenic lesion* is a radiographic lesion that can be seen in magnetic resonance imaging (MRI) or computed tomography (CT) and causes epileptic seizures. In cryptogenic epilepsy, the epileptogenic lesion is not visible. Naturally, not all radiographic lesions are epileptogenic, therefore they have to be cautiously verified using different diagnostic tools. The relation to EZ is similar to the seizure onset zone, where a complete resection of the lesion does not necessarily result in seizure freedom. This could be the case if the lesion is not intrinsically epileptogenic, but can induce seizures by causing reactions in the surrounding tissue. Another explanation could be an incomplete detection of the extent of the lesion, e.g. the tissue surrounding the lesion have a more subtle or diffuse pathology and thus not be detected by MRI. This is frequently the case with focal cortical dysplasia.

The *seizure onset zone* is an area of the cortex that generates clinical seizures and is typically localized using scalp or invasive electroencephalogram (EEG) methods, like depth or subdural electrodes to detect the electrical activity representing an epileptic seizure, as well as ictal single-photon emission computed tomography (SPECT), which can identify a regional increase in blood flow in response to the high metabolic demand of an epileptic

seizure. Unlike the irritative zone, the seizure onset zone generates repetitive discharges that are strong enough to generate clinical ictal symptoms. However, this cannot be confused with the EZ. Often the EZ is more extensive than the seizure onset zone indicating that a complete resection of the seizure onset zone alone will not result in seizure freedom, if some of the EZ remains unresected. This happens when the seizure onset zone has multiple thresholds within a single EZ. Only the seizure zone of the lowest threshold is detected prior to surgery, therefore another seizure onset zone with a higher threshold may become clinically visible after the resection of the previous zone. Occasionally, the seizure onset zone is larger than EZ and partial resection of the seizure onset zone can still lead to seizure freedom if the entire EZ was resected.

The *irritative zone* is an area of the cortex that produces interictal spikes (also called interictal epileptiform discharge), measured by scalp EEG. Interictal spikes are short (<250ms) events observed in EEG that occur between seizures and usually isolated and independent spikes will not produce any clinical symptoms. The presence of interictal spikes strongly supports the diagnosis of epilepsy.

The *symptomatogenic zone* is an area of the cortex, which produces ictal symptoms during a seizure. It is common for this zone to reach beyond the EZ, because seizures are dynamic events, propagating through the brain over time. Some parts of the brain, when electrically stimulated are silent, i.e. a focal seizure in this area would not cause visible clinical symptoms. During a seizure, occasionally symptoms are generated only when the electrical activity spreads to adjacent eloquent cortex.

The *epileptogenic zone (EZ)* is defined as the area of the cortex that is indispensable for the generation of epileptic seizures and whose resection is necessary and sufficient for seizure control in pharmaco-resistant focal epilepsy. Unfortunately, there is currently no

diagnostic modality that can measure the EZ directly. Therefore, the location of the zone must be measured indirectly, by defining the above-mentioned zones.

It has been suggested, that in some cases, the EZ is not bound to only one region, but is interconnected to other regions (Buser and Bancaud, 1983). One example is the corticocortical facilitatory connections, which describe fronto-temporal epilepsy (Bancaud and Talairach, 1992).

The *functional deficit zone* is defined as regions of the cortex, which are functionally abnormal during the interictal period. The spatial extent of the functional deficit zone usually reaches beyond the EZ and can be investigated directly with neurological examination, neuropsychological assessment and indirectly with EEG, SPECT and PET. Generally, the functional deficit zone can only lateralize and estimate the localization of the EZ to the lobe affected in focal epilepsy, but is not specific. However, it does provide complementary information to the other five zones during the pre-surgical evaluation.

The *eloquent cortex* is cortex that carries a specific, relevant function and must be spared during surgery. The aim of the surgery is to resect the complete EZ with good boundaries, but at the same time sparing the eloquent cortex in order to avoid additional deficit for the patient. To identify eloquent areas, the cortex can be electrically stimulated to test whether this results in a functional impairment or not. However, in situations where the eloquent cortex overlaps with the EZ, sparing of the eloquent cortex has the priority and would only allow partial resection of the EZ with lower chances for post-surgical seizure freedom. If a patient is a candidate for surgery, then the individual risk factors have to be discussed with the patient prior to the resection.

### 1.1.2. PATHOLOGY

Focal epilepsy can be caused by different underlying pathologies and the consequences of seizures on the brain are complex affecting both brain function and structure. The structural alterations are present at different levels, such as cellular, synaptic and molecular, some of which may be permanent (Thom, 2011). To achieve seizure freedom in pharmaco-resistant focal epilepsy, the EZ must be resected using a number of diagnostic tools to outline the borders of the EZ (see Section 1.1.3).

The histopathology of resected tissue in cFE often shows malformations of cortical development (MCD), which is an outcome of abnormal prenatal development of the brain. The pathology involves neuronal proliferation, migration and organization of the cerebral cortex. MCD occurs in cFE, however, focal cortical dysplasia (FCD) is a more frequent pathology, especially in pharmaco-resistant focal epilepsy (Blümcke et al., 2011).

FCD includes a wide spectrum of abnormalities in the grey and white matter and is characterized by the occurrence of histological abnormalities of the organization of the cortex, blurring of the grey and white matter border, dysmorphic neurons, balloon cells and ectopic neurons in the subcortical white matter (Besson et al., 2008; Blümcke et al., 2011). FCD can be diffuse or focal and can vary in severity. More severe forms of FCD can typically be detectable in MRI scans (**Figure 1**).

FCD has a wide spectrum of characteristics and often it is difficult to reach a consensus for the classification of the histopathological specimen amongst neuropathologists (Chamberlain et al., 2009). Currently FCD can be classified into Type I and Type II, and recently Type III has been proposed (Blümcke et al., 2011).

Type I subdivides into Type IA and IB. Type IA shows architectural alterations of the cortical lamination, whereas Type IB additionally includes hypertrophic pyramidal neurons. Type II FCD can also be subdivided into IIA and IIB types of pathology. The hallmark of FCD Type IIA are dysmorphic neurons and Type IIB also includes balloon cells.

The pathology can be located anywhere in the cortex and the extent of the pathology varies. Some types of FCD are more frequent in certain regions of the brain than others, e.g. FCD Type II is more commonly occurring in extratemporal areas, particularly in the frontal lobe (Blümcke et al., 2011).

Neuroimaging techniques have been used extensively for diagnosing FCD. However, it has been proven to be limited. Neuroimaging is not able to reliably identify the FCD subtypes and often cannot detect subtle forms of FCD or the total extent of the pathology, making the delineation more difficult. Additionally, often patients diagnosed with the same FCD subtype according to Palmini's classification system show different imaging characteristics (Lerner et al., 2009).

The histopathology of the resective tissue in cryptogenic focal epilepsy often shows mild MCD (mMCD), which entails subtler end of the spectrum of cortical abnormalities than MCD or FCD and are often referred to as mild architectural changes (Lüders, 2008; Thom, 2011), such as blurring of the grey and white matter border and excess of cortical neuronal clusters. The diagnosis of mMCD is a challenging one, as there is no established immunohistochemical method that labels the 'ectopic' neurons from the normal neuronal population. This of course leads to less consensus on the diagnosis of mMCD compared to other, more severe forms of FCD (Thom, 2011).

### 1.1.3. PRE-SURGICAL EVALUATION

An extensive diagnostic investigation is needed to determine whether a patient with pharmacoresistant focal epilepsy is a candidate to undergo resective surgery. The aim of such a surgery is to remove the EZ, while sparing the eloquent cortex. To achieve this, several diagnostic tools are used, like scalp EEG with video monitoring, MRI, Positron Emission Tomography (PET) and SPECT (Rosenow and Lüders, 2001).

Typically, T<sub>1</sub>-, T<sub>2</sub>-weighted and FLAIR sequences are used for basic MRI evaluation. FLAIR sequences are particularly successful for localizing the epileptogenic lesions (**Figure 1**). On the other hand, T<sub>1</sub> and T<sub>2</sub>-weighted sequences can show the blurring of the grey and white matter border, which is characteristic of FCD.

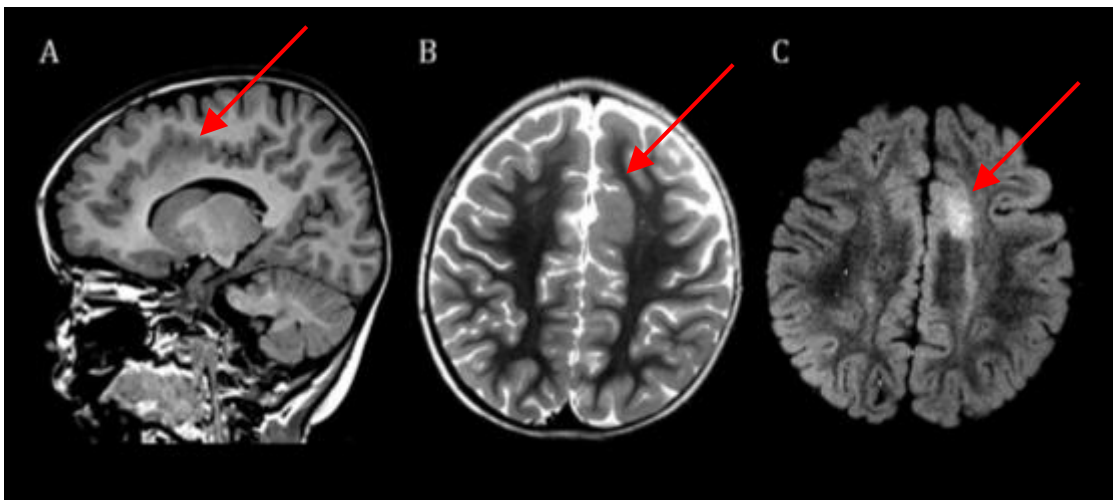


**Figure 1 Epileptogenic lesion seen in T2 and T2-FLAIR.** At the Epilepsy Centre, patients routinely obtain neuroimages including A) T1 showing blurred grey and white matter junction B) T2 showing cortical thickening and C) T2-FLAIR, where the signal is enhanced around the epileptogenic lesion. Courtesy of Dr. Christian Vollmar.

Scalp EEG is another important diagnostic tool, essential in the pre-surgical evaluation of epilepsy. It measures the electrical activity of the brain and is able to lateralize and localize the seizure onset zone in majority of cases. Currently, video-EEG monitoring is the gold standard for defining the irritative and seizure onset zones (see Section 1.1.1)

when recording a sufficient amount of ictal and interictal EEG (Lüders, 2008; Rosenow and Lüders, 2001).

One limitation of scalp EEG is low sensitivity to deep cortical areas, such as mesial frontal or fronto-orbital regions, due to the large distances between the scalp electrodes and those cortical areas. Usually, scalp electrodes are only able to detect the discharges after they have spread considerably. Scalp EEG is typically combined with video monitoring to assess the seizure semiology.

Seizure semiology allows for the localization of the symptomatogenic zone, which is usually in close proximity to the epileptogenic zone. Thereby seizure semiology contributes localizing information to the pre-surgical evaluation and can be particularly helpful in cFE. There are several established lateralizing and localizing signs of auras and seizures (described in detail in Lüders et al., 1999; Tufenkjian and Lüders, 2012) and some of these signs have a correct lateralization rate of > 95%. For example, clonic movement of the left hand indicates an epileptic activation of the right precentral cortex. If this occurs early in the seizure, chances are high that the epileptogenic zone is in close proximity to the right motor cortex.

If scalp EEG and seizure semiology do not allow for the exact localization or lateralization of the seizure onset zone, then additional methods are needed, including intracranial EEG recording, such as depth or subdural electrodes. Information obtained from scalp EEG and MRI guides the implantation of intracranial EEG recording. Even though the pre-surgical evaluation for the resection relies mainly on intracranial EEG for delineating the EZ (Rosenow and Lüders, 2001; Zhang et al., 2014), it is crucial to have a strong clinical hypothesis for the location of the EZ, when planning the implantation of the depth electrodes. This is because depth electrodes record activity from a very localized and

limited region and the total number of electrodes that can be implanted is limited. However, they are highly sensitive due to the direct contact with the brain matter and accurately record the epileptic activity. On the other hand, the subdural grid is more invasive than depth electrodes and has higher risk of complications, but it covers a larger area of the cortex, which can be beneficial when the location of the EZ is not clear (Zhang et al., 2014).

Another important diagnostic test is the ictal SPECT, which is based on cerebral metabolic and perfusion coupling. During a seizure, neurons are hyperactive resulting in an increased metabolic demand and a regional increase in blood flow. This ictal hyperperfusion can be depicted with a SPECT scan, if the tracer is injected early during the seizure, preferably within 20 seconds after the seizure onset (Van Paesschen, 2004). The evaluation of ictal and interictal SPECT can be challenging. The sensitivity of SPECT in localizing the EZ increases when computer-aided subtraction ictal SPECT co-registered to MRI (SISCOM) is applied (O'Brien et al., 1998).

Another nuclear medicine technique, called positron emission tomography (PET), often can reliably identify dysfunctional cortex with hypometabolism. It is often acquired in cFE and in some cases the EZ can be visible because of a change in glucose metabolism in the affected region of the brain reflecting the regions of functional deficit (Lüders, 2008).

All of the above mentioned methods reflect different aspects of the epileptogenic network and provide complementary information when combined, thus increasing the sensitivity and specificity of the diagnosis. The need to use all of the methods show how complex the pre-surgical evaluation of focal epilepsy is. This process becomes even more challenging in cFE.

#### *1.1.4. CRYPTOGENIC FOCAL EPILEPSY*

Cryptogenic, or MRI-negative, focal epilepsy is a classification of epilepsy where the lesion is not visible in conventional MRI. The diagnostic protocol remains the same as for lesional focal epilepsy. The only difference is that there is no visible lesion in MRI, which would be a valuable clue, where to look first. In cFE, the diagnosis relies almost exclusively on EEG, semiology and nuclear medicine like SPECT and PET.

## 1.2. DIFFUSION MRI

Diffusion weighted MRI is a specific MRI acquisition that allows for the quantification of water diffusion in tissue. The process of diffusion is influenced by the structure of the tissue, like cell membranes, cytoskeleton and macromolecules (Le Bihan, 2014). This enables indirect inferences on the cellular integrity and pathology of the tissue. The diffusivity depends on the angle between the fiber track and the applied magnetic field gradient. The diffusivity is largest when the magnetic field gradient is parallel to the fiber direction and smallest when it is perpendicular (Basser et al., 1994). Application of gradients to enhance the diffusion attenuation introduces a contrast mechanism creating diffusion-weighted images (DWI).

In grey matter, the measured diffusivity is mainly isotropic, i.e. uniform in all directions. Therefore, the diffusion characteristics can be measured using a single apparent diffusion coefficient (ADC). However, white matter tissue is anisotropic, where the diffusivity is dependent upon the orientation of the axonal bundles and a single ADC is not sufficient (Basser et al., 1994). A more complex model has to be applied in order to account for the anisotropic properties of the axonal bundles by implementing a diffusion tensor of water.

### 1.2.1. DIFFUSION TENSOR IMAGING

A tensor is a  $3 \times 3$  matrix representing the orientation of the anisotropic diffusion with respect to the three orthogonal axes of the reference frame (Stejskal and Tanner, 1965). Diffusion tensor imaging (DTI) is a technique measuring the diffusion tensor from each voxel in the brain (Basser et al., 1994). This allows for the calculation of diffusivity

(degree of diffusion), anisotropy (directionality of the diffusion) and principal direction, therefore providing information on the microstructure of the tissue and white matter tracts that cannot be obtained in standard MRI.

There are two main DTI-based scalars: fractional anisotropy (FA) and mean diffusivity (MD). FA shows the degree of directionality of water diffusion, where a high FA indicates a diffusion restriction along one direction, and low FA indicates unconstrained diffusion equally in different directions. MD on the other hand shows the total degree of diffusivity, regardless of the directionality. In the vicinity of a lesion, FA is often decreased and MD increased (Dumas de la Roque et al., 2005). Even though both of these measures, FA and MD, have shown alterations in many neurological diseases, in focal epilepsy these changes often remain non-specific (Winston, 2015).

### 1.2.2. TRACTOGRAPHY

Tractography is currently the only available tool for identifying white matter pathways non-invasively and *in vivo* in humans. It is based on the fundamental assumption that when axons align along a common axis, the diffusion of water is greater along than across the axis (Behrens et al., 2003). Tractography is a process of integrating voxel-wise fiber orientations into a pathway (Behrens et al., 2009) by streamlining through a vector field. The streamlines can be reconstructed at any starting seed by following the main direction of water diffusion (**Figure 2**), it moves on to the next vector and so on until it reaches the stopping vector. Streamline tractography has many advantages, including fast reconstruction of fibers, does not require special computational equipment or training and is able to reconstruct many major white matter tracts.

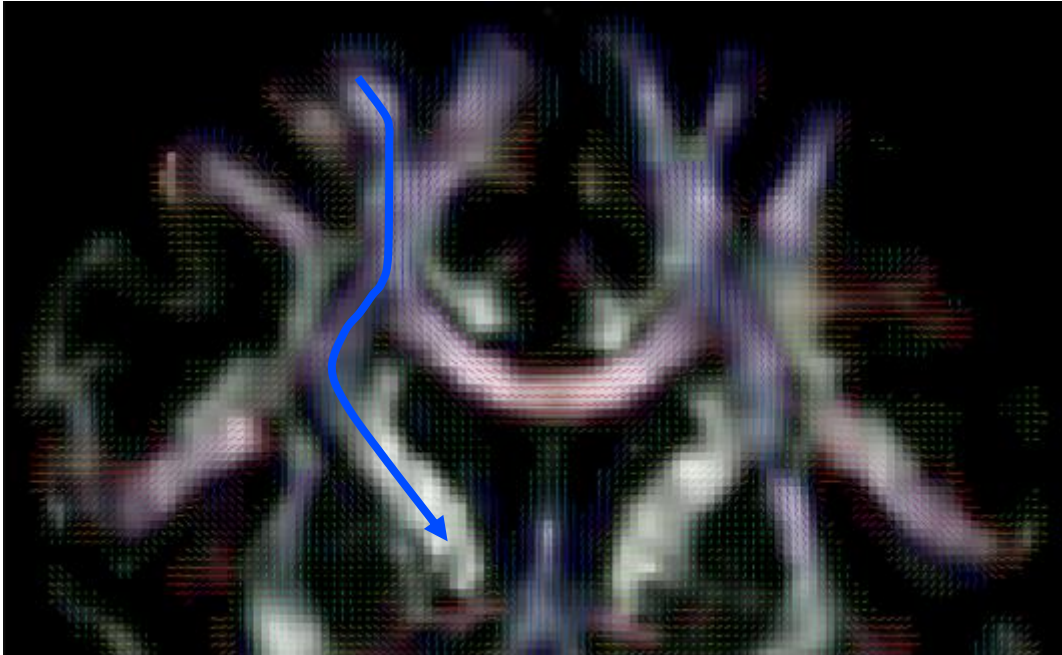


**Figure 2 Streamline tractography.** The blue line represents the streamline that follows the orientation of the diffusion. Image was created by the author of this thesis.

Although streamline tractography allows for non-invasive research, it can be prone to errors. One key limitation of diffusion tensor model is that it can only recognize a single fiber orientation in each voxel. Therefore, the model might fail at locations with crossing or kissing fibers. There are multiple alternative models and algorithms that recover more information about the fiber orientation from a single voxel, such as high angular resolution diffusion imaging (HARDI) (Tuch et al., 2002), QBall imaging (Tuch, 2004) or constrained spherical deconvolution (CSD) (Anderson and Ding, 2002), which can be helpful to delineate a more complex topography in regions with crossing fibers.

### *1.2.3. DTI IN EPILEPSY*

Alterations related to pathology like FCD and MCD (see Section 1.1.2) have been described in DTI, mainly by reduced anisotropy and increased diffusivity within the proximity of the EZ in patients with MRI-visible FCD (Dumas de la Roque et al., 2005;

Eriksson et al., 2001). In some patients, the extent of the alterations exceeded beyond the borders of MCD visible on conventional T<sub>1</sub>- and T<sub>2</sub>-weighted images (Eriksson et al., 2001).

Diffusion Tensor Tractography (DTT) has been shown to detect structural changes in cFE (Vollmar and Diehl, 2011), where the number of tracts was reduced in the epileptogenic zone compared to the healthy contralateral side.

The specificity of DTI in localizing the EZ is higher for extratemporal than temporal lobe epilepsy (Thivard et al., 2006), possibly due to the higher prevalence of dysplastic lesions in extratemporal epilepsy, as opposed to hippocampal sclerosis in temporal epilepsy. Thivard et al (2006) also suggested that the epileptic networks associated with extratemporal and temporal epilepsy differ in structural connections and cytoarchitecture.

### **1.3. AIMS OF THE THESIS**

The aim of this PhD thesis is to establish a new diagnostic method that localizes the epileptogenic zone in patients with pharmaco-resistant cryptogenic focal epilepsy (cFE) by quantifying the density of short association fibers, called U-fibers, obtained through DTI.

The main objectives are:

1. To compare the sensitivity and specificity of the conventional DTI-based measures FA and MD with track density images (TDI), including whole brain TDI and U-fiber TDI, for the detection of the epileptogenic zone in individual patients with cFE.
2. To compare the results of the method to the electroclinical data obtained from the hospital.
3. To compare different options throughout the pre-processing pipeline, to optimize the pre-processing steps of the method.
4. To investigate the effects of the control population on the results of the quantification.

## **CHAPTER 2. FROM FA TO U-FIBERS**

### **2.1. CONTRIBUTIONS**

The work was done under the supervision of Dr. Christian Vollmar (CV). Joanna Goc (JG) and CV designed the research. JG, CV and Dr. Elisabeth Hartl (EH) recruited and scanned participants. JG designed the method and carried out the research and analysis and together with CV discussed the results. JG wrote the article.

## **Performance of different DTI-based measures to localize the epileptogenic zone in cryptogenic focal epilepsy**

J. Goc<sup>1,2</sup>, E. Hartl<sup>1</sup>, K. Ernst<sup>1</sup>, S. Noachtar<sup>1</sup>, C. Vollmar<sup>1,3\*</sup>

<sup>1</sup>Dept. of Neurology, Epilepsy Centre, University of Munich Hospital, Munich, Germany

<sup>2</sup>Graduate School of Systemic Neurosciences, Ludwig Maximilians University, Munich, Germany

<sup>3</sup>Dept. of Neuroradiology, University of Munich Hospital, Munich, Germany

\*Correspondence to:

Dr. Christian Vollmar

Marchioninstr. 15

81377 Munich

Germany

+4989440072682

Christian.vollmar@med.uni-muenchen.de

### **Keywords:**

cryptogenic epilepsy, focal epilepsy, fractional anisotropy, diffusion tensor imaging, U-fibers, mean diffusivity

**Abstract**

Pharmacoresistant focal epilepsy may be treated surgically by removing the epileptogenic zone (EZ). However, in patients with cryptogenic epilepsy no structural lesion is visible in clinical MRI, challenging the localization of the EZ and planning of the resective surgery. Here, we show a DTI analysis approach based on a quantification of regional track density images (TDI) and compare that to conventional FA and MD maps to localize previously undetected structural abnormalities in the EZ.

Ten patients with MRI-negative focal epilepsy with clear clinical localization of the EZ were compared against 42 controls. DTI data was acquired on a 3T GE Signa HDx Scanner with 64 diffusion-weighted directions and b-value of 1000 s/mm<sup>2</sup>. DTI data was processed and FA and MD maps were created. Whole brain streamline tracking was performed and three TDI were created. These track density images were spatially normalized together with FA and MD to a common template space. Statistical comparison to the healthy control population was carried out to identify alterations in individual patients. The resulting significant alterations were compared to clinical data.

All DTI-based measures showed alterations in patients with epilepsy, beyond the range seen in healthy controls. However, the extent and specificity of these alterations varied. The quantification of U-fiber track density images correctly identified the EZ in 80% of the patients, compared to only 20% and 10% for FA and MD, respectively, showing that these frequently used DTI measures are not ideal to localize specific alterations in the EZ.

**Abbreviations:** DTI = diffusion tensor imaging; MRI = magnetic resonance imaging; PET = positron emission tomography; SPECT = single-photon emission computed tomography; SPM = statistical parametric mapping; CVA = conventional visual analysis; cFE = cryptogenic focal epilepsy; HP = healthy population; CTR = control; FA = fractional anisotropy; MD = mean diffusivity; TDI = fiber density image; EZ = epileptogenic zone

## 1. Introduction

Epilepsy is one of the most commonly occurring neurological diseases affecting up to 1% of the population and is typically treated with medication. However, according to World Health Organization (WHO, 2016), 30% of patients do not respond sufficiently to medication (pharmacoresistant epilepsy) and for some of these patients resective epilepsy surgery might be an effective treatment option (Rosenow and Lüders, 2001). Up to half of the candidates for epilepsy surgery have non-lesional, “cryptogenic” focal epilepsy (cFE), where conventional MRI does not show underlying structural lesions and the localization of the epileptogenic zone (EZ) depends on complementary diagnostic methods. The success rate of resective surgery in cryptogenic epilepsy (measured by the absence of seizures) is often lower than in lesional epilepsy (Martin et al., 2015). The outcome of surgery depends on multiple factors, starting from the type of underlying histopathology (Yao et al., 2014) to correct localization and complete resection of the EZ, which is not straight forward in MRI-negative patients.

One of the most frequent causes of focal drug-resistant epilepsy is focal cortical dysplasia (FCD), a structural pathology characterized by histological abnormalities of the laminar layers of the cortex, blurring of the white and grey matter border, dysmorphic neurons, balloon cells and ectopic neurons in the subcortical white matter (Besson et al., 2008; Blümcke et al., 2011). More severe forms of FCD are detectable with conventional MRI and occasionally with diffusion tensor imaging (DTI) (Dumas de la Roque et al., 2005; Eriksson et al., 2001; Rugg-Gunn et al., 2001; Widjaja et al., 2011). However, mild malformations of the cortical development (MCD) are often missed even with an optimized epilepsy MRI protocol.

In recent years, DTI has become more popular in clinical diagnostics. Most commonly used DTI-derived scalars include: fractional anisotropy (FA) and mean diffusivity (MD). FA shows the degree of directionality of water diffusion, where a high FA indicates a diffusion restriction along one direction, and low FA indicates unconstrained diffusion in different directions. MD on the other hand shows the total degree of diffusivity, regardless of the directionality. In the vicinity of a lesion, FA is often decreased and MD increased (Dumas de la Roque et al., 2005; Eriksson et al., 2001; Rugg-Gunn et al., 2001). Even though both of these measures, FA and MD, have shown alterations in many neurological diseases, in focal epilepsy, these changes often remain non-specific (Winston, 2015).

An alternative DTI-based measure to FA or MD is track density imaging (TDI) (Calamante et al., 2015, 2010), a tractography mapping technique that has already been applied in various neurological disorders. The TDI maps are typically based on whole brain streamline tracking and represent the number of streamlines passing through any voxel.

The possible microstructural alterations in cFE, like the blurring of the white and grey matter border could have an effect on fibers that are located in the proximity of the white-grey matter border, like on local short association fibers, called the U-fibers (Colombo et al., 2003). These microstructural changes might affect the tracking enough to yield a more specific effect than FA or MD. Thus, using alternative DTI-based measures based on fiber-tracking, like TDI, could improve the identification of subtle structural alterations in cFE.

In this study we compared sensitivity and specificity of the conventional DTI measures FA and MD with different types of track density images (TDI) including a specific TDI for U-fibers only, for mapping the EZ in individual patients with cFE.

## 2. **Methods and Participants**

### 2.1. *Participants*

A group of 10 patients diagnosed with drug-resistant, cryptogenic focal epilepsy (cFE) [mean age of 30 years (SD: 9.9), 8 males] was investigated. All patients had conventional structural MRI at 3T using a specific epilepsy protocol, including high resolution 3D T1 and 3D FLAIR images, coronal FLAIR T2 and inversion recovery T1 images, not showing any structural epileptogenic lesions. All patients underwent a series of neurological examinations including routine EEG and non-invasive EEG-video-monitoring, FDG-PET, SPECT and in most cases invasive intracranial EEG (n=8). All patients had a clear clinical hypothesis as for the localization of the EZ based on the conclusive interpretation of the aforementioned tests: bilateral frontal (n=1), right frontal (n=1), left frontal (n=4), right temporal (n=2), left temporal (n=1) and right parietal (n=1).

A healthy population (HP) of 42 participants with no history of neurological or psychiatric disease [mean age of 29.4 years (SD: 6.1), 27 males] was scanned for comparison.

Additionally, 10 controls (CTR) were individually compared to the HP group using identical procedures as for the cFE patients.

The University of Munich Ethics Committee approved the study and all participants gave written and informed consent.

### 2.2. *DTI acquisition*

All participants had additional DTI data acquisition on a 3T GE Signa HDx Scanner using a DTI-acquisition scheme with 64 diffusion-weighted directions, a b-value of 1000 s/mm<sup>2</sup>, 60 axial slices with 2.4 mm slice thickness, a 96x96 in-plane matrix with a 220mm

field of view, TR 16000 ms, TE 90.2 ms, flip angle 90° and parallel imaging with a SENSE factor 2.

### 2.3. *DTI Processing*

The processing of DTI data involved several steps. Firstly, the images were resampled to isotropic 1mm voxel size and corrected for movement and distortions artefacts caused by eddy currents using FMRIB Software Library Version 4.1.6 (FSL; <http://fsl.fmrib.ox.ac.uk>). The diffusion weighted images were skull-stripped using the Brain Extraction Tool implemented in FSL. Next, using FSL dtifit, we created the two most commonly used DTI-based scalars: fractional anisotropy (FA) and mean diffusivity (MD).

### 2.4. *Streamline Tractography*

Deterministic streamline tracking was performed using the Diffusion Toolkit (<http://trackvis.org/blog/tag/diffusion-toolkit/>) seeding from every voxel within the brain. Tracking used a 2<sup>nd</sup>-order Runge Kutta propagation algorithm with an angular threshold of <math>35^\circ</math> between neighboring voxels. The termination criteria of the tracking were either exiting the brain or reaching a voxel with an FA value <math><0.1</math>. The average whole brain track counts for cFE and HP were 979461 and 1034048, respectively. Visual quality check of the streamlines was performed using TrackVis (<http://trackvis.org/>).

### 2.5. *Track-density imaging (TDI)*

The population of U-fibers was selected from the whole brain streamline data using the following selection parameters: length 20-60mm, curvature 2-10 and a U-factor, describing the shape of a fiber between 0.6-1.

Using TrackVis, three types of track density images (TDI) were created: 1) whole brain TDI (wbTDI), 2) enhanced whole brain TDI (ewbTDI) and U-fiber TDI (ufTDI). To account for the underrepresentation of peripheral curved U-fibers in comparison to major deep white matter tracts (Girard et al., 2014) we created the ewbTDI map. It combines the wbTDI and the ufTDI multiplied by a factor of 5 to enhance the fiber density at the periphery of the dataset. In each density map, every voxel represents the number of fibers passing through it.

### 2.6. *Spatial Normalization*

The FA map was spatially normalized to the FMRIB58\_FA template in MNI space using SPM5 software (<http://www.fil.ion.ucl.ac.uk/>) with the following settings: Source Image Smoothing 5mm FWHM, Non-linear Frequency cut-off 12mm, non-linear Regularization 0.1, non-linear iterations 128. The determined transformation from individual DTI space to MNI template space was then applied to all five DTI-based images: FA, MD, wbTDI, ewbTDI and ufTDI.

### 2.7. *Voxel-wise Statistical Analysis*

Spatially normalized FA, MD, wbTDI, ewbTDI and ufTDI of an individual brain were used for further voxel-wise statistical analysis. Every patient with MRI-negative focal epilepsy is different and therefore each patient has to be analyzed individually using an

approach suggested by Henson (Henson., 2006). First, the differences between one individual patient and each of the 42 healthy participants were calculated for each DTI-based measure. The resulting 42 difference images were analyzed with one-sample T-test using SPM5 software for each patient, identifying voxels with significant deviations from the healthy population. We specifically tested for reduced FA, increased MD and reduced track density, correcting for multiple comparisons with the family-wise error method and thresholding at  $p < 0.001$ .

### *2.8. Regional Quantification*

To compare the sensitivity and specificity of the five different DTI-based measures, we divided each brain into 8 regions (left and right: frontal, parietal, temporal and occipital lobes) in MNI-space using MNI structural Atlas obtained from FSL software. Using `fsfstats`, implemented in FSL, two parameters were determined from the statistical analysis of each DTI-based measure for each region: the highest T-score per region and the number of voxels in each region with a T-score larger than 8.

To further evaluate the specificity of the DTI-based measures we assessed, for each cFE patient, how many lobes showed alterations larger than  $20\text{cm}^3$  (Table I).

Differences between cFE and CTR were assessed with two-sample t-test.

## **3. Results**

### *3.1. Visualization of voxel-wise statistical analysis*

In cFE, the visual inspection showed more widespread, bilateral and non-specific alterations in FA, MD and wbTDI. The alterations in ewbTDI were less extensive than in FA or MD, but still were more widespread than in uFTDI, where alterations were most

circumscribed and localized to one region (Fig. 1). In comparison to cFE, the alterations seen in 10 CTR were significantly smaller for all five DTI-based measures (Fig. 1).

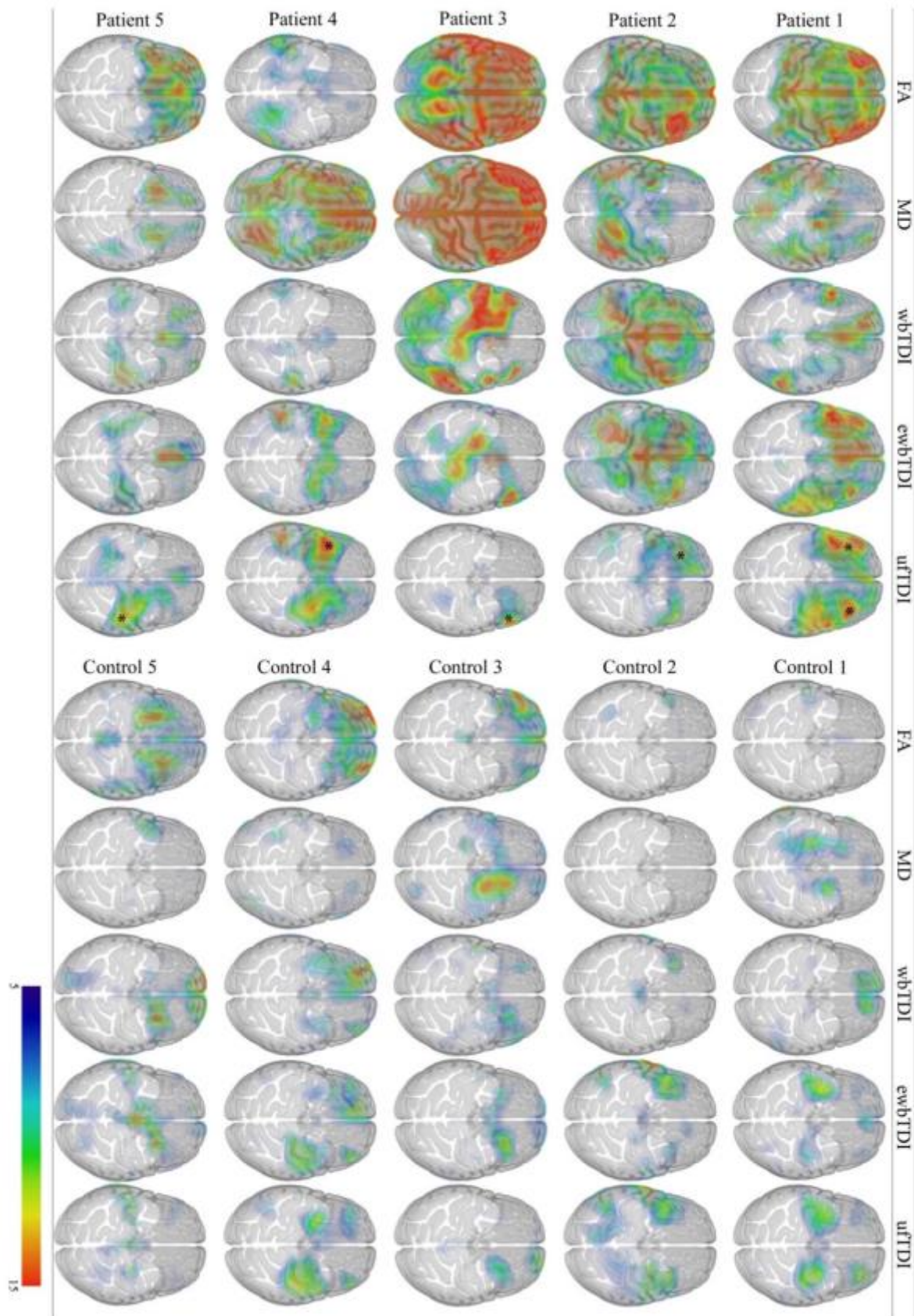


**Figure 1. Visualization of voxel-wise statistical analysis.**

Examples of five cFE patients and five CTR participants are used to show the differences in distribution of T-scores and volume alterations in five DTI-based measures: FA, MD, wbTDI, ewbTDI and ufTDI, with low (blue) to high T-score (red). The results of SPM quantification were rendered together with a MNI template at a threshold T-score > 5. The transparency of the template was increased to allow for the appreciation of the extent of alterations. For cFE patients, the clinical localization of the EZ is marked with an asterisk.

*3.2. Number of lobes with alterations*

Using a threshold of 20cm<sup>3</sup> per lobe, FA quantification showed the most unspecific alterations. Only 10% of the patients had reductions in intensity in only one lobe of the brain, 20% of patients showed alterations in up to three lobes and 60% showed alteration in more than three lobes including 40% with FA reductions in all eight lobes (Table I). MD alterations were restricted to one lobe in only 10% of patients and 80% of patients showed alterations spreading to more than three lobes. The extent of the alterations was more restricted with TDI-based quantifications. A restriction of alterations to only one lobe was seen in 20% and 30% for wbTDI and ewbTDI, respectively. ufTDI alterations were most localized, in 60% of patients the alterations were restricted to only one lobe and the remaining 40% of the patients showed changes in up to three lobes (Table I).

No. of lobes	FA	MD	wbTDI	ewbTDI	ufTDI
8	4	3	2	0	0
7	0	2	0	0	0
6	0	1	0	1	0
5	2	2	1	2	0
4	0	0	2	1	0
3	1	0	0	2	2
2	1	0	1	0	2
1	1	1	2	3	6

**Table I. Number of lobes showing alterations in different DTI-based measures for all cFE patients.**

At a threshold of alteration volume of 20cm<sup>3</sup>, the frequency of alterations in eight lobes was counted for all DTI-based measures in 10 patients. The number of patients is color-coded with a gradient, where red represents the highest number of patients. Only in a few patients the alteration volume did not reach 20cm<sup>3</sup> in any lobes for FA (n=1), MD (n=1), wbTDI (n=2) and ewbTDI (n=1).

### 3.3. *Correlation with clinical data*

Statistical analysis of FA, MD, wbTDI, ewbTDI and uFTDI for 10 individual cFE patients and its regional quantification was compared to the clinical location of the EZ. The quantification of FA, wbTDI and ewbTDI showed the peak T-score of alterations in the lobe of the EZ in 20% of patients and MD identified the correct region in only 10%. In uFTDI quantification, 80% of patients showed the peak T-score in the correct region.

Assessing the number of voxels above the threshold of T-score of 8 led to similar results as the peak T-score. Only 20% of FA, MD and ewbTDI and only 10% in wbTDI showed the correct lobe. uFTDI performed better than any other measure, with the highest number of voxels in the correct lobe in 60%.

### 3.4. *Differences between cFE and CTR quantification*

To determine the range of alterations in our DTI-based measures in healthy controls, the data of 10 CTR participants were analyzed, using the same quantitative procedure as for the 10 cFE patients.

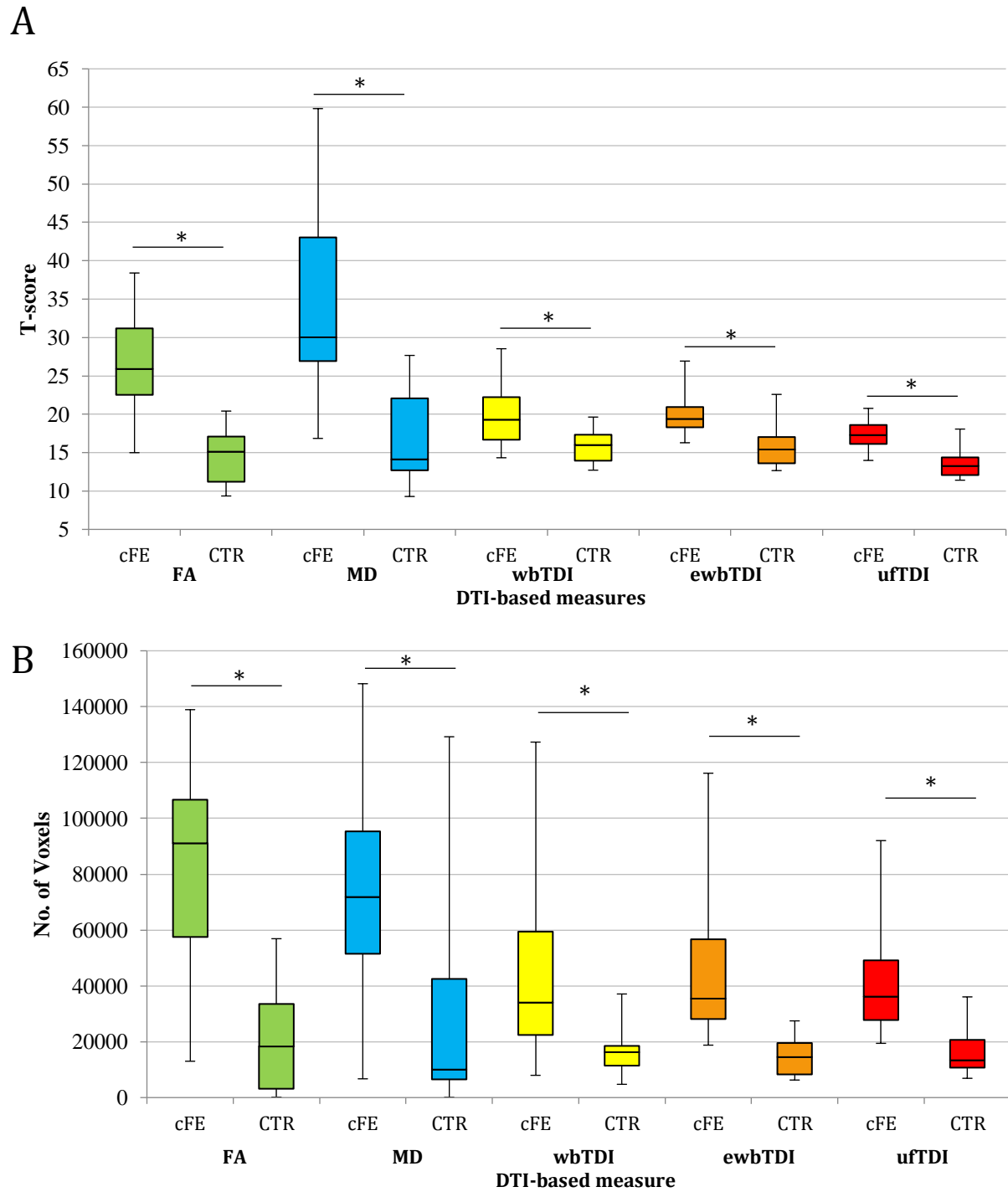
For all DTI-based measures, the peak T-scores of observed alterations were significantly higher in cFE than in CTR (FA  $p=0.0001$ , MD  $p=0.0015$ , wbTDI  $p=0.007$ , ewbTDI  $p=0.002$ , uFTDI  $p=0.001$ ; Fig. 2A).

The volumes of alterations with a T-score  $>8$  of all measures in cFE were also significantly larger in cFE than in CTR (Fig. 2B), which can also be appreciated visually (Fig. 1). Within the CTR group, the median volume of significant alterations falls below  $20\text{cm}^3$  for all five measures, whereas for cFE the median is above  $30\text{cm}^3$ . In the cFE group, FA quantification showed a wide distribution (Fig. 2B) with a median alteration volume of

91cm<sup>3</sup>. On the other hand, the volume of FA decrease for CTR was significantly lower with a median volume of 18cm<sup>3</sup> ( $p=6.6\times 10^{-5}$ ).

The quantification of MD showed an increase in intensity. In the cFE group, the volume of this alteration had a median of 72cm<sup>3</sup> compared to 10cm<sup>3</sup> in the CTR group ( $p=0.01$ ). MD alterations showed a larger variability in CTR than FA accounting for the relatively high differences in p value 0.01.

The quantification of track density images showed much smaller alteration volumes. For wbTDI the median volume of significant reductions is 34cm<sup>3</sup> for cFE and 16cm<sup>3</sup> in CTR ( $p=0.006$ ), similar to that of ewbTDI with a median of 35cm<sup>3</sup> in cFE and 14cm<sup>3</sup> in CTR ( $p=0.0008$ ) and ufTDI with a median of 36cm<sup>3</sup> and 13cm<sup>3</sup> for cFE and CTR ( $p=0.0008$ ), respectively.



#### 4. Discussion

The localization of the epileptogenic zone (EZ) in patients with pharmacoresistant cryptogenic focal epilepsy considered for resective epilepsy surgery is challenging with current diagnostic methods.

To increase the yield of MRI, different processing strategies have been proposed (other methods discussed in a review by (Kini et al., 2016)). Voxel-based morphometry (VBM) (Ashburner and Friston, 2000) using either T1 or T2 FLAIR has also been applied in MRI-negative epilepsy. However, similarly to FA and MD quantification, the yield was low. One study using VBM of FLAIR-images identified focal changes in 14.3% of 70 patients of which only half correlated with clinical data (Focke et al., 2009). Another study using morphometric analysis programme detected 1% more histologically proven FCD Type IIb than in conventional visual analysis (CVA), where CVA detected FCD in 91% of 74 cases (Wagner et al., 2011). This method was more successful at detecting FCD Type IIa pathology, where morphometric analysis detected 82% of histologically proven lesions compared to 65% using CVA (n=17).

Recently, DTI has also been used as an additional diagnostic tool in a variety of diseases. Here we compared the diagnostic accuracy of different DTI-based measures to identify cryptogenic lesions in patients with focal epilepsy and showed that conventionally used DTI measures, like FA and MD, are not optimal in localizing the EZ.

This is consistent with the few studies that used DTI for localization in MRI-negative patients, where the analyses of FA and MD maps have been disappointing. A study using voxel-wise statistical quantification identified an increase in MD in 8 of 30 MRI-negative patients of which only half corresponded to the ictal EEG recordings and two patients that showed alterations in FA, but only one was confirmed with ictal EEG (Rugg-Gunn et al.,

2001). Another study, showed that increased MD identified the EZ, determined by the intracranial EEG, in 8 out of 20 patients (40%) (Thivard et al., 2011). Similarly to these studies, our quantification of FA and MD maps showed widespread alterations throughout the brain in most patients, insufficient to specifically identify the EZ. Specific changes restricted to the EZ were seen in only 20% of the patients. Our analysis with one sample t-test of difference images increases sensitivity for single subject studies, which could explain the higher detection rate than what was reported in the aforementioned study (Rugg-Gunn et al., 2001), but this procedure does not improve specificity. The high specificity of our uFTDI quantification shows that uFTDI reflects different tissue properties than FA and MD, selectively detecting changes in the EZ of focal epilepsy. Perhaps FA and MD are more sensitive to secondary effects of epilepsy, seizures or medication, which cannot be distinguished from the primary alterations in the EZ.

There is evidence of cytoarchitectural alterations at the grey-white matter border in the resected epileptogenic tissue from cFE patients (Blümcke et al., 2011), which might influence the tractography, by tracking fewer fibers in the vicinity of these epileptogenic changes. From our 5 DTI-based measures, uFTDI is most specific for the grey-white matter border and this could explain why uFTDI correlated best with clinical data, in 80% of our patients, which to our knowledge has not been achieved before in MRI-negative epilepsy.

It is a common conception that every healthy brain is different. Therefore, it comes to no surprise that regional alterations of all DTI-based measures were also observed in the 10 CTR participants we investigated, reflecting individual anatomic variability. However, these alterations had a much lower T-score and smaller volume than the alterations we saw in epilepsy patients for all five DTI-based measures. So in spite of their poor localizing value, even FA and MD could still separate healthy subjects from patients.

#### 4.1. *Limitations*

In this study, a rather small sample of 10 cFE patients were analyzed and confirmation of our results in a larger cohort is warranted. Another potential limitation is that the locations of DTI alterations are compared to the available clinical data. So far, only two patients underwent resective surgery, definitely confirming the EZ. However, for all patients there was conclusive clinical evidence for the location of the EZ, with no contradictory information from any diagnostic modality. Also, we have used a standard streamline tracking algorithm and perhaps more sophisticated algorithms, like HARDI (Tuch et al., 2002) or Q-Ball (Berman et al., 2008), would lead to different results. We are also aware of another DTI-based measure, called Neurite Orientation Dispersion and Density Imaging (NODDI) (Zhang et al., 2012). However, this requires a two shell DTI acquisition scheme, not readily available in a clinical setting and has not been applied to cryptogenic epilepsy.

#### 4.2. *Conclusion*

Quantification of U-fiber track density images provides a novel diagnostic method of mapping the EZ in MRI-negative focal epilepsy, with much higher sensitivity and specificity than the currently used DTI measures FA and MD. We assume this reflects specific microstructural alterations at the grey-white matter border, where U-fibers are located.

### **Acknowledgement**

This study was supported by the Friedrich-Baur-Stiftung and the Herta-Riehr Stiftung.

## 5. References

- Ashburner, J., Friston, K.J., 2000. Voxel-Based Morphometry—The Methods. *Neuroimage* 11, 805–821. doi:10.1006/nimg.2000.0582
- Berman, J.I., Chung, S., Mukherjee, P., Hess, C.P., Han, E.T., Henry, R.G., 2008. Probabilistic streamline q-ball tractography using the residual bootstrap. *Neuroimage* 39, 215–22. doi:10.1016/j.neuroimage.2007.08.021
- Besson, P., Andermann, F., Dubeau, F., Bernasconi, A., 2008. Small focal cortical dysplasia lesions are located at the bottom of a deep sulcus. *Brain* 131, 3246–3255. doi:10.1093/brain/awn224
- Blümcke, I., Thom, M., Aronica, E., Armstrong, D.D., Vinters, H. V, Palmini, A., Jacques, T.S., Avanzini, G., Barkovich, a J., Battaglia, G., Becker, A., Cepeda, C., Cendes, F., Colombo, N., Crino, P., Cross, J.H., Delalande, O., Dubeau, F., Duncan, J., Guerrini, R., Kahane, P., Mathern, G., Najm, I., Ozkara, C., Raybaud, C., Represa, A., Roper, S.N., Salamon, N., Schulze-Bonhage, A., Tassi, L., Vezzani, A., Spreafico, R., 2011. The clinico-pathologic spectrum of focal cortical dysplasias: a consensus classification proposed by an ad hoc Task Force of the ILAE Diagnostic Methods Commission. *Epilepsia* 52, 158–74. doi:10.1111/j.1528-1167.2010.02777.x
- Calamante, F., Smith, R.E., Tournier, J., Raffelt, D., Connelly, A., 2015. Quantification of voxel-wise total fiber density: Investigating the problems associated with track-count mapping. *Neuroimage* 117, 284–293. doi:10.1016/j.neuroimage.2015.05.070
- Calamante, F., Tournier, J.-D., Jackson, G.D., Connelly, A., 2010. Track-density imaging (TDI): super-resolution white matter imaging using whole-brain track-density mapping. *Neuroimage* 53, 1233–43. doi:10.1016/j.neuroimage.2010.07.024

- Colombo, N., Tassi, L., Galli, C., Citterio, A., Lo Russo, G., Scialfa, G., Spreafico, R., 2003. Focal cortical dysplasias: MR imaging, histopathologic, and clinical correlations in surgically treated patients with epilepsy. *Am. J. Neuroradiol.* 24, 724–733.
- Dumas de la Roque, A., Oppenheim, C., Chassoux, F., Rodrigo, S., Beuvon, F., Daumas-Duport, C., Devaux, B., Meder, J.-F., 2005. Diffusion tensor imaging of partial intractable epilepsy. *Eur. Radiol.* 15, 279–85. doi:10.1007/s00330-004-2578-8
- Eriksson, S.H., Rugg-Gunn, F.J., Symms, M.R., Barker, G.J., Duncan, J.S., 2001. Diffusion tensor imaging in patients with epilepsy and malformations of cortical development. *Brain* 124, 617–626. doi:10.1093/brain/124.3.617
- Focke, N.K., Bonelli, S.B., Yogarajah, M., Scott, C., Symms, M.R., Duncan, J.S., 2009. Automated normalized FLAIR imaging in MRI-negative patients with refractory focal epilepsy. *Epilepsia* 50, 1484–1490. doi:10.1111/j.1528-1167.2009.02022.x
- Girard, G., Whittingstall, K., Deriche, R., Descoteaux, M., 2014. Towards quantitative connectivity analysis: reducing tractography biases. *Neuroimage* 98, 266–278. doi:10.1016/j.neuroimage.2014.04.074
- Henson, R., 2006. Comparing a single patient versus a group of controls (and SPM) 1–5.
- Kini, L.G., Gee, J.C., Litt, B., 2016. Computational analysis in epilepsy neuroimaging: A survey of features and methods. *NeuroImage Clin.* 11, 515–529. doi:10.1016/j.nicl.2016.02.013
- Martin, P., Bender, B., Focke, N.K., 2015. Post-processing of structural MRI for individualized diagnostics. *Quant. Imaging Med. Surg.* 5, 188–203. doi:10.3978/j.issn.2223-4292.2015.01.10

- Rosenow, F., Lüders, H., 2001. Presurgical evaluation of epilepsy. *Brain* 124, 1683–700.  
doi:10.4103/1817-1745.40593
- Rugg-Gunn, F.J., Eriksson, S.H., Symms, M.R., Barker, G.J., Duncan, J.S., 2001. Diffusion tensor imaging of cryptogenic and acquired partial epilepsies. *Brain* 124, 627–636.  
doi:10.1093/brain/124.3.627
- Thivard, L., Bouilleret, V., Chassoux, F., Adam, C., Dormont, D., Baulac, M., Semah, F., Dupont, S., 2011. Diffusion tensor imaging can localize the epileptogenic zone in nonlesional extra-temporal refractory epilepsies when [(18)F]FDG-PET is not contributive. *Epilepsy Res.* 97, 170–82. doi:10.1016/j.epilepsyres.2011.08.005
- Tuch, D.S., Reese, T.G., Wiegell, M.R., Makris, N., Belliveau, J.W., Van Wedeen, J., 2002. High angular resolution diffusion imaging reveals intravoxel white matter fiber heterogeneity. *Magn. Reson. Med.* 48, 577–582. doi:10.1002/mrm.10268
- Wagner, J., Weber, B., Urbach, H., Elger, C.E., Huppertz, H.J., 2011. Morphometric MRI analysis improves detection of focal cortical dysplasia type II. *Brain* 134, 2844–2854.  
doi:10.1093/brain/awr204
- WHO, 2016. Epilepsy. World Heal. Organ. URL  
<http://www.who.int/mediacentre/factsheets/fs999/en/>
- Widjaja, E., Geibprasert, S., Otsubo, H., Snead III, O.C., Mahmoodabadi, S.Z., 2011. Diffusion Tensor Imaging Assessment of the Epileptogenic Zone in Children with Localization-Related Epilepsy. *Am. J. Neuroradiol.* 32, 1789–1794.
- Winston, G.P., 2015. The potential role of novel diffusion imaging techniques in the understanding and treatment of epilepsy. *Quant. Imaging Med. Surg.* 5, 279–287.

doi:10.3978/j.issn.2223-4292.2015.02.03

Yao, K., Mei, X., Liu, X., Duan, Z., Liu, C., Bian, Y., Ma, Z., Qi, X., 2014. Clinical characteristics, pathological features and surgical outcomes of focal cortical dysplasia (FCD) type II: correlation with pathological subtypes. *Neurol. Sci.* 35, 1519–26. doi:10.1007/s10072-014-1782-9

Zhang, H., Schneider, T., Wheeler-Kingshott, C.A., Alexander, D.C., 2012. NODDI: practical in vivo neurite orientation dispersion and density imaging of the human brain. *Neuroimage* 61, 1000–16. doi:10.1016/j.neuroimage.2012.03.072

## **CHAPTER 3. ON THE CLINICAL SIDE**

### **3.1. CONTRIBUTIONS**

The author of this doctoral thesis, Joanna Goc (JG), contributed to the study by recruiting and scanning the patients and controls with Dr. Christian Vollmar (CV). JG also contributed by carrying out the research and analysis and together with CV discussed the results. CV wrote the article.

**Looking at the Dark Side of Diffusion Tensor Imaging Data –  
U-Fiber Track Density Imaging Identifies Specific Structural Changes in  
Non-lesional Focal Epilepsy**

C. Vollmar<sup>1,2</sup>, J. Goc<sup>1,3</sup>, E. Hartl<sup>1</sup>, S. Noachtar<sup>1</sup>

<sup>1</sup>Dept. of Neurology, Epilepsy Centre, University of Munich Hospital, Germany

<sup>2</sup>Dept. of Neuroradiology, University of Munich Hospital, Munich, Germany

<sup>3</sup>Graduate School of Systemic Neurosciences, Ludwig Maximilian University, Munich, Germany

**Abstract**

Epilepsy surgery is the most efficient treatment for selected patients with medically refractory focal epilepsy. However, epilepsy surgery is challenging in non-lesional patients when conventional magnetic resonance imaging (MRI) fails to identify the underlying epileptogenic lesion. Here, we present a novel analysis method for single-subject Diffusion Tensor Imaging (DTI), based on reconstruction, quantification and statistical analysis of regional U-fibers, the most peripheral, short association fibers of the brain, located at the grey-white-matter junction. This new approach identifies previously undetected structural changes in 95% of 22 epilepsy patients with normal conventional MRI compared to normal controls. Seventy-five percent of these changes are localized in brain regions consistent with the epileptogenic zone. This novel diagnostic approach is a valuable tool in patients considered for resective epilepsy surgery, when conventional MRI fails to identify a surgical target.

**Introduction**

Diffusion tensor imaging (DTI) is a recent MRI method, which allows in vivo studies of brain white matter and significantly contributed to important advances in clinical and theoretical neuroscience in the past years (Craddock et al. 2013). Traditionally, analyses of DTI data focused on fractional anisotropy (FA) images, which indicate the degree of directional bundling of white matter fibers. Anatomically, analyses have focused on the major white matter tracts which appear bright in FA images and which can be assessed reliably, even with low- or medium-quality DTI acquisitions. More recently, high-quality DTI acquisitions and processing methods provide rich datasets, with more detailed information on structural brain anatomy, from core white matter tracts to the most peripheral U-fibers of the brain. These peripheral regions appear dark in FA images (“dark side”) and deserve more attention and further investigation (Fig. 1).

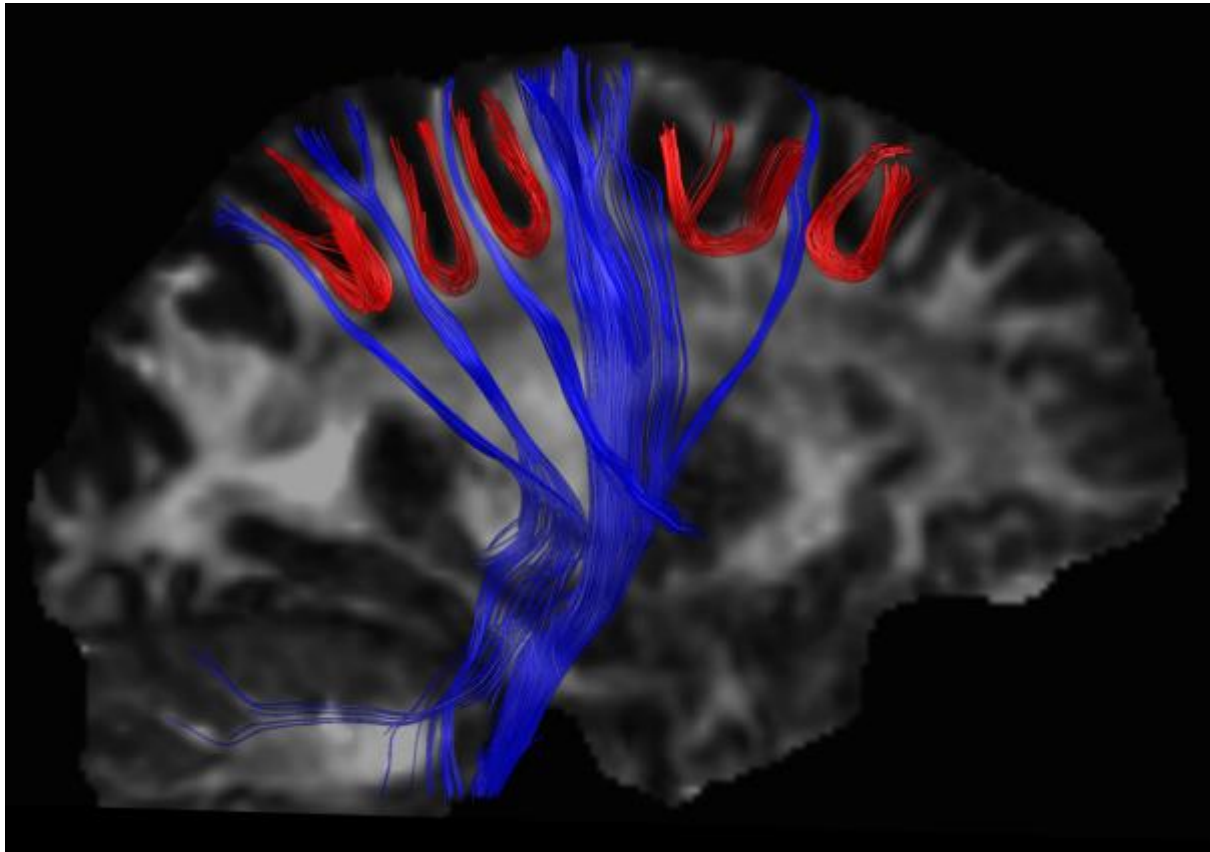


**Figure 1. U-fiber and long fiber projections tractography seen in a healthy brain.**

Epilepsy is a common serious neurological diseases and epilepsy surgery. i.e. the surgical resection of the epileptogenic zone is an effective and safe treatment for selected patients with pharmaco-resistant focal epilepsies (Kuzniecky & Devinsky 2007; Wiebe 2011). Presurgical evaluation aims to localize and delineate the epileptogenic zone using multiple diagnostic methods and depends strongly on neuroimaging (Duncan 2010). Patients with no visible structural lesion on conventional brain MRI scans typically have lower chances to become seizure free after surgery than patients with a lesion in MRI, providing a clear surgical target (Télez-Zenteno et al. 2010; Henry 2014). However, more recent studies in non-lesional focal epilepsy showed better surgical outcome, as good as in lesional epilepsies when there is sufficient localizing information from complementary

functional imaging data, consistent with the clinical and electrophysiological data (Lazow et al. 2012).

Improvement of imaging methods has led to higher detection rates of epileptogenic abnormalities, especially focal cortical dysplasia (FCD) (Mellerio et al. 2013). Despite these advances in neuroimaging, still up to 50% of referrals for epilepsy surgery in tertiary referral centers are patients with non-lesional or cryptogenic focal epilepsies (Nguyen et al. 2013) which require more extensive pre-surgical evaluation, including invasive EEG studies with intracranial electrodes (Wiebe & Jette 2012; So & Lee 2014).

Several neuroimaging approaches have been developed to improve localization of the epileptogenic zone in patients with non-lesional focal epilepsies (Madan & Grant 2009). These include analysis of conventional T1-weighted MRI data using morphometry, which has helped to identify hidden structural changes in some patients (Bernasconi et al. 2011; Huppertz et al. 2005). Advanced MRI acquisition schemes are also being developed (Feindel 2013) and high field strength MRI at 7 Tesla is evaluated (De Ciantis et al. 2016). Functional imaging, such as single photon emission tomography (SPECT) (Sulc et al. 2014) and glucose-metabolism-based positron emission tomography (FDG-PET) (Rheims et al. 2013) can also provide complementary information to localize functional abnormalities. Magnetencephalography (MEG) has contributed additional localizing information in a few selected patients (Jung et al. 2013). All of these methods have some limitations. T1-based morphometry has low yield, providing additional information in only 10-30% of patients (Wagner et al. 2011; Srivastava et al. 2005). MEG, FDG-PET and ictal SPECT which should be performed during continuous EEG-video-monitoring are not readily available outside tertiary referral centers. Both SPECT and FDG-PET are expensive and involve significant radiation exposure.

Focal epilepsy is mainly a grey matter disease, caused by cortical neuronal hyperexcitability, while DTI is usually used to analyze brain white matter. FCD is one of the most frequent etiologies in focal epilepsy in patients with normal conventional MRI, often diagnosed histopathologically in specimens from resective surgery (Wang et al. 2013). FCD is a malformation of cortical development associated with impaired neuronal migration and altered architecture of the cortex and underlying white matter (Blümcke et al. 2011). Hallmarks of FCD are cortical thickening, blurring of the grey-white-matter border and ectopic neurons in the subcortical white matter. Contemporary, high-quality DTI data acquisition and processing allow to reliably reconstruct a comprehensive network of white matter connections, including small peripheral U-fibers, spanning from one gyrus to the neighboring gyri (Fig. 2), directly underneath the cortex, where FCD causes architectural alterations. Quantification of regional U-fiber density is therefore a specific approach to assess the brains microstructural properties in the proximity of the grey-white-matter-border.

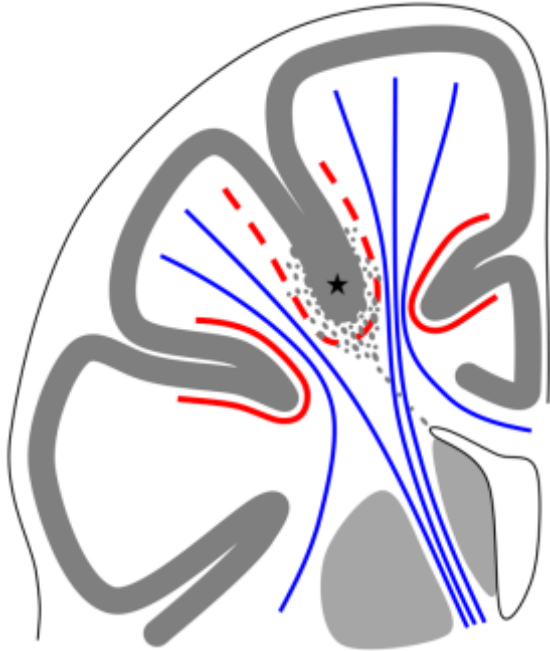


**Figure 2. Schematic diagram showing the affected U-fibers in focal cortical dysplasia.** Asterisk represents area affected by the pathology, which includes the blurring of the grey and white matter junction and the regional U-fibers.

Additionally, U-fibers are important for regional feedback mechanisms, controlling activity levels within a brain area. Cortical inhibition, facilitated by interneurons, has been shown to be impaired in focal epilepsy (Badawy et al. 2009; Werhahn et al 2000.). Axons of inhibitory interneurons contribute a large proportion of connections in regional U-Fibers, but this has not been studied systematically. In a patient with focal epilepsy following hypoxic brain damage and normal conventional MRI, we could show regional U-fiber reduction in the epileptogenic zone, leading to impaired cortical inhibition and epileptogenicity (Feddersen, 2015).

Here, we propose a novel analysis approach to DTI data, which can be easily acquired on a clinical routine MRI scanner. We show that reconstruction and statistical quantification of regional U-fiber density from DTI data can serve as a novel neuroimaging

biomarker, identifying regional structural changes at the grey-white-matter-border, which could not be detected by conventional MRI techniques in patients with focal epilepsy.

## **Results**

Thirty consecutive patients with refractory focal epilepsy referred for pre-surgical evaluation were investigated. In all of them epilepsy oriented (conventional) state of the art 3-Tesla MRI of the brain failed to reveal any structural lesion. Additional DTI images were acquired for all patients. All patients had prolonged Video-EEG monitoring and we included only those 22 with consistent clinical evidence for the localization of the epileptogenic zone.

Eleven of the 22 included patients had electroclinical evidence of a single localized epileptogenic zone (frontal, n=6; temporal, n=3; central, n=2). Six patients had evidence for two epileptogenic zones in one hemisphere and five patients had clinical evidence for bilateral seizure onset.

Fourteen patients were re-examined with invasive EEG after implantation of subdural electrodes (n=2) or stereotactic depth electrodes (n=12). Seven patients went on to have epilepsy surgery, and six are since seizure free (follow-up 6-18 months). In three patients, intracranial EEG showed bilateral epileptogenic zones, prohibiting resective epilepsy surgery. Four patients are currently awaiting surgery.

In total, 48 clusters of voxels with significant reductions in U-fiber track density images (ufTDI) were found in 21 of 22 patients (95%): One single cluster was identified in three patients (14%), two clusters in ten (45%), three clusters in seven (32%) and four clusters in two patients (9%) (Fig. 3). Of these 48 clusters, 36 (75%) were consistent with clinically suspected epileptogenic regions, twelve (25%) did not match the clinical data. Three additional regions were clinically suspected in two patients but did not show

significant uFTDI reductions (6%). Of the twelve clusters not matching the clinical data, eight were ipsilateral to the epileptogenic zone and four were in the contralateral hemisphere.

In the 14 patients with invasive EEG, 26 clusters were detected, 22 of which were covered by the intracranial electrodes. Intracranial EEG recording showed seizure onset in 17 of these 22 clusters (77%).

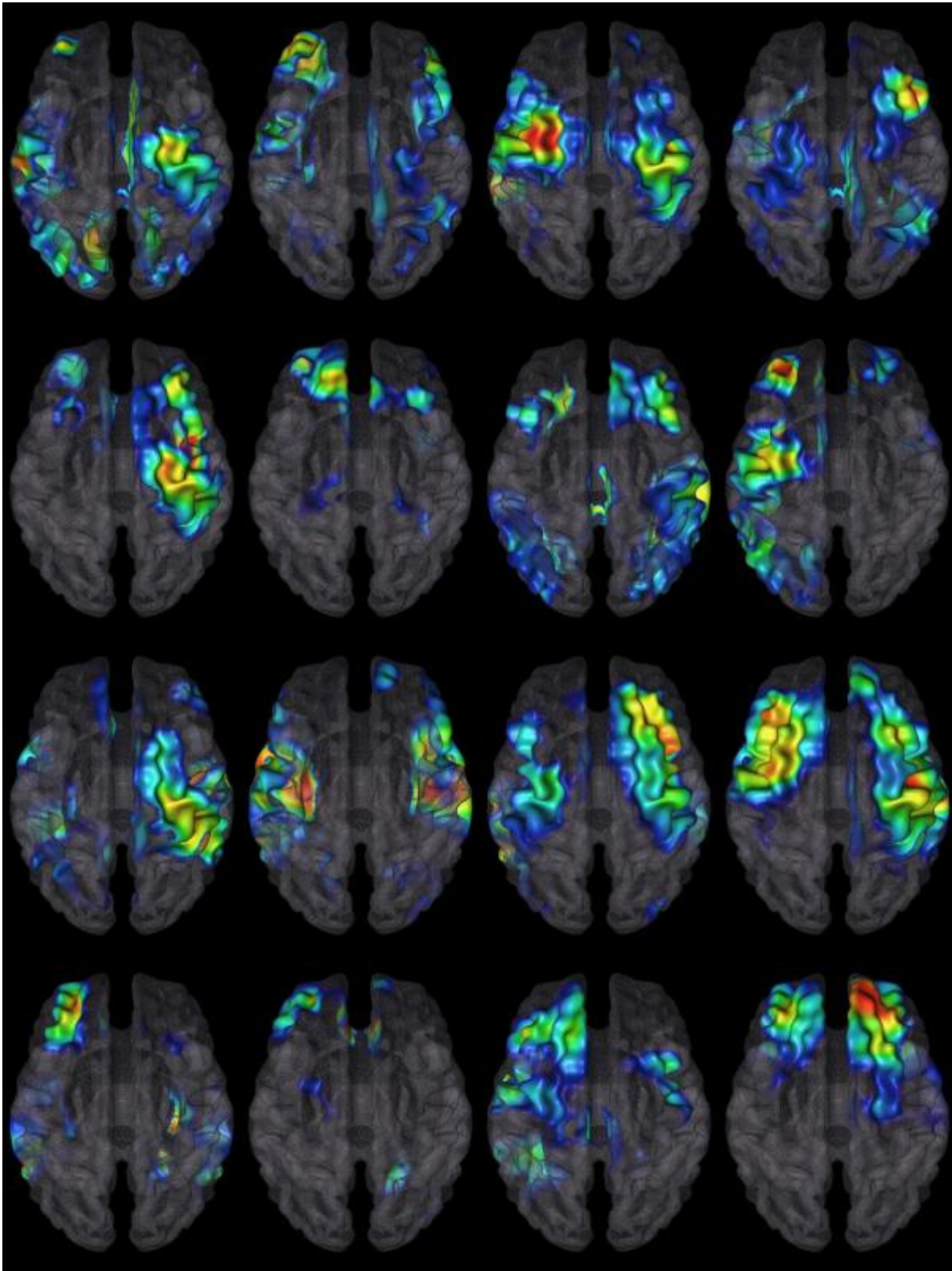


**Figure 3. Fiber tracking and results from quantitative analysis of uTDI data for the first 16 consecutive patients.** These examples reflect the diversity in the cluster shape, size and locations in different patients. Red color shows the hotspot or the peak of the cluster.

Of the five patients with clinical evidence for bilateral epileptogenic zones, 4 showed extensive, bilateral changes in the quantitative uFTDI analysis. Bilateral seizure onset was confirmed by intracranial EEG recordings in three of them, precluding these patients from resective epilepsy surgery. One of these patients has subsequently undergone implantation of deep brain stimulation electrodes in the anterior thalamus, improving seizure control, and one had a vagal nerve stimulator implanted.

Histopathological analysis of resected surgical specimen was performed in the seven operated patients, and showed mild architectural disturbances with blurred grey-white-matter border and ectopic neurons (n=5), ganglioglioma (n=1) and normal brain tissue (n=1).

We also investigated one additional patient with severe hypoxic brain damage, a pathology known to predominantly affect U-fibers. This patient had normal conventional MRI but uFTDI quantification showed extensive bilateral reductions of U-fiber density, to a degree and extent not seen in our epilepsy patients (Fig. 4). This serves as proof of concept and demonstrates the sensitivity of our method to detect damage to U-fibers.

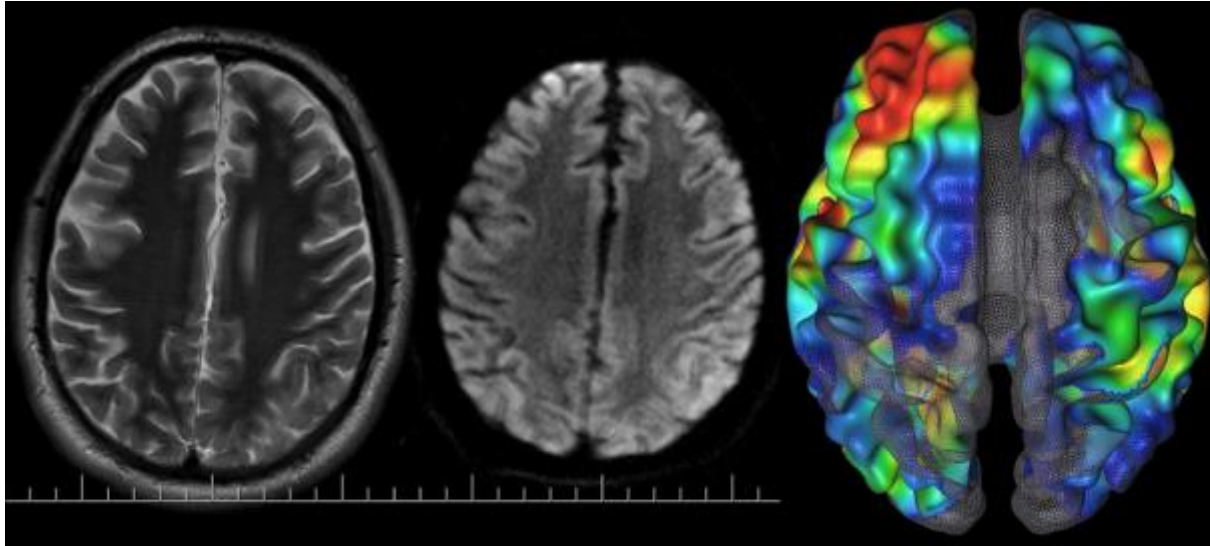


**Figure 4. uFTDI quantification in a patient with hypoxic brain damage.** Images from the left to right: T2, conventional diffusion weighted images (DWI) and uFTDI quantification results. uFTDI showed extensive bilateral reductions, whereas neither T2 nor DWI showed any abnormalities.

### **Discussion**

We present a novel analysis method for DTI data, based on tracking and quantification of regional U-fibers. U-Fiber track density images (uFTDI) were statistically compared with a sample of healthy controls. This novel approach identifies focal structural changes in patients with so-called cryptogenic focal epilepsy, where state-of-the-art 3 Tesla conventional MRI had failed to show the epileptogenic lesions. This method provides a new neuroimaging biomarker for microstructural alterations at the grey-white-matter-border, not visible in conventional epilepsy oriented MRI. DTI data was acquired on a 9-year-old clinical routine 3T Scanner, not requiring any specific hardware or software. Similar data can be acquired on almost all currently available MRI scanners.

Almost all previous studies using DTI in epilepsy have been performed in patients with visible brain lesions, such as hippocampal sclerosis, and investigated DTI alterations beyond and remote from the lesion (Ahmadi et al. 2009) or their correlation with cognitive parameters (McDonald et al. 2014).

DTI has rarely been used as additional localizing method in non-lesional focal epilepsy. One of the few studies with a larger cohort used statistical analysis of mean diffusivity (MD) images in 20 epilepsy patients and reported regional MD increases with a sensitivity of 40% and specificity of 60% (Thivard et al. 2011). One recent DTI study also included patients with non-lesional temporal lobe epilepsy and failed to identify abnormalities in the major white matter tracts (Campos et al. 2015). However, this study only evaluated major, “bright” white matter tracts, which are less affected by focal cortical dysplasias. In contrast, our current study addressed U-fibers, in the “dark” and so far unexplored periphery of DTI images, specifically investigating the grey-white matter border, affected by FCD. Previous voxel based morphometry studies in epilepsy have repeatedly shown focal alterations of the grey-white matter border (Wagner et al. 2011), but with a much lower yield than with our approach. We recently compared uTDTI quantification against the conventional DTI measures FA and MD showed a much higher sensitivity and specificity of uTDTI for the detection of the epileptogenic zone in non-lesional focal epilepsy (Goc, 2016, submitted).

### True positive findings

With our approach, we were able to show clusters of reduced U-fiber track density, representing focal microstructural brain changes in 95% of the patients, and 75% of these clusters were consistent with clinical evidence on the epileptogenic zone. This sensitivity and specificity is higher than for other complementary neuroimaging methods in non-lesional focal epilepsy (Thivard et al. 2011). The correct identification of the epileptogenic zone in previously non-lesional patients has several clinical consequences:

- 1) Some patients, where complementary functional investigations also remained inconclusive, would have been excluded from epilepsy surgery. Here, uFTDI facilitates that these patients benefit from surgery, by providing a target region for further investigation.
- 2) If patients are candidates for epilepsy surgery but require intracranial EEG recordings, uFTDI can help in guiding the implantation of invasive electrodes, increasing the yield of the procedure and reducing the number of required electrodes, and thereby minimizing the risk of complications.
- 3) Further, uFTDI showed extensive bilateral U-fiber reductions in all patients, where invasive recordings confirmed bilateral epileptogenic zones (Fig. 5). In these patients, not suitable for resective surgery, our new approach may help in the future to identify these patients earlier and to avoid the risks of invasive EEG recordings.

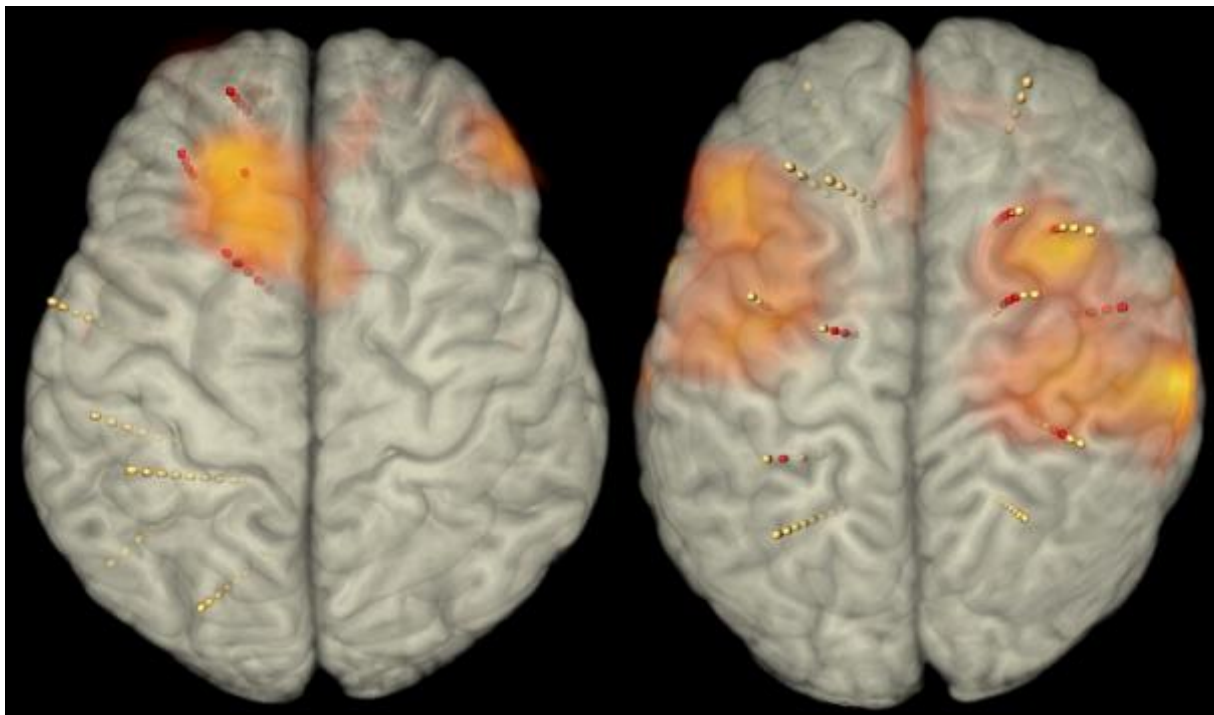


**Figure 5. Co-registration of intracranial EEG electrodes and clusters of significant uFTDI reductions.** These images show co-localization of seizure onset (red electrodes) with uFTDI alterations.

### False positive findings

In about half of our patients, uFTDI showed more widespread changes, including additional clusters of uFTDI reductions outside the clinically determined epileptogenic zone. These additional areas were located ipsilateral to the epileptogenic zone in eight patients, but also included clusters in the contralateral hemisphere in four patients. Only one of those four contralateral clusters was the main (primary) cluster, the other three were smaller (secondary or tertiary clusters) in addition to the primary, correctly localizing cluster. There are different possible explanations for these additional clusters:

1) False positive clusters may reflect secondary effects of chronic focal epilepsy, where areas remote from, but well connected to the epileptogenic onset zone, can show secondary changes. This would be typical for homologue areas in the contralateral hemisphere where lacking physiological input from the diseased side leads to inactivity or even regional atrophy on the contralateral side. Such remote effect may also be seen in areas belonging to the same functional system, similar to ipsilateral frontal hypometabolism observed in patients with mesial temporal epilepsy (Arnold et al. 1995; Wong et al. 2010). Follow-up scans of patients rendered seizure-free by surgery, may allow us to determine if some of these remote effects are reversible after seizure cessation.

2) These false positive clusters may not be false positive after all. Not all patients who undergo resective epilepsy surgery become seizure free, and some develop recurrent seizures after a variable time of seizure freedom following surgery (Rosenow & Lüders 2001). There are several reasons for this, such as incomplete resection, but also including dual pathology, where a second epileptogenic zone exists, but had not been detected at the time of the pre-surgical evaluation, probably because it was not yet epileptically active at that time. The fact that patients with non-lesional focal epilepsy tend to have a less

favorable outcome may indicate a higher proportion of such remote pathologies, extending beyond the assumed epileptogenic zone (Bernhardt et al. 2013). Clinically uncorrelated clusters of uFTDI reductions may represent such brain areas with structural alterations, currently not epileptogenic, but with the potential to become secondary seizure generators later on (Rosenow & Lüders 2001).

3) Finally, these additional clusters could be unrelated to epilepsy and simply reflect more pronounced individual anatomical variations. In our current control population, we have not observed clusters larger than 5 cm<sup>3</sup> at the threshold we use for analyses in epilepsy patients, but this does not preclude larger anatomical variations without pathological value.

#### False negative findings

No corresponding changes were seen in uFTDI for three brain regions with strong clinical evidence of the epileptogenic zone. This may be due to different reasons, which ultimately result in a reduced number of reconstructed U-fibers and hence may reduce the sensitivity or statistical power of our method. 1) Some brain areas have a lower amount of regional U-fibers than others, or a higher inter-individual variability reducing the statistical power. 2) Our selection criteria to identify U-fibers may not be ideal for all brain areas, for example, our length constrain of 20 - 60 mm may be too short to include longer U-fibers around a deeper sulcus, artificially reducing fiber density. 3) Technical artifacts, specific to some brain areas, may interfere with DTI data quality, such as susceptibility artifacts from the skull base, which interfere with the reconstruction of basal temporal fiber tracts.

### Patient population, gold standard and confirmation

All patients in our study underwent pre-surgical video-EEG monitoring, more than half of them with intracranial EEG recordings, the gold standard for identification and delineation of the epileptogenic zone in non-lesional focal epilepsy. Our uTfDI quantification could identify clusters of focal reductions in all of these patients, and intracranial EEG confirmed seizure onset in 77% of the identified clusters.

In those without intracranial EEG, the epileptogenic zone was defined by conclusive interpretation of all available diagnostic information, including non-invasive video-EEG monitoring, ictal SPECT, PET and clinical data. The percentage of correlation was not significantly different in these patients, with 73% of uTfDI clusters correlating with the clinical data. This indicates, that our observed correlations do not depend on the way, the epileptogenic zone was identified.

### Histopathology

The most frequent histopathological finding in resected surgical specimen from our patients is a mild architectural disturbance with blurred grey-white-matter border and ectopic neurons in the subcortical white matter, not enough to fulfil the current histopathological criteria for FCD (Blümcke et al. 2014). We assume, that these subtle histological changes disrupt the DTI tracking algorithm through a less consistent fiber alignment, disturbed by ectopic neurons in the white matter. It is important to clarify that, rather than showing white matter fibers directly, DTI and tractography actually show reconstructed pathways of water diffusion, resembling the white matter fibers described in anatomical studies. Hence, the reduction of U-fiber density we observe in our patients may

reflect an actual reduction of the number of anatomical U-fibers but could also reflect focal changes interfering with the tracking algorithm.

Further correlation with histopathology results from more patients, the comparison of different fiber types and different tracking algorithms, and the inclusion of additional parametric DTI and other MR images will allow us to look into the biological nature of the underlying alterations in more detail. Should different alteration patterns emerge, this may allow us to predict histological changes from specific profiles of alterations in DTI data. That we currently do not know the exact mechanism underlying our observed reductions in uFTDI does not decrease its important clinical value for patients with medically refractory non-lesional focal epilepsy.

### Conclusion

Our novel user-independent DTI analysis method is able to identify subtle focal structural changes at the grey-white-matter border not seen in conventional MRI. This approach should be considered in patients with “non-lesional” focal epilepsy to localize the epileptogenic zone. This additional localizing information has an impact on the management of these patients, by helping to identify candidates for intracranial evaluation and guidance of the electrode implantation. This same method may also be suitable to identify patients with extensive bilateral alterations, who are not candidates for resective surgery, sparing them unnecessary invasive investigations.

### Outlook

Further analyses of different fiber populations and long-term follow-up of patients will further our understanding of the mechanisms of epileptogenesis, seizure propagation

and secondary epileptogenesis, as well as compensation mechanisms and long-term effects of chronic focal epilepsy.

Similar changes, with subtle alteration of peripheral fibers may also be found to underlie other neurological disorders, such as neurodegenerative disease, where state-of-the-art structural MRI fails to show specific pathological changes in early stages of the disease and where the dark side of DTI data also has not been explored so far.

**(Online) Methods***Study population*

We investigated 30 patients with refractory focal epilepsy referred for pre-surgical evaluation at the University of Munich Hospital between 2013 and 2015. All patients had more than one conventional MRI, including a dedicated epilepsy protocol on a 3T scanner evaluated by at least 2 experienced neuroradiologists and epileptologists, all MRI scans were reported normal. Comprehensive pre-surgical evaluation allowed hypothesizing a single seizure onset zone in 22 of the 30 patients, based on the conclusive interpretation of scalp EEG, seizure semiology, ictal SPECT imaging (n=11) and FDG-PET (n=13). In the remaining 6 patients, the pre-surgical evaluation was inconclusive, i.e. the epileptogenic zone could not be lateralized or was only lateralized to one hemisphere but with no further lobar localization. All patients are candidates for further invasive evaluation, using intracranial depth or subdural electrodes.

For comparison we have scanned 31 age- and gender matched healthy controls with no prior history of neurological disease and normal structural MRI scan.

Figure 6 shows the workflow of the method starting with the pre-processing of the diffusion weighted images to ufTDI quantification in SPM.

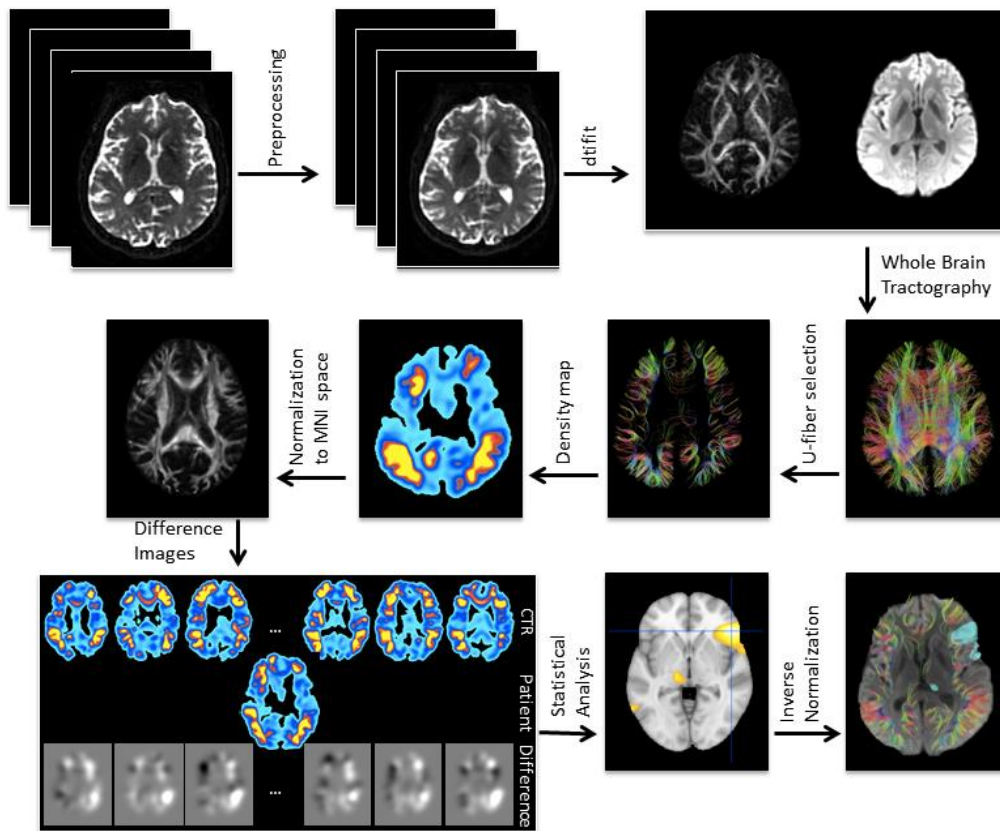


**Figure 6. Workflow of DTI data processing and analysis.**

### *MRI*

Clinical MRI was performed on a GE Signa HDx 3T scanner, using a dedicated epilepsy protocol, including 3D T1, coronal T1 inversion recovery, coronal T2, coronal and axial 2D FLAIR and a 3D sagittal FLAIR sequence.

### *DTI imaging*

DTI data was acquired on the same scanner in a different session, using an acquisition scheme with 64 diffusion-weighted directions, a b-value of  $1000\text{m/s}^2$ , 2.4 mm slice

thickness and a 96x96 matrix within a 220mm field of view, resulting in a 2.3 mm in-plane resolution. Using one excitation per volume, the acquisition time was 17:36 minutes.

### *DTI processing*

Image volumes were resampled to isotropic 1mm voxel size and realigned to correct for movement and eddy current induced distortions with FSL software (<http://fsl.fmrib.ox.ac.uk>). Diffusion tensors were fitted and fractional anisotropy (FA) and mean diffusivity (MD) maps were created. The resulting FA maps were spatially normalized to a FA template in MNI (Montreal Neurological Institute) space using SPM5 software (<http://www.fil.ion.ucl.ac.uk/spm>) to determine a nonlinear transformation with a 12mm frequency cutoff, a regularization of 0.1 and 128 nonlinear iterations. Whole-brain deterministic streamline tractography was performed in native individual subject space with diffusion toolkit (<http://trackvis.org>), using an FA threshold of 0.1 and an angular threshold of 35° between voxels, resulting in an average of 1.04 million fiber tracts per subject (range 0.87 - 1.22million). From these fiber tracts, we selected U-fibers with the command-line tool `track_vis`, using a length constraint of 20 - 60 mm, curvature of 5 - 10 and a U-factor, which estimates the shape of a fiber, of 0.6 - 1 (range -1 to 1). This resulted in an average of 84 thousand U-fibers per subject (range 65 - 107), which were used for subsequent analyses.

### *Statistical analysis and quantification of DTI data*

For user-independent, automatic analysis of U-fibers, we subsequently created U-Fiber track density images (ufTDI), where each voxel is assigned the number of U-fibers passing through it. The ufTDI were then spatially normalized to MNI space, applying the

transformation previously determined from the FA normalization. Spatially normalized ufTDI were smoothed with an 8mm FWHM kernel.

For the clinical purpose of localizing the previously undetermined epileptogenic area of a patient, each patient needs to be analyzed as a single individual. We have, therefore, chosen the approach suggested by Henson (R. Henson 2006) for single subject analysis, where difference images are created for every patient, subtracting the ufTDI of every single control from the ufTDI of the patient.

The resulting 31 difference images were then analyzed using a one sample t-test in SPM, identifying areas of consistent decrease of U-fiber density.

We chose the threshold of  $p < 0.001$ , with family-wise error correction for multiple comparisons and a spatial extend threshold of at least 5000 contiguous voxels (equivalent to 5 cm<sup>3</sup> volume) to eliminate small volume noise.

Clusters of decreased U-fiber density were visualized in SPM glass brain view, sectional images overlay and 3D surface rendering. Clusters were also back-normalized from MNI-space into the patient's individual DTI data and superimposed with the U-fiber rendering to allow visual inspection of fiber tracts in the regions detected as statistically significant.

For the purpose of this study, regional increases in ufTDI were not analyzed. However, future studies should address this in view of potential compensatory changes outside the epileptogenic zone.

## **References**

- Ahmadi, M.E. et al., 2009. Side matters: diffusion tensor imaging tractography in left and right temporal lobe epilepsy. *AJNR*, 30(9), pp.1740–7. Available at: <http://www.pubmedcentral.nih.gov/articlerender.fcgi?artid=2759860&tool=pmcentrez&rendertype=abstract> [Accessed August 2, 2014].
- Badawy, R. a B., Harvey, A.S. & Macdonell, R. a L., 2009. Cortical hyperexcitability and epileptogenesis: Understanding the mechanisms of epilepsy - part 2. *Journal of clinical neuroscience*, 16(4), pp.485–500. Available at: <http://www.ncbi.nlm.nih.gov/pubmed/19230676> [Accessed August 13, 2013].
- Bernasconi, A. et al., 2011. Advances in MRI for “cryptogenic” epilepsies. *Nature reviews. Neurology*, 7(2), pp.99–108. Available at: <http://www.ncbi.nlm.nih.gov/pubmed/21243016> [Accessed August 15, 2014].
- Bernhardt, B.C. et al., 2013. Imaging structural and functional brain networks in temporal lobe epilepsy. *Frontiers in human neuroscience*, 7(October), p.624. Available at: <http://www.pubmedcentral.nih.gov/articlerender.fcgi?artid=3787804&tool=pmcentrez&rendertype=abstract> [Accessed December 22, 2013].
- Besson, P. et al., 2008. Small focal cortical dysplasia lesions are located at the bottom of a deep sulcus. *Brain*, 131(Pt 12), pp.3246–55. Available at: <http://www.ncbi.nlm.nih.gov/pubmed/18812443> [Accessed August 13, 2013].
- Blümcke, I. et al., 2011. The clinico-pathologic spectrum of focal cortical dysplasias: a consensus classification proposed by an ad hoc Task Force of the ILAE Diagnostic Methods Commission. *Epilepsia*, 52(1), pp.158–74. Available at:

<http://www.pubmedcentral.nih.gov/articlerender.fcgi?artid=3058866&tool=pmcentrez&rendertype=abstract> [Accessed April 2, 2014].

Burzynska, A.Z. et al., 2013. A scaffold for efficiency in the human brain. *The Journal of neuroscience*, 33(43), pp.17150–9. Available at:

<http://www.ncbi.nlm.nih.gov/pubmed/24155318> [Accessed March 19, 2014].

Campos, B.M. et al., 2015. White matter abnormalities associate with type and localization of focal epileptogenic lesions. *Epilepsia*, 56(1), pp.125–132. Available at:

<http://doi.wiley.com/10.1111/epi.12871>.

De Ciantis, A. et al., 2016. 7T MRI in focal epilepsy with unrevealing conventional field strength imaging. *Epilepsia*, p.n/a–n/a. Available at:

<http://doi.wiley.com/10.1111/epi.13313>.

Colombo, N. et al., 2012. Focal cortical dysplasia type IIa and IIb: MRI aspects in 118 cases proven by histopathology. *Neuroradiology*, 54(10), pp.1065–77. Available at:

<http://www.ncbi.nlm.nih.gov/pubmed/22695739> [Accessed April 13, 2014].

Craddock, R.C. et al., 2013. Imaging human connectomes at the macroscale. *Nature methods*,

10(6), pp.524–39. Available at: <http://www.ncbi.nlm.nih.gov/pubmed/23722212>

[Accessed December 12, 2013].

Duncan, J.S., 2010. Imaging in the surgical treatment of epilepsy. *Nature reviews. Neurology*,

6(10), pp.537–50. Available at: <http://www.ncbi.nlm.nih.gov/pubmed/20842185>

[Accessed August 13, 2013].

Feindel, K.W., 2013. Can we develop pathology-specific MRI contrast for “MR-negative” epilepsy? *Epilepsia*, 54 Suppl 2(2009), pp.71–4. Available at:

<http://www.ncbi.nlm.nih.gov/pubmed/23646976> [Accessed January 3, 2014].

Hader, W.J. et al., 2013. Complications of epilepsy surgery: a systematic review of focal surgical resections and invasive EEG monitoring. *Epilepsia*, 54(5), pp.840–7. Available at: <http://www.ncbi.nlm.nih.gov/pubmed/23551133> [Accessed November 17, 2013].

Henry, T.R., 2014. Resecting without detecting the lesion in extratemporal lobe epilepsy? *Neurology*. Available at: <http://www.ncbi.nlm.nih.gov/pubmed/24532278> [Accessed March 2, 2014].

Huppertz, H.-J. et al., 2005. Enhanced visualization of blurred grey-white matter junctions in focal cortical dysplasia by voxel-based 3D MRI analysis. *Epilepsy research*, 67(1-2), pp.35–50. Available at: <http://www.ncbi.nlm.nih.gov/pubmed/16171974> [Accessed August 4, 2010].

Jung, J. et al., 2013. The value of magnetoencephalography for seizure-onset zone localization in magnetic resonance imaging-negative partial epilepsy. *Brain*, 136(Pt 10), pp.3176–86. Available at: <http://www.pubmedcentral.nih.gov/articlerender.fcgi?artid=3784280&tool=pmcentrez&rendertype=abstract> [Accessed December 16, 2013].

Kuzniecky, R. & Devinsky, O., 2007. Surgery Insight: surgical management of epilepsy. *Nature clinical practice. Neurology*, 3(12), pp.673–81. Available at: <http://www.ncbi.nlm.nih.gov/pubmed/18046440> [Accessed August 5, 2014].

- Lazow, S.P. et al., 2012. Outcome of frontal lobe epilepsy surgery. *Epilepsia*, 53(10), pp.1746–55. Available at: <http://www.ncbi.nlm.nih.gov/pubmed/22780836> [Accessed January 19, 2015].
- Madan, N. & Grant, P.E., 2009. New directions in clinical imaging of cortical dysplasias. *Epilepsia*, 50 Suppl 9, pp.9–18. Available at: <http://www.ncbi.nlm.nih.gov/pubmed/19761449> [Accessed January 21, 2015].
- McDonald, C.R. et al., 2014. White matter microstructure complements morphometry for predicting verbal memory in epilepsy. *Cortex*, 58, pp.139–150. Available at: <http://dx.doi.org/10.1016/j.cortex.2014.05.014>.
- Mellerio, C. et al., 2013. 3T MRI improves the detection of transmantle sign in type 2 focal cortical dysplasia. *Epilepsia*, 55(1), p.n/a–n/a. Available at: <http://doi.wiley.com/10.1111/epi.12464> [Accessed November 17, 2013].
- Nguyen, D.K. et al., 2013. Prevalence of non-lesional focal epilepsy in an adult epilepsy clinic. *The Canadian journal of neurological sciences*, 40(2), pp.198–202. Available at: <http://www.ncbi.nlm.nih.gov/pubmed/23419568> [Accessed April 13, 2014].
- Von Oertzen, J. et al., 2002. Standard magnetic resonance imaging is inadequate for patients with refractory focal epilepsy. *Journal of neurology, neurosurgery, and psychiatry*, 73(6), pp.643–7. Available at: [http://www.ncbi.nlm.nih.gov/entrez/query.fcgi?cmd=Retrieve&db=PubMed&dopt=Citation&list\\_uids=12438463](http://www.ncbi.nlm.nih.gov/entrez/query.fcgi?cmd=Retrieve&db=PubMed&dopt=Citation&list_uids=12438463) [Accessed August 10, 2014].

Paus, T. et al., 1999. Structural maturation of neural pathways in children and adolescents: in vivo study. *Science*, 283(5409), pp.1908–11. Available at:

<http://www.ncbi.nlm.nih.gov/pubmed/10082463> [Accessed January 19, 2015].

Rheims, S., Jung, J. & Ryvlin, P., 2013. Combination of PET and Magnetoencephalography in the Presurgical Assessment of MRI-Negative Epilepsy. *Frontiers in neurology*, 4(November), p.188. Available at:

<http://www.pubmedcentral.nih.gov/articlerender.fcgi?artid=3836027&tool=pmcentrez&rendertype=abstract> [Accessed January 3, 2014].

Rosenow, F. & Lüders, H., 2001. Presurgical evaluation of epilepsy. *Brain*, 124(Pt 9), pp.1683–700. Available at: <http://www.ncbi.nlm.nih.gov/pubmed/11522572>.

See, S.-J. et al., 2013. Surgical outcomes in patients with extratemporal epilepsy and subtle or normal magnetic resonance imaging findings. *Neurosurgery*, 73(1), pp.68–76; discussion 76–7. Available at: <http://www.ncbi.nlm.nih.gov/pubmed/23615090> [Accessed December 12, 2013].

Seo, J.H. et al., 2011. Multimodality imaging in the surgical treatment of children with nonlesional epilepsy. *Neurology*, 76(1), pp.41–8. Available at: <http://www.pubmedcentral.nih.gov/articlerender.fcgi?artid=3030221&tool=pmcentrez&rendertype=abstract>.

So, E.L. & Lee, R.W., 2014. Epilepsy surgery in MRI-negative epilepsies. *Current opinion in neurology*, 27(2), pp.206–12. Available at: <http://www.ncbi.nlm.nih.gov/pubmed/24553461> [Accessed September 14, 2014].

- Srivastava, S. et al., 2005. Feature-based statistical analysis of structural MR data for automatic detection of focal cortical dysplastic lesions. *NeuroImage*, 27(2), pp.253–66. Available at: <http://www.ncbi.nlm.nih.gov/pubmed/15993628> [Accessed April 13, 2014].
- Sulc, V. et al., 2014. Statistical SPECT processing in MRI-negative epilepsy surgery. *Neurology*, 82(11), pp.932–9. Available at: <http://www.ncbi.nlm.nih.gov/pubmed/24532274> [Accessed March 2, 2014].
- Téllez-Zenteno, J.F. et al., 2010. Surgical outcomes in lesional and non-lesional epilepsy: a systematic review and meta-analysis. *Epilepsy research*, 89(2-3), pp.310–8. Available at: <http://www.ncbi.nlm.nih.gov/pubmed/20227852> [Accessed April 6, 2014].
- Thivard, L. et al., 2011. Diffusion tensor imaging can localize the epileptogenic zone in nonlesional extra-temporal refractory epilepsies when [(18)F]FDG-PET is not contributive. *Epilepsy research*, 97(1-2), pp.170–82. Available at: <http://www.ncbi.nlm.nih.gov/pubmed/21885254> [Accessed August 13, 2013].
- Wagner, J. et al., 2011. Morphometric MRI analysis improves detection of focal cortical dysplasia type II. *Brain*, 134(Pt 10), pp.2844–54. Available at: <http://www.ncbi.nlm.nih.gov/pubmed/21893591> [Accessed August 13, 2013].
- Wang, Z.I. et al., 2013. The pathology of magnetic-resonance-imaging-negative epilepsy. *Modern pathology*, 26(8), pp.1051–8. Available at: <http://www.ncbi.nlm.nih.gov/pubmed/23558575> [Accessed August 5, 2014].

- Wiebe, S., 2011. Epilepsy. Outcome patterns in epilepsy surgery--the long-term view. *Nature reviews. Neurology*, 8(3), pp.123–4. Available at:  
<http://www.ncbi.nlm.nih.gov/pubmed/22290572> [Accessed January 4, 2014].
- Wiebe, S. & Jette, N., 2012. Pharmacoresistance and the role of surgery in difficult to treat epilepsy. *Nature reviews. Neurology*, 8(12), pp.669–77. Available at:  
<http://www.ncbi.nlm.nih.gov/pubmed/22964510> [Accessed January 27, 2014].
- Wong, C.H. et al., 2010. The topography and significance of extratemporal hypometabolism in refractory mesial temporal lobe epilepsy examined by FDG-PET. *Epilepsia*, 51(8), pp.1365–73. Available at: <http://www.ncbi.nlm.nih.gov/pubmed/20384730>.

## **CHAPTER 4. EFFECTS OF PRE-PROCESSING**

### **4.1. CONTRIBUTIONS**

The work was done under the supervision of Dr. Christian Vollmar (CV). CV developed the initial hypothesis and together with Joanna Goc (JG) designed the research. JG, CV and Dr. Elisabeth Hartl (EH) recruited and scanned participants. JG developed the method and Nadia Khalilieh (NK) optimized spatial normalization procedures that JG later used in the study. JG carried out the research and analysis and together with CV discussed the results. JG wrote the article.

## **The effects of pre-processing pipeline steps on statistical DTI tract quantification in cryptogenic focal epilepsy**

J. Goc<sup>1,2</sup>, E. Hartl<sup>1</sup>, N. Khalilieh<sup>1</sup>, S. Noachtar<sup>1</sup>, C. Vollmar<sup>1,3\*</sup>

<sup>1</sup>Dept. of Neurology, Epilepsy Centre, University of Munich Hospital, Germany

<sup>2</sup>Graduate School of Systemic Neurosciences, Ludwig Maximilian University, Munich, Germany

<sup>3</sup>Dept. of Neuroradiology, University of Munich Hospital, Munich, Germany

\*Correspondence to:

Dr. Dr. Christian Vollmar

Marchioninstr. 15

81377 Munich

Germany

+49 89440072682

Christian.vollmar@med.uni-muenchen.de

### **Keywords:**

cryptogenic epilepsy, epileptogenic zone, uFTDI, localization, spatial normalization, DTI

**Abstract**

A recent approach to localize the epileptogenic zone (EZ) in patients with cryptogenic focal epilepsy (cFE) based on the quantification of U-fiber track density images (ufTDI) showed better results than the quantification of FA or MD. However, the analysis involves a complex processing pipeline, where every processing step should be evaluated and optimized. Here, we looked at the effects of three different spatial normalization procedures, a U-fiber-specific masking and two different tracking algorithms on the final ufTDI results.

22 patients with MRI-negative focal epilepsy were compared against 31 healthy controls. DTI data was acquired on a 3T GE Signa HDx Scanner with 64 diffusion-weighted directions and b-value of 1000 s/mm<sup>2</sup>. DTI data was pre-processed, whole brain deterministic streamline tracking and HARDI tracking were performed and ufTDI were created, counting the number of U-fibers passing through any voxel. The ufTDI of each participant was spatially normalized to a template in MNI-space using three different approaches: SPM with default settings (SPMd) and optimized parameters (SPMo) and Advanced Normalization Tools (ANTs). A statistical comparison to the healthy control population was carried out, using a whole brain mask or the U-fiber-specific mask. The resulting clusters of significant ufTDI reductions, in every individual patient, were compared to the clinical localization of the EZ.

All three spatial normalization procedures showed comparable results, identifying primary clusters of reductions at similar locations with an average overlap of 71.5%. Results based on the SPMo spatial normalization showed the highest correlation with the clinical data and strongest statistical significance. Using a U-fiber-specific mask, instead of the MNI152\_T1 whole brain mask reduced the volume of false-positive clusters by 31.6%.

Deterministic streamline tracking showed fewer tertiary clusters than when using HARDI tracking.

Quantification of uFTDI is a robust method to localize the EZ in cFE. However, optimization of several processing steps along the analysis pipeline can help to increase sensitivity and specificity of the results, mostly by reducing the number of false positive findings.

**Abbreviations:** DTI = diffusion tensor imaging; MRI = magnetic resonance imaging; SPM = statistical parametric mapping; ANTs = advanced normalization tool; cFE = cryptogenic focal epilepsy; CTR = control; EZ = epileptogenic zone; uTfDI = U-fiber track density image

## 1. Introduction

Epilepsy is one of the most common neurological disorders affecting up to 1% of the population, where 30% of patients have pharmaco-resistant epilepsy. In some of these patients, resective epilepsy surgery can be an effective treatment option (Rosenow and Lüders, 2001). Up to 50% of the candidates for surgery have “non-lesional”, cryptogenic focal epilepsy (cFE), where conventional MRI does not show the underlying structural lesion. No single diagnostic method alone is available for the localization of the epileptogenic zone (EZ) (Kudr et al., 2013). The correct localization of the EZ and its complete resection are crucial for postoperative seizure freedom. The most frequent structural pathology in focal epilepsy is focal cortical dysplasia (FCD) characterized by histological abnormalities of the laminar layer of the cortex, blurring of the white and grey matter border, dysmorphic neurons and balloon cells (Besson et al., 2008; Blümcke et al., 2011). More severe forms of FCD can be detected by conventional MRI, but the changes can also be subtle and then may be easily overlooked on visual inspection of MRI or may not be visible in conventional MRI at all (Besson et al., 2008).

The use of diffusion tensor imaging (DTI) for identifying hidden lesions in cFE patients is less common. Quantification of the track density images (TDI) of short association fibers, called U-fibers, obtained from DTI has been shown to localize the EZ more effectively than quantitative analysis of fractional anisotropy (FA), mean diffusivity (MD) or whole brain track density images (Goc et al., submitted). This approach provides a novel and efficient diagnostic tool in cFE, offering additional valuable information for the localization of the EZ (Vollmar et al., in prep).

The ability to accurately compare DTI data across brains of many individuals relies on spatial normalization to transform individual brain scans onto a common template thus

allowing further comparison and voxel wise analyses. There are two types of approaches: volume-based and surface-based. The former, more common type, uses voxel intensities to steer the spatial normalization and uses full brain volume (Ghosh et al., 2010; Klein et al., 2009), whereas the latter takes into account the cortical surface alone, i.e. the shape of sulci and gyri (Fischl et al., 1999). The choice of the type of spatial normalization is likely to affect the results of cross subject analyses. Here we are interested in the reductions in fiber density and therefore volume-based spatial normalization is more applicable for this purpose.

Here we report the effects of the software and parameters for volume-based spatial normalization, a U-fiber-specific masking and different tracking algorithms on the quantification of U-fiber track density images (ufTDI).

## **2. Methods and Participants**

### *2.1. Participants*

A group of 22 patients [mean age of 31 (SD: 12.4), 11 males] diagnosed with drug-resistant cryptogenic focal epilepsy (cFE) was investigated. All patients had conventional structural MRI at 3T, not showing any structural epileptogenic lesions and underwent a series of neurological examinations including scalp EEG and video monitoring, FDG-PET, SPECT and in some cases invasive intracranial EEG.

31 healthy participants with no previous neurological or psychiatric history were included in the control (CTR) group [mean age of 28 years (SD: 6.4), 24 males].

The University of Munich Ethics Committee approved the study and all participants have given a written and informed consent.

### 2.2. DTI acquisition and pre-processing

All participants had additional DTI data acquisition on a 3T GE Signa HDx Scanner with an 8-channel head coil using 64 diffusion-weighted directions, a b-value of 1000 s/mm<sup>2</sup>, 60 axial slices with 2.4 mm slice thickness, a 96x96 in-plane matrix with a 220mm field of view, TR 16000 ms, TE 90.2 ms, flip angle 90° and parallel imaging with a SENSE factor of 2.

DTI-images were resampled to isotropic 1mm voxel size and corrected for movement and distortions caused by eddy currents using FSL software (<http://fsl.fmrib.ox.ac.uk>). Skull-stripped, realigned images were processed with FSL dtifit to create fractional anisotropy (FA) maps.

### 2.3. Tracking and U-fiber selection

Deterministic streamline tracking (DST) seeding from every voxel within the brain was performed with the Diffusion Toolkit (<http://trackvis.org/>) using a 2<sup>nd</sup>-order Runge Kutta propagation algorithm with an angular threshold of 35°. The termination criteria of the tracking were either exiting the brain or when the FA value in a voxel was <0.1. The streamlines were then visually analyzed in TrackVis (<http://trackvis.org/>) to check for erroneous tracking. The average whole brain track counts for cFE and CTR were 951699 and 1025380, respectively.

Additionally, in the first 10 cFE patients, the same DTI data was used for a high angular resolution diffusion imaging (HARDI) tracking performed with Diffusion Toolkit. The termination criteria, visual verification and U-fiber selection were the same as for DST tractography, except for an angular threshold of 45°. The average whole brain track counts for cFE and CTR using HARDI tracking were 1136809 and 1240378, respectively.

The population of U-fibers was selected from the whole brain tracking data using the following selection parameters: length 20-60mm, curvature 2-10 and U-factor, describing the shape of a fiber, between 0.6-1. These were then used to create U-fiber track density images (ufTDI) (Goc et al., submitted).

#### 2.4. *Spatial Normalization*

We compared two commonly used volume-based programs for affine and nonlinear spatial normalizations: SPM (Ashburner et al., 1999) and Advanced Normalization Tools (ANTs) (Avants et al., 2011). The FA maps were spatially normalized to the FMRIB58\_FA template in MNI space provided by FSL. The following three different spatial normalization procedures were compared:

**SPM default** (SPMd) – using default parameters provided by SPM5.

**SPM optimized** (SPMo) – with the following adjustments: source image smoothing (from 8 to 5mm), non-linear frequency cut-off (from 25 to 12mm), non-linear regularization (from 1 to 0.1) and non-linear iterations (from 16 to 128).

**ANTs optimized** (ANTs) – using the SyN algorithm with a regularization of SyN 0.5, smoothing 5mm and a 4x2x1 subsampling scheme with 30x90x150 nonlinear iterations.

The determined transformation from individual FA maps to the FA template was then applied to ufTDI before further statistical analyses.

#### 2.5. *Voxel-wise Statistical Analysis*

Spatially normalized ufTDI of an individual brain was used for the voxel-wise statistical analysis based on the method described elsewhere (Goc et al., submitted). First,

the differences in uTDI maps between each individual patient and the group of 31 controls were calculated (Henson, 2006). The resulting 31 difference images were analyzed with one-sample t-test using SPM to identify clusters of voxels with decreased track density compared to the CTR group. After family wise error (FWE) correction for multiple comparisons, the results were analyzed at the threshold of  $p < 0.001$  and a spatial extent threshold of  $> 5000$  voxels ( $5\text{cm}^3$ ).

### 2.6. *U-fiber-specific explicit mask*

Additionally, a U-fiber-specific mask was created to constrain statistical analysis to regions with a sufficient U-fiber density by averaging the spatially normalized uTDIs of all participants. This average was then smoothed with 8mm FWHM, thresholded at 3 and binarised. Using FSL atlas tool, subcortical structures (brainstem, caudate, putamen, pallidum, thalamus and lateral ventricles) and cerebellum were subtracted from the mask. This U-fiber-specific mask was compared to the conventionally used MNI152\_T1 whole brain mask before statistical analysis in a sample of 10 cFE patients using the SPMo normalization.

### 2.7. *Classification of clusters*

In most of the patients, the quantification of uTDI showed multiple clusters of voxels with uTDI reductions varying in spatial extent and degree of significance. Occasionally, there are clusters with a high T-score that are unlikely to be true findings, usually located in regions where no U-fibers are present, presumably due to e.g. DTI acquisition or spatial normalization artefacts. Therefore, to overcome these issues, we have ranked clusters based on their weight defined by:

$$\text{cluster weight} = (\text{cluster volume}) \times (\text{cluster peak T-score})$$

**Equation 1. Calculating the cluster weight.**

Cluster volume is based on the number of voxels thresholded at  $p < 0.001$  and cluster T-score is the maximum T-score of any voxel within this cluster.

The primary cluster is the one with the highest cluster weight per participant. Tertiary clusters have a cluster weight smaller than 10% of the primary cluster. Secondary clusters are all clusters in between.

### 3. Results

#### 3.1. *Spatial normalization procedures*

The quantification of uTfDI showed clusters of statistically significant decrease in track density in all patients for all three spatial normalization procedures. Overall uTfDI quantification identified 45, 49 and 51 clusters for SPMd, SPMo and ANTs, respectively. We restricted further analyses to the primary cluster of every patient. Compared to the clinical information about the localization of the EZ, the uTfDI quantification correctly identified the EZ in 79%, 85% and 74% of primary clusters using SPMd, SPMo and ANTs normalization, respectively.

In general, the three spatial normalization procedures lead to very similar statistical results. However, there are differences, which can be appreciated visually and quantitatively. On average, the volume of primary clusters was bigger in SPMd by 3% compared to SPMo. The volume of the clusters was bigger in ANTs than SPMo by 6.5% and SPMd by 3.9%.

The peak T-score obtained by the quantification of uTfDI was significantly higher in cFE than in CTR for all three spatial normalization procedures (Fig.1). The average peak T-

scores for primary clusters in CTR and cFE groups were 12.0 and 15.1 for SPMd ( $p=4 \times 10^{-3}$ ), 12.2 and 16.3 for SPMo ( $p=8.66 \times 10^{-7}$ ) and 12.2 and 16.0 for ANTs ( $p=1.46 \times 10^{-5}$ ), respectively, showing that the difference between cFE and CTR was most significant using the SPMo spatial normalization procedure.

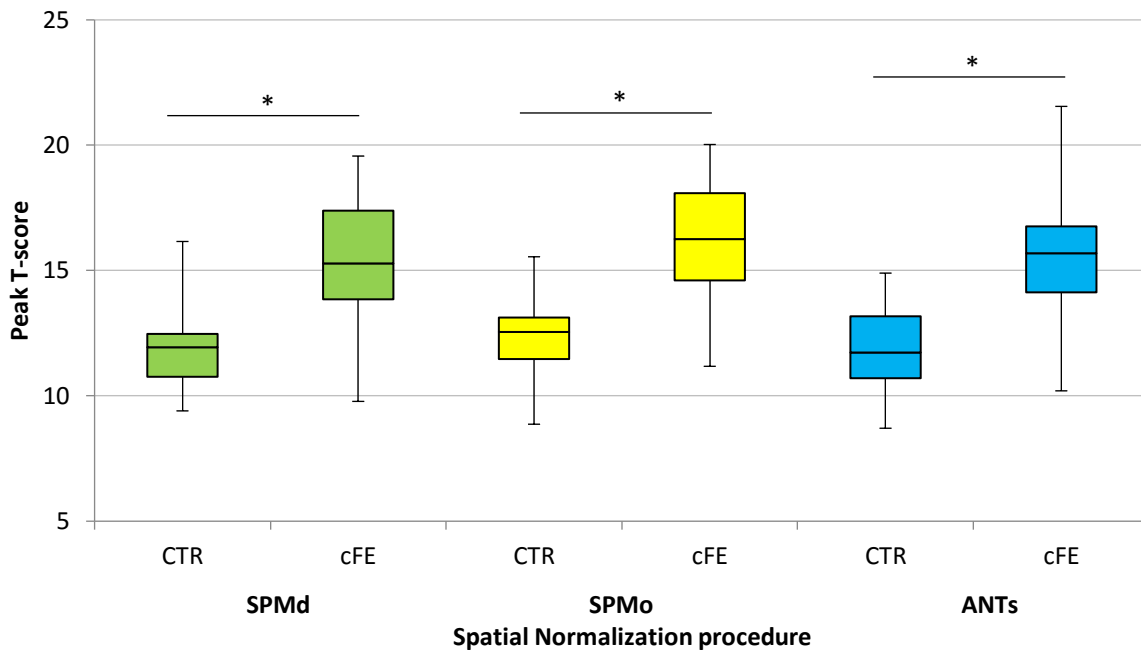


**Figure 1. Significance of uFTDI reductions in CTR and cFE patients based on three different spatial normalization procedures.**

For each spatial normalization procedure, the average peak T-score of uFTDI quantification and its corresponding interquartile range was calculated for each group.

The quantification based on all three spatial normalization procedures showed the clusters in similar regions (Fig. 2) with 71.5% average overlap of the three clusters in each patient (Table 1).

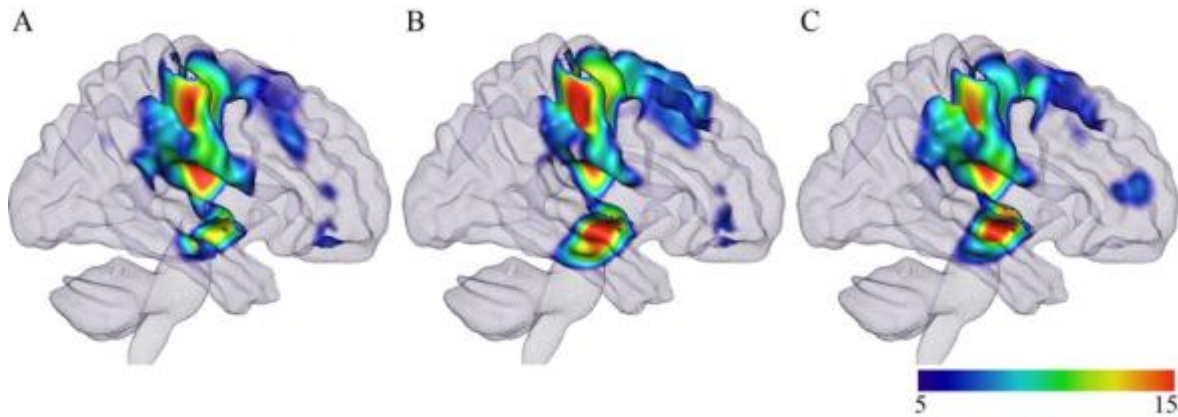


**Figure 2. Visualisation of the uFTDI quantification based on three different spatial normalization procedures in the same patient.**

uFTDI quantification showing a single cluster extending from the right postcentral gyrus in the parietal lobe to the temporal lobe. Clinically, the patient had somatosensory auras with tingling of the left hand consistent with the postcentral location of the cluster. SPMo shows the most significant reduction in the postcentral gyrus comparing to SPMd and ANTs. The 3D mesh is rendered at the smoothed grey-white-matter border of the MNI152T1 template. The color-coded overlay shows one patient's statistically significant reductions of the uFTDI compared to controls.

		and	SPMd	SPMo	ANTs
Overlap between clusters	SPMd	-		69%	67%
	SPMo	73%		-	70%
	ANTs	75%	75%		-

**Table 1. Average degree of overlap between quantifications based on different spatial normalization procedures.**

The percentage of the overlap of clusters from two different quantifications was calculated. The top row indicates what the overlap was for a particular quantification, e.g. the overlap between SPMd and SPMo was 69% of SPMo-based cluster and 73% of SPMd-based cluster.

### 3.2. U-fiber specific mask

The effects of a U-fiber-specific mask on the cluster volume obtained in quantification and visual impression were evaluated in 10 cFE patients. Quantification of uFTDI using a U-fiber-specific explicit mask, resulted on average in 31.6% smaller volume of

clusters compared to using the MNI152\_T1 whole brain mask. With the U-fiber-specific mask, several of the false-positive clusters were removed from anatomical regions where U-fibers are not typically present (Fig. 3). For this reason, the remaining analyses were based on the quantification using the U-fiber-specific explicit mask.

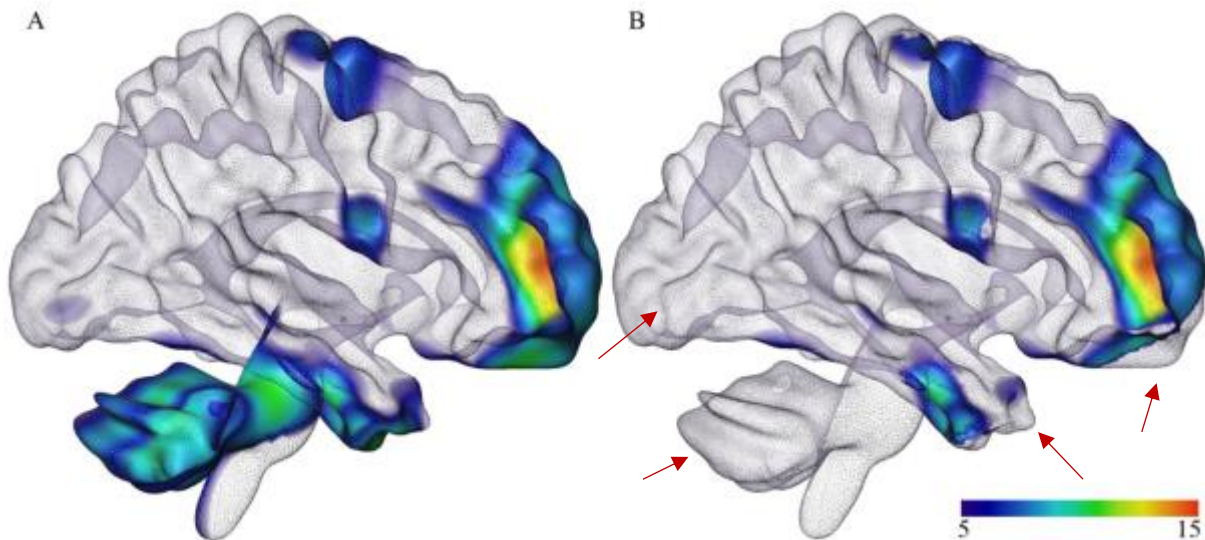


**Figure 3. Effects of masking on uFTDI quantification.**

(A) SPMo-based quantification using MNI152\_T1 whole brain mask showed clusters in regions where U-fibers are not typically found, e.g. cerebellum. Those clusters are masked out using (B) U-fiber-specific mask.

### 3.3. *DST versus HARDI tracking*

The comparison of the effects of DST and HARDI tracking algorithms on the quantification of uFTDI was performed for 10 cFE patients using SPMo spatial normalization and the U-fiber-specific mask. On average, HARDI tracking resulted in 16% more whole-brain fibers and 36% more U-fibers than DST.

The uFTDI quantification based on HARDI tracking showed a slightly lower average T-score for primary clusters (16.26) than DST (16.98). The total number of clusters detected in these 10 patients was higher in HARDI (n=34) than in DST (n=23). Typically, the additional clusters were tertiary clusters or noise (Fig. 4).

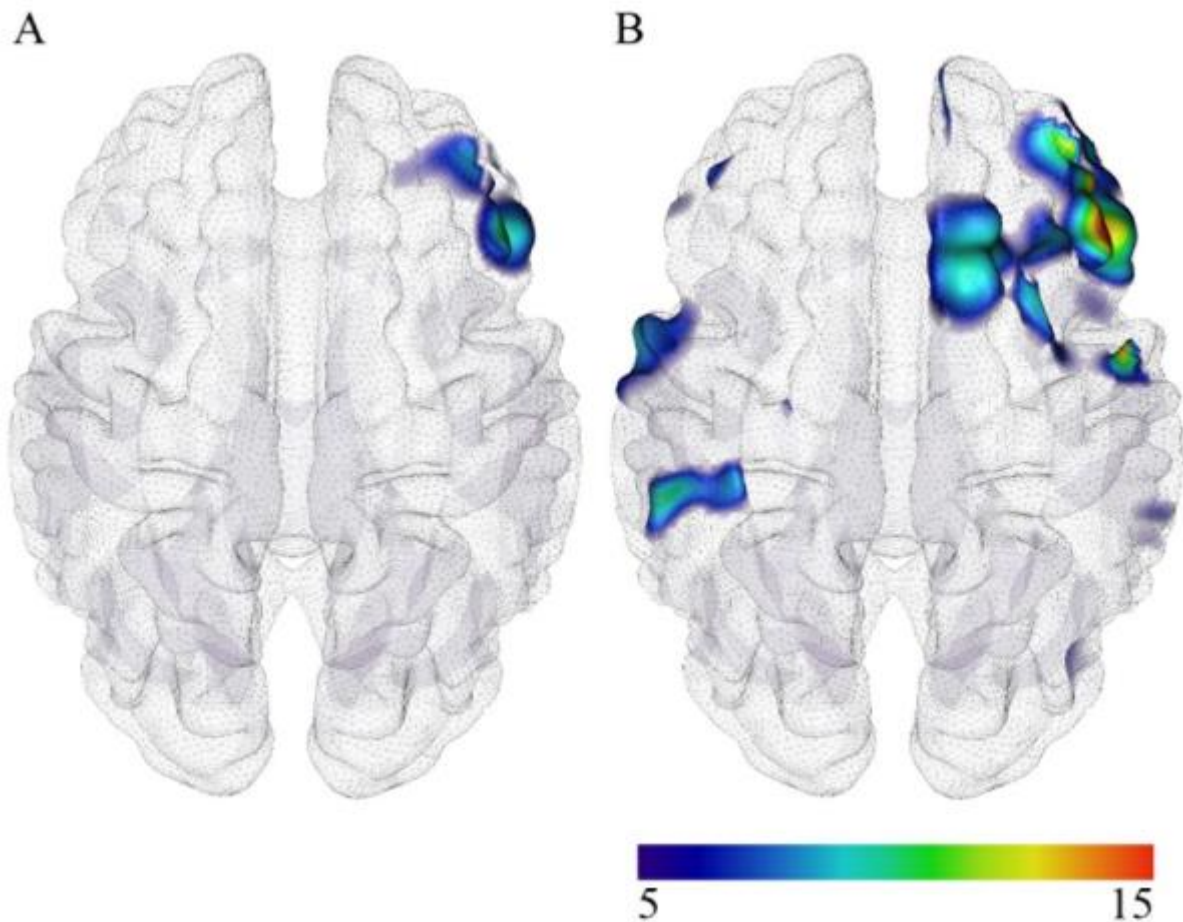


**Figure 4. Visualisation of the uFTDI quantification based on different tracking algorithms in the same patient.**

uFTDI quantification results based on (A) DST and (B) HARDI tracking.

Generally, the primary clusters were detected at similar locations and had a comparable shape for all patients. In terms of correlation with the electroclinical data, the same primary clusters were correctly identified in all 10 cFE patients with both DST and HARDI tracking. However, of all known clusters, including secondary clusters, 76% matched the clinical localization of the EZ when using DST and 65% in HARDI.

#### 4. Discussion

In cryptogenic focal epilepsy (cFE), localization of the epileptogenic zone (EZ) is challenged by the absence of a visible lesion in conventional MRI and relies on complementary diagnostic methods. DTI might be able to detect microscopic changes due to disruptions of the cortical laminations (Rugg-Gunn et al., 2001; Martin et al., 2015; Goc et al., submitted; Vollmar et al., in prep) in the area causing epilepsy. The use of DTI data allows for the analysis of structural differences in regions of the hypothesized EZ by quantifying U-fiber track density images (ufTDI). However, the processing pipeline of such analyses is complex, involving pre-processing, tracking, spatial normalization, masking, etc. and each step may affect the final results. Here, we focused on evaluating the effects of the spatial normalization and masking. We chose two commonly used volume-based software packages for this purpose: SPM and ANTs.

We expected for this step to be important, as it might directly relate to the accuracy and reliability of the results later on (Ghosh et al., 2010). However, we showed that the type of normalization and the optimization of parameters do not fundamentally influence the results of the quantification, i.e. the majority of primary clusters remain at the same location in all three spatial normalization procedures. The type of spatial normalization has an impact on the amount of secondary and tertiary clusters and the amount of general noise. It has been reported that ANTs performs better at registering the native brain to a reference image than SPM does (Ghosh et al., 2010). In our data, the apparent changes in ufTDI are robust enough that the different spatial normalization procedures do not significantly change the results of statistical quantification.

It is difficult to assess which spatial normalization procedure is best to improve the quantification. We still do not know whether presence of more or fewer clusters is better or

worse. We do know that altogether, SPMd normalization lead to the lowest number of clusters, however, cluster location based on SPMo correlated best with the clinical data. Here, we only evaluated the primary clusters, but we do know that in some patients, the EZ might extend to more than just one region. SPMd showed higher correlation of the primary clusters with the clinical data than ANTs did by 5%, whereas SPMo identified 6% more clusters than SPMd did. All three are within a close range and the clusters largely overlapped. It is important to take into account the computation time and ANTs has shown to be more demanding and time-consuming than SPMo (Ghosh et al., 2010), while the results were similar.

On the other hand, the U-fiber-specific explicit mask used in the quantification had a major effect on the results. All primary clusters remained at the same location, but the total size of all clusters significantly decreased by 31.6%, mostly by eliminating artefactual secondary and tertiary clusters.

Every brain has its own individual characteristics, meaning that there will be clusters of reduced uFTDI present in every brain including healthy controls (Goc et al., submitted). To determine the threshold, separating CTR from cFE, we have also performed statistical uFTDI quantification in the CTR group and compared the results to those from cFE patients. The distribution of T-scores clearly separates CTR and cFE groups (see Fig. 1). Together with other indications (e.g. cluster weight, cluster shape, etc.), this separation might be used as a threshold to determine the validity of the cluster.

We have compared uFTDI quantifications based on both DST and HARDI tracking algorithms, which have both correctly identified the same primary clusters. But –similarly to the spatial normalization procedures – changes in the tracking algorithms affected the amount of noise and false-positive clusters. In our series, HARDI-based quantification

showed more clusters that were not correlated with the electroclinical data. Compared to a simple DST tracking algorithm, HARDI is optimized to decipher multiple fiber orientations within a single voxel (Tuch et al., 2002) and is more capable to overcome crossings. This could account for a different distribution of reconstructed tracts and the additional clusters seen in HARDI-based quantification. However, the effects of different tracking algorithms on uFTDI quantification to localize the EZ should be investigated in more detail.

#### *4.1. Conclusion*

For a complex analysis pipeline, such as statistical quantification of uFTDI, every step, from the data acquisition to the statistical analysis, matters and every step should be optimized to obtain the best results possible for a given question. None of the differences we investigated have resulted in a failure to correctly identify the primary cluster of uFTDI reductions, also illustrating the robustness of this approach. However, the choice of the most appropriate alternative for every step throughout the processing pipeline has reduced the number of false-positive findings, reduced the amount of noise, strengthened the separation of patients from controls and improved the specificity of findings.

## **5. Acknowledgements**

This study was supported by the Friedrich-Baur-Stiftung and the Herta-Riehr Stiftung.

## 6. References

- Ashburner, J., Andersson, J.L., Friston, K.J., 1999. High-dimensional image registration using symmetric priors. *Neuroimage* 9, 619–28. doi:10.1006/nimg.1999.0437
- Avants, B.B., Tustison, N.J., Song, G., Cook, P. a., Klein, A., Gee, J.C., 2011. A reproducible evaluation of ANTs similarity metric performance in brain image registration. *Neuroimage* 54, 2033–2044. doi:10.1016/j.neuroimage.2010.09.025
- Besson, P., Andermann, F., Dubeau, F., Bernasconi, A., 2008. Small focal cortical dysplasia lesions are located at the bottom of a deep sulcus. *Brain* 131, 3246–3255. doi:10.1093/brain/awn224
- Blümcke, I., Thom, M., Aronica, E., Armstrong, D.D., Vinters, H. V, Palmini, A., Jacques, T.S., Avanzini, G., Barkovich, a J., Battaglia, G., Becker, A., Cepeda, C., Cendes, F., Colombo, N., Crino, P., Cross, J.H., Delalande, O., Dubeau, F., Duncan, J., Guerrini, R., Kahane, P., Mathern, G., Najm, I., Ozkara, C., Raybaud, C., Represa, A., Roper, S.N., Salamon, N., Schulze-Bonhage, A., Tassi, L., Vezzani, A., Spreafico, R., 2011. The clinicopathologic spectrum of focal cortical dysplasias: a consensus classification proposed by an ad hoc Task Force of the ILAE Diagnostic Methods Commission. *Epilepsia* 52, 158–74. doi:10.1111/j.1528-1167.2010.02777.x
- Fischl, B., Sereno, M.I., Dale, a M., 1999. Cortical Surface-Based Analysis II: Inflation, Flattening, and a Surface-Based Coordinate System. *Neuroimage* 9, 195–207. doi:10.1006/nimg.1998.0396
- Ghosh, S.S., Kakunoori, S., Augustinack, J., Nieto-Castanon, A., Kovelman, I., Gaab, N., Christodoulou, J.A., Triantafyllou, C., Gabrieli, J.D.E., Fischl, B., 2010. Evaluating the validity of volume-based and surface-based brain image registration for developmental

cognitive neuroscience studies in children 4 to 11 years of age. *Neuroimage* 53, 85–93.  
doi:10.1016/j.neuroimage.2010.05.075

Henson, R., 2006. Comparing a single patient versus a group of controls (and SPM) 1–5.

Klein, A., Andersson, J., Ardekani, B.A., Ashburner, J., Avants, B., Chiang, M.C., Christensen, G.E., Collins, D.L., Gee, J., Hellier, P., Song, J.H., Jenkinson, M., Lepage, C., Rueckert, D., Thompson, P., Vercauteren, T., Woods, R.P., Mann, J.J., Parsey, R. V., 2009. Evaluation of 14 nonlinear deformation algorithms applied to human brain MRI registration. *Neuroimage* 46, 786–802. doi:10.1016/j.neuroimage.2008.12.037

Kudr, M., Krsek, P., Marusic, P., Tomasek, M., Trnka, J., Michalova, K., Jaruskova, M., Sanda, J., Kyncl, M., Zamecnik, J., Rybar, J., Jahodova, A., Mohapl, M., Komarek, V., Tichy, M., 2013. SISCOM and FDG-PET in patients with non-lesional extratemporal epilepsy: Correlation with intracranial EEG, histology, and seizure outcome. *Epileptic Disord.* 15, 3–13. doi:10.1684/epd.2013.0560

Martin, P., Bender, B., Focke, N.K., 2015. Post-processing of structural MRI for individualized diagnostics. *Quant. Imaging Med. Surg.* 5, 188–203. doi:10.3978/j.issn.2223-4292.2015.01.10

Rosenow, F., Lüders, H., 2001. Presurgical evaluation of epilepsy. *Brain* 124, 1683–700.  
doi:10.4103/1817-1745.40593

Rugg-Gunn, F.J., Eriksson, S.H., Symms, M.R., Barker, G.J., Duncan, J.S., 2001. Diffusion tensor imaging of cryptogenic and acquired partial epilepsies. *Brain* 124, 627–636.  
doi:10.1093/brain/124.3.627

Tuch, D.S., Reese, T.G., Wiegell, M.R., Makris, N., Belliveau, J.W., Van Wedeen, J., 2002. High

angular resolution diffusion imaging reveals intravoxel white matter fiber heterogeneity. *Magn. Reson. Med.* 48, 577–582. doi:10.1002/mrm.10268

## **CHAPTER 5. GENDER AND CONTROLS**

### **5.1. CONTRIBUTIONS**

The work was done under the supervision of Dr. Christian Vollmar (CV). Joanna Goc (JG) developed the initial hypothesis and designed the research. JG and Dr. Elisabeth Hartl (EH) recruited and scanned additional healthy controls. JG adjusted the previously mentioned method in Chapters 3 and 4. JG carried out the research and analysis and together with CV discussed the results. JG wrote the article.

## **Careful control selection improves the quantification of fiber density images in cryptogenic focal epilepsy**

J. Goc<sup>1,2</sup>, E. Hartl<sup>1</sup>, S. Noachtar<sup>1</sup>, C. Vollmar<sup>1,3\*</sup>

<sup>1</sup>Dept. of Neurology, Epilepsy Centre, University of Munich Hospital, Germany

<sup>2</sup>Graduate School of Systemic Neurosciences, Ludwig Maximilian University, Munich, Germany

<sup>3</sup>Dept. of Neuroradiology, University of Munich Hospital, Munich, Germany

\*Correspondence to:

Dr. med. Dr. phil. Christian Vollmar

Klinikum Großhadern

Marchioninstr. 15

81377 Munich

Germany

+49 89440072682

Christian.vollmar@med.uni-muenchen.de

### **Keywords:**

control population, gender, sex dimorphism, DTI, cryptogenic epilepsy, focal epilepsy, U-fibers, ufTDI

**Abstract**

DTI is becoming increasingly used as a diagnostic tool in neurology. Recently, we proposed a new DTI-based diagnostic method that localized the epileptogenic zone in patients with cryptogenic focal epilepsy (cFE) by quantifying U-fiber track density images (ufTDI) in comparison to a healthy control population. We also showed that optimizing the steps in the complex pre-processing pipeline improves the specificity of the ufTDI quantification. Another unexplored aspect of this approach is the effect of the control population on the quantification. In neuroimaging studies, there are still open questions regarding the composition of the correct control group and it may be selected inadequately. The effects of gender-matched control groups are rarely investigated and to our knowledge, no single-subject study has evaluated them.

Here, we investigated different effects of the composition of the group of healthy controls (n=60) on ufTDI quantification in cFE patients (n=48). DTI data was acquired for all participants on a 3T GE Signa HDx Scanner with 64 diffusion-weighted directions and b-value of 1000 s/mm<sup>2</sup>. DTI data was pre-processed and whole brain streamline tracking was performed and U-fibres were selected to create ufTDI. Statistical comparisons of single individual patients to the varying healthy population (HP) groups were carried out to identify changes in the final results of the ufTDI quantification.

The results showed that increasing size of the HP group increases the statistical significance of the ufTDI quantification and improves the separation of healthy controls from cFE patients. The separation was further strengthened by removing outliers from the biggest HP group. When using a gender-matched HP group, the overall volume of ufTDI reductions decreased by 17% for male and 21.5% for female patients. At the same time, the

primary clusters amongst all groups and patients remained at the same location and only the additional clusters, e.g. noise clusters, are affected.

In summary, we showed that careful selection of controls affects the amount of noise and additional clusters without fundamentally changing the primary cluster.

**Abbreviations:** DTI = diffusion tensor imaging; MRI = magnetic resonance imaging; ufTDI = U-fiber track density image; cFE = cryptogenic focal epilepsy; CTR = control; HP = healthy participants

## 1. **Introduction**

Identifying micro-structural lesions using diffusion tensor imaging in patients with ‘non-lesional’ cryptogenic focal epilepsy (cFE) is new. In drug-resistant patients, the correct localization of the epileptogenic zone (EZ) and its complete surgical resection are crucial to achieve seizure freedom (Rosenow and Lüders, 2001). Recently, a new approach of quantifying track density images (TDI) of short association fibers, called U-fibers, obtained from DTI has been introduced (Goc et al., submitted). It has shown to localize the EZ more effectively than a quantitative analysis of commonly-used fractional anisotropy (FA), mean diffusivity (MD) or whole brain track density images. A following study showed that optimizing steps of the pre-processing pipeline, like spatial normalization or the use of a U-fiber-specific mask, improved the sensitivity and specificity of the method (Goc et al., in prep). These studies did not yet evaluate the role of the control group for statistical comparison and its effects on the final statistical results.

The quantification of U-fiber track density images (ufTDI) is based on statistical comparison of one individual cFE patient against a group of healthy controls, which is able to identify clusters with significantly decreased track density in individual cFE patients. The primary cluster has been shown to correlate well with the clinically-determined EZ (Goc et al., in prep). Often there are additional, smaller clusters of reduced track density that are thought to represent false-positive findings. These could be due to a number of factors, e.g. individual anatomical variability, the sample size and composition of the control group.

In neuroimaging studies, there are still open questions regarding the composition of the correct control group and it is occasionally poorly selected (Greene et al., 2016). This is particularly true for new methodological approaches, such as the ufTDI quantification, where the sample size necessary for statistical analyses or comparisons is unknown.

Underpowered studies are prone to low chance of discovering a true effect and even if that effect is found, most likely the relative magnitude of that effect would be exaggerated (the so-called “Winner’s curse”, Button et al., 2013). Too small size of a control group could prevent the discovery of the true effect and increasing the number of controls might improve the power of a study. However, this association is not linear and beyond a certain number of controls, there is little improvement in the power of the study (Grimes and Schulz, 2005). Finding the optimal number of controls for neuroimaging studies remains a challenging task, especially for a single-subject study against group comparison that we perform here.

It has been shown that gender-specific differences are present in the human brain. A number of studies over the last decade studied sex dimorphism using neuroimaging methods, such as fMRI, voxel-based morphometry (VBM) and DTI (Sacher et al., 2013). Sexual dimorphism was investigated at great length, primarily looking into the overall brain size, where male brain volume is larger than female’s brain, or investigating the proportion of white to grey matter, where women showed to have a higher proportion of grey matter (Sacher et al., 2013). These differences can influence statistical analyses such as our uFTDI quantification and could result in both reduced sensitivity and false-positive findings and increased noise in case of gender mismatch. Additionally, recent structural studies have shown regional differences in brain volume, where men showed an increased volume of midbrain, left inferior temporal gyrus, right middle temporal gyrus and cerebellum (Chen et al., 2007). Women showed greater volume in cingulate cortices (Chen et al., 2007) and auditory and language-related areas (Brun et al., 2009).

In most neuroimaging studies, mixed control groups are used and the gender of the controls is not necessarily considered, e.g. for mixed patient group, a mixed control group is

assembled. Occasionally, when a gender-related disease is investigated, e.g. prostate cancer, then naturally it would involve a male control group. However, the effects of using a gender-specific control group are rarely investigated and to our knowledge, no single-subject study has evaluated the effects of single-patients against mixed control group compared to a gender-specific control group.

Basically, the control population should be similar to the patients in all regards, except for the disorder in question (Grimes and Schulz, 2005; Schulz and Grimes, 2002). Therefore, here we evaluated the effects of the size and gender of the control group on the uTfDI quantification of individual patients with cFE.

## **2. Methods and Participants**

### *2.1. Participants*

A group of 48 patients [26 males with mean age 31.4 (SD: 11.5), 22 females with mean age 29.1 (SD: 9.2)] diagnosed with MRI-negative cryptogenic focal epilepsy (cFE) was investigated. 20 of those patients had a clinically clearly defined epileptogenic zone and were used for further analyses. All patients had conventional structural MRI at 3T using a specific epilepsy protocol, including high resolution 3D T1 and 3D FLAIR images, coronal FLAIR T2 and inversion recovery T1 images, not showing any structural epileptogenic lesions. All patients underwent a series of neurological examinations including scalp EEG and Video Monitoring, FDG-PET, ictal SPECT and in some cases invasive intracranial EEG.

60 healthy controls (CTR) with no previous history of neurological or psychiatric disease were included in the healthy population (HP) group [mean age of 28.7 years (SD: 7.1), 30 males and 30 females].

The University of Munich Ethics Committee approved the study and all participants gave written and informed consent.

### *2.2. DTI acquisition and pre-processing*

All participants had additional DTI data acquisition on a 3T GE Signa HDx Scanner with an 8-channel head coil using 64 diffusion-weighted directions, a b-value of 1000 s/mm<sup>2</sup>, 60 axial slices with 2.4 mm slice thickness, a 96x96 in-plane matrix with a 220mm field of view, TR 16000 ms, TE 90.2 ms, flip angle 90° and parallel imaging with a SENSE factor of 2.

DTI-images were resampled to isotropic 1mm voxel size and corrected for movement and distortions caused by eddy currents using eddy-correct function in FSL 4.1.9 software (<http://fsl.fmrib.ox.ac.uk>). Skull-stripped, realigned images were processed with FSL dtifit to create fractional anisotropy (FA) maps.

### *2.4. Streamline Tractography and U-fiber selection*

Deterministic streamline tracking seeding from every voxel within the brain was performed using the Diffusion Toolkit 0.6.2.1 (<http://trackvis.org/>). This was based on 2<sup>nd</sup>-order Runge Kutta propagation algorithm with an angular threshold of 35°. The termination criteria of the tracking were either exiting the brain or when the FA value in a voxel was <0.1. The streamlines were then visually analyzed in TrackVis 0.5.2.1 (<http://trackvis.org/>) to check for erroneous tracking.

The population of U-fibers was selected from the whole brain tracking data using the command line tool `track_vis` with the following selection parameters: length 20-60mm, curvature 2-10 and U-factor 0.6-1 (more information available in the help command in

track\_vis, as part of TrackVis). These were then used to create U-fiber track density images (ufTDI) (Goc et al., submitted), where the value at each pixel represents the number of U-fibers passing through it.

### *2.5. Spatial Normalization*

The FA maps were spatially normalized to the FMRIB58\_FA template in MNI space using SPM5 software (<http://www.fil.ion.ucl.ac.uk/>) with the following settings: Source Image Smoothing 5mm, Non-linear Frequency cut-off 12mm, non-linear Regularization 0.1, non-linear iterations 128. The determined transformation from individual DTI space to MNI template space was then applied to ufTDI.

### *2.6. Voxel-wise Statistical Analysis*

Spatially normalized ufTDI of an individual brain was used for the voxel-wise statistical analysis based on the method described elsewhere (Vollmar et al., in prep; Goc et al., submitted; Henson, 2006). In short, for each patient ufTDI difference images are calculated by subtracting each CTR ufTDI from a patient's ufTDI. These difference images are then analyzed using a one-sample t-test for each individual cFE patient. This was also repeated for each individual CTR in the same way.

Additionally, to limit the false-positive results, a U-fiber-specific mask was created by averaging the spatially normalized ufTDIs of all participants. This was then smoothed by FWHM 8, thresholded at 3. and binarised. Using the FSL Atlas tool, subcortical structures (brainstem, caudate, putamen, pallidum, thalamus and lateral ventricles) and cerebellum were subtracted from the mask.

Four analyses were performed. 1) We investigated the effects of the size of the HP group on the quantification results on uFTDI in 20 individual cFE patients, in which case the number included in the HP group varied: 20, 30, 40, 50 and 60 HP. Each individual CTR was also analyzed against the whole group of HP in the same way as the 20 cFE patients. 2) In the second part of the study, we investigated the importance of “cleaned” up HP group, where outliers were removed, in comparison to the 60HP group. The average and standard deviation (SD) of t-scores of individual CTR from the 60HP-quantification were calculated and CTR participants that had t-score higher than the average plus one standard deviation were excluded with the aim of selecting CTR with a normal distribution and no outliers. The re-selected “cleaned-up” HP group consisted of 49 healthy controls. 3) Additionally, a two sample t-test was performed comparing the male and female G-HP groups. 4) The last part of the study evaluated the effects of using a gender-specific healthy population (G-HP) on the quantification including 30 HP each for a male and female G-HP.

The resulting clusters of decreased uFTDI were analyzed at the threshold of  $p < 0.001$  after family wise error (FWE) correction for multiple comparisons of and with a spatial extent threshold of  $> 5000$  voxels.

### **3. Results**

#### *3.1. Size of the Control Group*

The analysis was performed based on a comparison of 20 cFE patients against groups of controls of: 20, 30, 40, 50 and 60 HP.

The average t-score of the primary clusters gradually increased with the increase in the size of the control group showing a high  $R^2$  value for a non-linear regression model ( $R^2=0.993$ ; Fig. 1). With the increasing HP group, the distinction between CTR and cFE

becomes stronger and the t-scores are higher for cFE than CTR. While the smallest HP of 20 resulted in similar t-scores in cFE and CTR ( $p=0.09$ ), increasing the number of HP allowed for a better separation of cFE and CTR, (30HP:  $p=2.14 \times 10^{-5}$ ; 40HP:  $p=1.00 \times 10^{-4}$ ; 50HP:  $p=1.00 \times 10^{-4}$ ; 60HP:  $p=4.09 \times 10^{-5}$ ; Fig. 1).

The resulting peak t-score increased with the increasing number of HP, therefore the threshold had to be adjusted accordingly. This implies that the clusters cannot be compared based on t-score alone. To be able to compare them, cluster weight was calculated by multiplying the t-score and the cluster size for each individual patient against 30HP at  $p < 0.001$  and extend threshold of  $5\text{cm}^3$ . The threshold was then adjusted for each analysis to match the cluster weight of the primary cluster of the same patient at 30HP.

Importantly, the primary clusters of every cFE patient remained at the same location for all variations of HP, therefore the size of the control group did not fundamentally affect the primary results. Additionally, as the size of the HP group increases, the volume of additional, false-positive clusters decreased, providing more “cleaned up” results (Fig. 1).

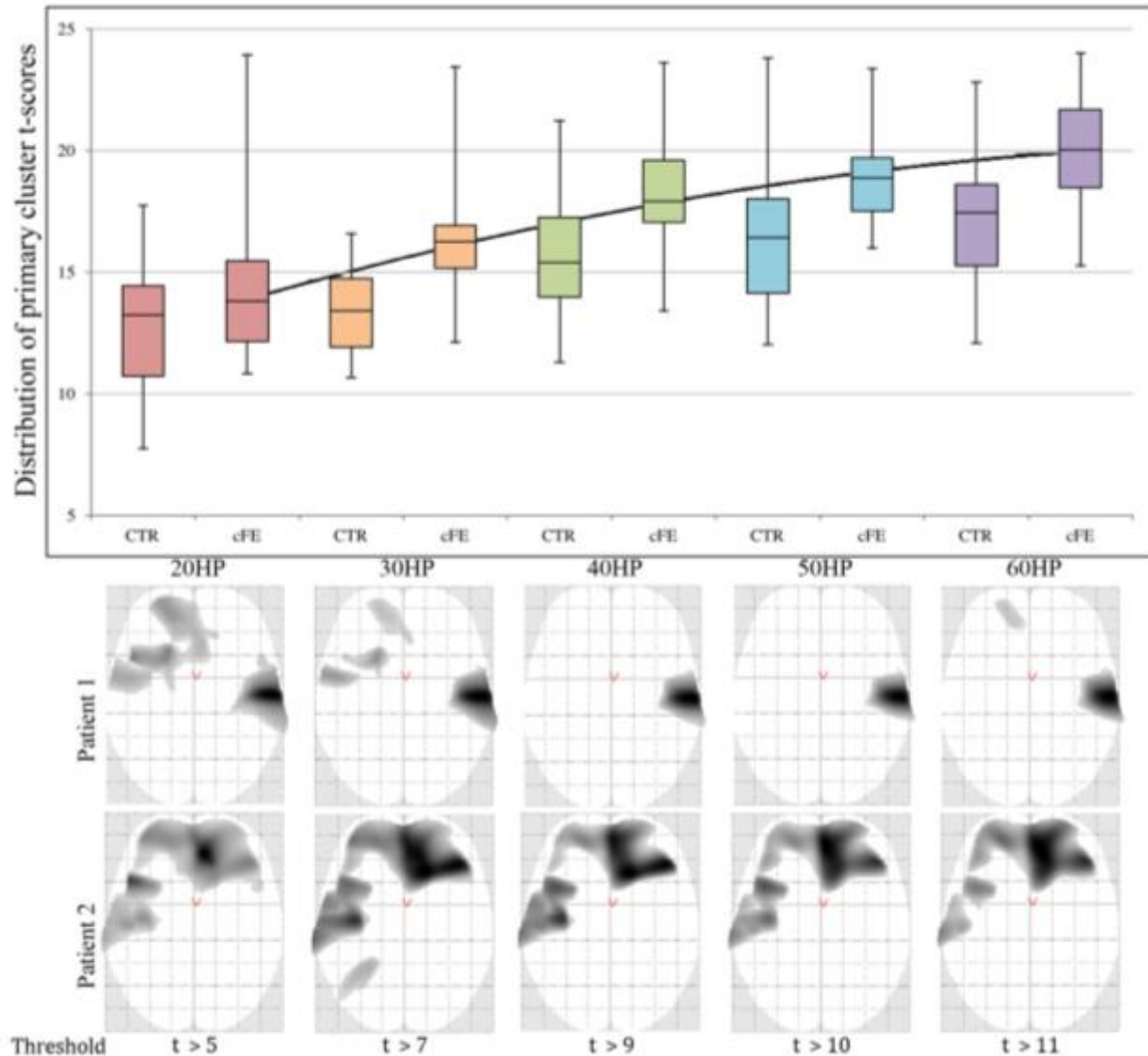


**Figure 1 Graphical representation of peak t-scores in cFE group against HP groups of different sizes.** The uFTDI were quantified for 20 cFE patients. Each box and whisker plot represents the peak t-score of the primary cluster in patients for a given HP group. The thick black line represents polynomial regression of the average t-score per each HP group ( $R^2= 0.993$ ). Underneath the graph are two examples showing the changes in cluster volume in glass brain, as the number of controls increases in the HP group.

### 3.2. Re-selected HP Group

The peak t-scores of uFTDI reductions seen in individual CTR differed significantly between 60HP and 49HP groups ( $p=0.0047$ ) with the average t-score of 17.18 and 15.84, respectively (Fig. 2). On the other hand, the peak t-scores for cFE were similar in both 60HP and 49HP groups ( $p=0.44$ ) with average t-score of 20.26 and 19.66, respectively.

Consequently, the re-selected 49 HP group did further strengthen the separation between CTR and cFE ( $p=5.25 \times 10^{-6}$ ) and decreased the cluster volume of secondary and tertiary clusters by 8%. In some patients, the quantification using 49 HP group resulted in new additional clusters (Fig. 2, Patient 1), which could indicate regions implicated in epilepsy that were previously “hidden” in quantification based on a larger, but less homogenous HP group.

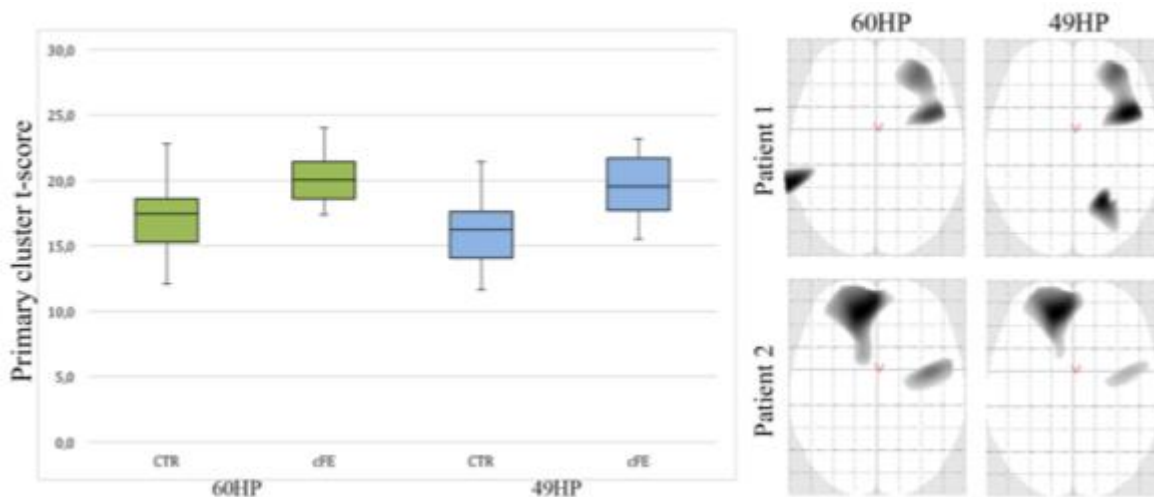


**Figure 2** uFTDI quantification of CTR and cFE against re-selected HP group. Box and whisker plot showing t-scores of primary clusters for CTR and cFE against two HP groups: 60HP and 49HP. The latter HP group is a re-selected group based on the uFTDI quantification of CTR against 60HP where mild outliers were excluded. A two-tailed two-sampled student’s t-test was performed showing a significant difference between CTR and cFE in 60HP ( $p=1.37 \times 10^{-5}$ ) and 49hp ( $p=5.25 \times 10^{-6}$ ). On the right are two examples of cFE patients using re-selected group quantification showing redistribution of t-scores within the clusters are reduced cluster volume.

### 3.3. Structural differences between male and female brains

A two sample t-test was performed comparing male and female G-HP groups. The differences were minor (at  $p < 0.05$  uncorrected). Females showed higher U-fiber track density in the superior frontal gyrus, posterior temporal neocortex and left occipital lobe. Males showed increased uFTDI in inferior central region above the Sylvian fissure (Fig. 3).

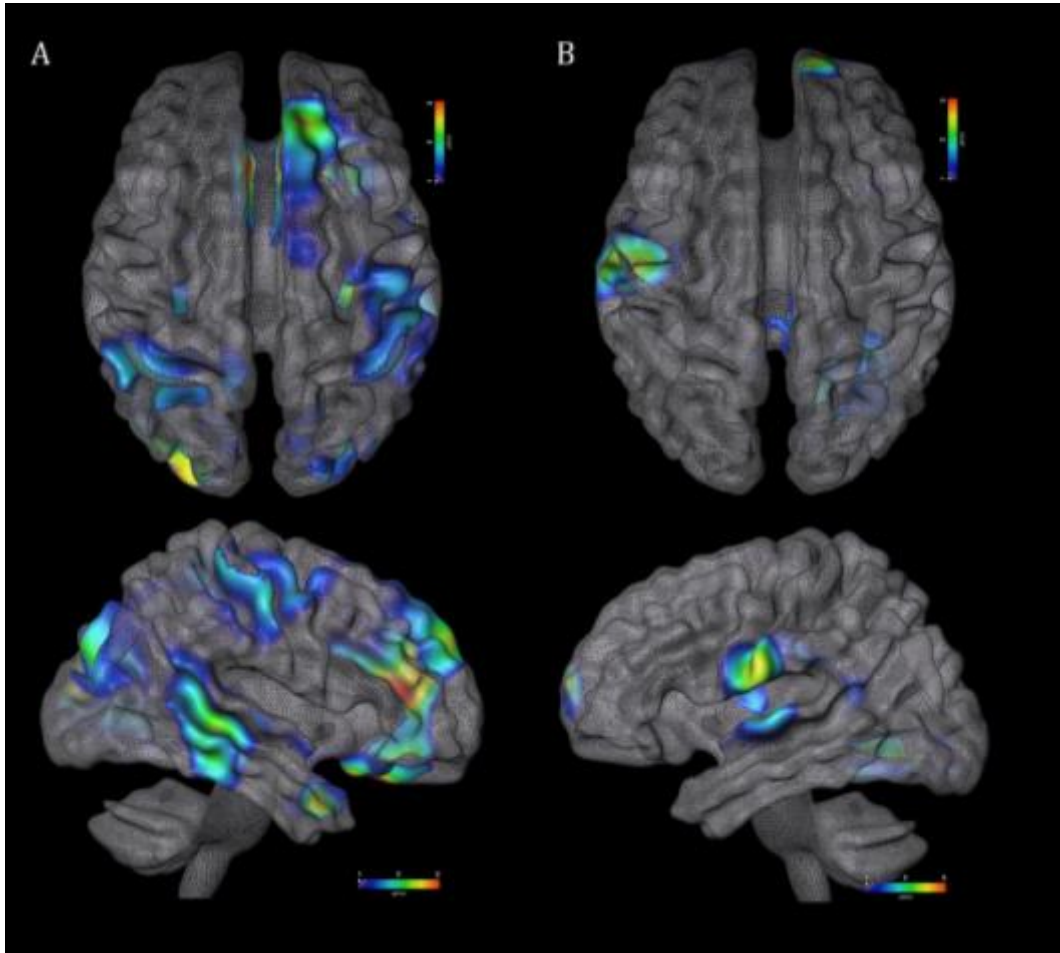


**Figure 3. Differences in uFTDI between female and male control population.** Results of two sample t-test where female and male healthy brains were compared. Increased uFTDI seen in A) female brains compared to male, B) male brains compared to female at  $p < 0.05$ , uncorrected.

### *3.4. Gender-specific quantification*

The uFTDI of all 48 cFE patients were individually quantified using mixed HP group of 30 healthy controls and compared to quantification using 30 gender-matched controls. The primary clusters in all cFE patients were located in the same region (Fig. 4), but the peak t-scores were lower when using the G-HP group. The overall volume of all the clusters in both male and female groups for cFE and CTR groups decreased with a higher reduction in cFE compared to CTR (Table 1.)

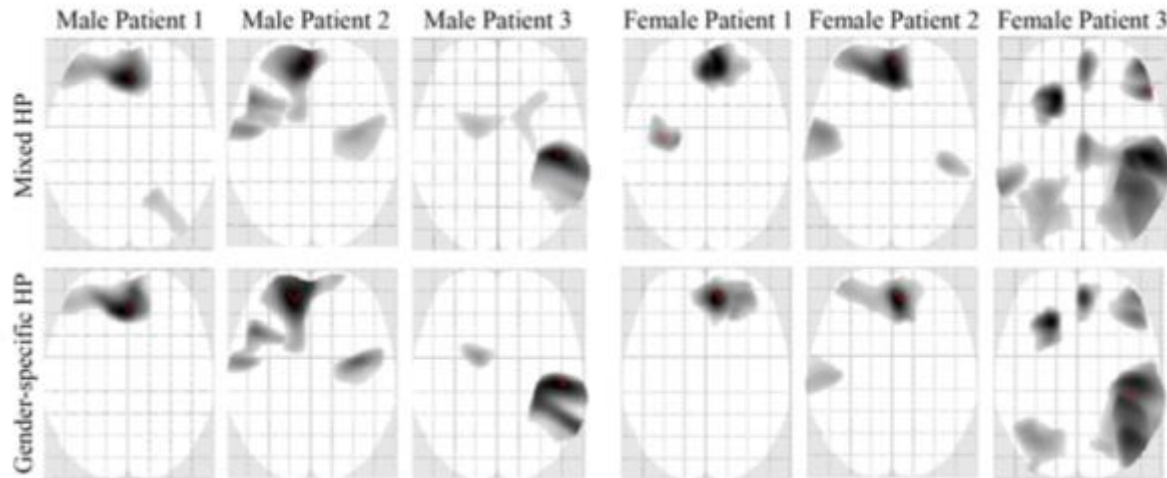


**Figure 4 Glass-brains of patients comparing mixed HP to G-HP quantification.** Shows 3 male and 3 female cFE patients at FWE  $p < 0.001$  and extent threshold of  $5\text{cm}^3$ . The primary clusters remain in the same location when using G-HP group, whereas the additional clusters either disappear or become smaller. In G-HP-based quantification, the t-scores within the primary cluster are redistributed giving a higher contrast within the cluster and increased specificity.

		Average no. of clusters		Average volume of all clusters ( $\text{cm}^3$ )		average difference in volume of all clusters ( $\pm$ SD)
		Mixed HP	Gender-matched HP	Mixed HP	Gender-matched HP	
Patients	Male	2.8	2.7	137.0	120.0	-17.0% ( $\pm 15.0\%$ )
	Female	3.1	2.8	123.8	101.2	-21.5% ( $\pm 25.3\%$ )
Controls	Male	2.9	2.8	69.6	65.4	-1.3% ( $\pm 25.0\%$ )
	Female	2.3	2.1	68.6	55.3	-24.8% ( $\pm 30.6\%$ )

**Table 1 Cluster volume differences between mixed HP group and G-HP group.**

#### 4. Discussion

It is common understanding that the control population for statistical analysis in neuroimaging should resemble the tested population in all aspects, except for what is being tested, in this case the diagnosis of cryptogenic focal epilepsy (cFE). Here, we showed that careful selection of the control population might not fundamentally change the results, but it might reduce the amount of noise and additional clusters.

How many healthy participants are needed for such a statistical analysis? We evaluated the effects of increasing number of HP and there were two main effects. First, the number of additional and false-positive clusters has decreased. Second, with an increase in control population statistical significance in the form of t-score also increases. In a single-subject study, increasing the number of controls increases the statistical significance of the method. The highest number of HP used in this study was 60 and the plateau of the peak t-score of the primary cluster was not yet reached, which could indicate that an even larger HP group would still result in higher t-scores.

Healthy participants in the HP groups were randomized. By chance the distribution of the t-scores of CTR in 30HP was close to normal, but other groups showed much higher variability (Fig. 1). Obviously by introducing additional CTR with an unusual distribution of Fibers. For this reason, we decided to investigate a “cleaner” HP group, where we excluded 11 healthy participants from the 60HP group with the highest individual variability of their U-fiber density. The results showed a stronger separation between CTR and cFE groups, which is clinically more relevant. This shows that the t-score alone is not the determining factor of what an effective method is. The reselected HP group of 49 participants had a more homogenous distribution and a better separation between CTR and cFE, thus showing that the size of the group alone is not enough and does not outweigh the importance of homogenous control population.

Similarly, using gender-matched HP group also resulted in decreased average t-score for both CTR and cFE and it also improved the separation of CTR from cFE patients and reduced the total cluster volume in the form of additional clusters. We have shown that absolute t-scores are not comparable and other factors are equally, if not more, important,

such as cluster size, cluster weight, distribution of the t-scores within a cluster, number of clusters per subject, etc.

While visually inspecting the results of the quantification for each subject, we noticed certain clusters of minor significance that appeared in the same region in patients of the same gender, e.g. a cluster in right posterior temporal lobe was often seen in male patients, when compared to the mixed HP and often this was no longer present when using the gender-matched control population. To counteract the possibly-artefactual and potentially-confusing clusters, we decided to investigate the effects of gender-matched HP group. We performed a two sample t-test comparing healthy male and female brains and found increases in uTDI in regions previously reported, e.g. females showed increased volume in the cingulate cortex (Chen et al., 2007).

We found that in gender-matched uTDI quantification, there is an overall decrease in cluster volume, primarily of the additional clusters, in patients by 17-21.5%. Introducing gender-matched HP groups “cleaned” up the results, making it easier for clinicians to interpret results, even though this did not fundamentally alter the results or did not increase the statistical value. Additionally, the distribution of the t-scores, as seen in the glass brain, shows a greater contrast, thus making it clearer to determine where the peak isolated within a large primary cluster.

An optimal composition of the control population is particularly important for single-subject studies like this. Careful selection of control population allows for improved results, while the fundamental, primary cluster remains at the same location. In patients, it can reduce the volume of additional or false-positive clusters in the range of 17-21.5% and improve the specificity of the method.

## **5. Acknowledgements**

This study was supported by the Friedrich-Baur-Stiftung and the Herta-Riehr Stiftung.

## 6. References

- Brun, C.C., Leporé, N., Luders, E., Chou, Y.-Y., Madsen, S.K., Toga, A.W., Thompson, P.M., 2009. Sex differences in brain structure in auditory and cingulate regions. *Neuroreport* 20, 930–5. doi:10.1097/WNR.0b013e32832c5e65
- Button, K.S., Ioannidis, J.P.A., Mokrysz, C., Nosek, B.A., Flint, J., Robinson, E.S.J., Munafò, M.R., 2013. Power failure: why small sample size undermines the reliability of neuroscience. *Nat. Rev. Neurosci.* 14, 365–76.
- Chen, X., Sachdev, P.S., Wen, W., Anstey, K.J., 2007. Sex differences in regional gray matter in healthy individuals aged 44-48 years: a voxel-based morphometric study. *Neuroimage* 36, 691–9. doi:10.1016/j.neuroimage.2007.03.063
- Greene, D.J., Black, K.J., Schlaggar, B.L., 2016. Considerations for MRI study design and implementation in pediatric and clinical populations. *Dev. Cogn. Neurosci.* 18, 101–112. doi:10.1016/j.dcn.2015.12.005.CONSIDERATIONS
- Grimes, D. a., Schulz, K.F., 2005. Compared to what? Finding controls for case-control studies. *Lancet* 365, 1429–1433. doi:10.1016/S0140-6736(05)66379-9
- Henson, R., 2006. Comparing a single patient versus a group of controls (and SPM) 1–5.
- Rosenow, F., Lüders, H., 2001. Presurgical evaluation of epilepsy. *Brain* 124, 1683–700. doi:10.4103/1817-1745.40593
- Sacher, J., Neumann, J., Okon-Singer, H., Gotowiec, S., Villringer, A., 2013. Sexual dimorphism in the human brain: Evidence from neuroimaging. *Magn. Reson. Imaging* 31, 366–375. doi:10.1016/j.mri.2012.06.007
- Schulz, K.F., Grimes, D. a., 2002. Case-control studies: research in reverse. *Lancet* 359, 431–434. doi:10.1016/S0140-6736(02)07605-5

## CHAPTER 6. GENERAL DISCUSSION

### 6.1. OVERVIEW

Patients with pharmaco-resistant focal epilepsy may benefit from resective surgery, in which the epileptogenic zone (EZ) is removed. Typically, patients undergo a series of neurological tests, including scalp EEG, MRI and in some cases ictal SPECT or PET studies and invasive EEG recordings. In cryptogenic focal epilepsy (cFE) conventional MRI does not show any structural lesion and the localization of the EZ is often more challenging. Imprecise localization of the EZ in these patients can result in poorer surgical outcome. For this reason, there have been a number of studies investigating alternative MRI approaches that would improve the localization of the EZ, starting with voxel based morphometry using  $T_1$  (Huppertz et al., 2005) or  $T_2$  FLAIR images (Focke et al., 2009) to FA and MD quantitative analyses (Eriksson et al., 2001; Rugg-Gunn et al., 2001; Thivard et al., 2011).

In focal epilepsy, one of the most commonly occurring pathologies is focal cortical dysplasia (FCD), whose histopathological characteristics include blurring of the grey and white matter border and cytoarchitectural alterations (Blümcke et al., 2011). For that reason, I focused on the role of short association fibers, called U-fibers. They are located directly at the border between grey and white matter and might be affected by FCD.

The clinical features of cFE are hugely variable between different patients, thus preventing conventional group comparisons. Instead, each patient needs to be analyzed individually. The new diagnostic method for cryptogenic focal epilepsy introduced and discussed throughout this thesis, uses a tractography mapping approach of track density images (TDI) (Calamante et al., 2010). A density image of U-fibers can be calculated by selecting U-fibers from whole brain streamline tracking data of an individual, thus creating

a U-fiber track density image (ufTDI), for every participant. The ufTDI were used to calculate difference images between individual patients with cFE and a group of healthy participants. These difference images were then used in one-sample t-test. This statistical analysis approach, proposed by Henson increases the sensitivity and allows a single-subject statistical tests (Henson, 2006).

DTI-based research commonly uses either FA or MD maps, therefore the first step was to compare the effectiveness of ufTDI quantification against the conventionally used DTI-based measures FA and MD in a sample of cFE patients (n=10) with a clear clinical localization of the EZ (see Chapter 2. From FA to U-). The ufTDI quantification successfully localized the EZ in 8 out of 10 patients, whereas the FA quantification correctly localized EZ in only 2 out of 10 patients and MD in only one patient, which is similar to the low yield in previously reported studies for both FA and MD (Rugg-Gunn et al., 2001; Thivard et al., 2011). The alterations in ufTDI showed circumscribed and confined changes, whereas FA and MD maps were often unspecific and widespread. This indicated that our ufTDI approach is more sensitive and specific than the conventional DTI measures. The additional step of performing streamline tracking and selecting U-fibers suggests that there might be specific microstructural alterations at the grey-white matter border, which interfere with the simple tracking algorithm.

Quantifying ufTDI proved to perform better than FA or MD and in a more extensive analysis, which included 22 patients, the reductions in ufTDI were more closely analyzed and compared to the clinical data (see Chapter 3. On The Clinical Side). Each patient with cFE showed different extent, severity and pathology of the disorder and this diversity is reflected in the observed clusters of reduced U-fiber track density. Results showed a wide range of clusters ranging from a single, small and circumscribed cluster to multiple or

larger clusters extending to both hemispheres. One or more cluster was detected in 95% of all patients and 75% of all clusters correlated with the clinical data, such as EEG recording, PET and/or ictal SPECT. This sensitivity and specificity is higher than any other reported neuroimaging method in cryptogenic focal epilepsy (Thivard et al., 2011). The remaining clusters could mean a number of things as mentioned in Chapter 3. However, most likely some of the false-positive clusters are unrelated to epilepsy and reflect individual anatomical variations.

The false-positive clusters could be due to e.g. individual subject variability or inadequately selected parameters in the pre-processing pipeline. Therefore, the next step involved the optimization of the uFTDI quantification pipeline to further enhance the specificity of the method and to reduce the amount epilepsy-unrelated clusters (see Chapter 4. Effects of Pre-processing). I evaluated different steps within the pipeline starting with the parameters for spatial normalization to tracking algorithms and using a U-fiber-specific mask. Here, the clusters were described in more detail, i.e. number of clusters per patient, the t-score of each cluster and the cluster weight. Based on the additional information, I was able to suggest a ranking of clusters: primary, secondary and tertiary to reflect the significance of the cluster in relation to the clinical data. The primary cluster represents the highest cluster weight and was further verified by correlation to the clinical data.

In neuroimaging, one of the most important pre-processing step is spatial normalization. It allows for the comparison between subjects by aligning each brain to a common space, e.g. MNI-space. There is a variety of software options and algorithms that are able to perform this spatial normalization. We have compared two commonly used software packages: SPM and ANTs, where I analyzed the default (SPMd) and optimized (SPMo) parameter settings in SPM and optimized settings in ANTs. The results showed that

both SPMo and ANTs performed better than SPMd with a higher specificity and fewer false-positive findings. However, the type of normalization did not fundamentally influence the outcome of the quantification, i.e. the primary cluster remained present and at the same location in all three spatial normalization procedures further supporting the initial hypothesis that regional U-fibers are affected in cFE patients.

A U-fiber-specific mask was created, where an averaged and binarised density map of U-fibers was generated. Conventionally, a whole brain mask in MNI space is used for analyses in SPM. However, when using the whole brain mask, clusters of reduced “U-fibers” were observed in areas where U-fibers are not expected to be present. Therefore, a U-fiber-specific mask allows for a focused analysis restricted to the regions of the brain that we are interested in. Using this mask resulted in fewer secondary and tertiary false-positive clusters by 31.6%, whilst leaving the primary cluster at the same location with the same statistical significance in all patients.

During a pilot study, the number of healthy participants was only 18, but even then the ufTDI quantification already showed promising results. The next study included 30 healthy participants, which resulted in fewer additional clusters. This confirmed that the role of the control group has a greater impact on the statistical analysis. Therefore, Chapter 5 explores the effects of control population on the results of the ufTDI quantification. In that study, I investigated two main aspects: 1) the effects of the size of the healthy population and 2) gender-matching of the population (see Chapter 5. Gender and Controls).

Increasing the size of the healthy population strengthens the statistics, improves the sensitivity of the method and reduces the number of false-positive clusters. The biggest healthy population group that was analyzed in Chapter 5 included 60 healthy participants and the average t-score of the primary clusters among cFE patients was the highest.

However, a remaining question was, which is more important: quantity or quality of the healthy population? To answer that question, I re-selected healthy participants from the pool of all controls available (n=60) based on the variability within group, thus excluding 11 participants as mild outliers. The comparison of the uFTDI quantification of the cFE patients based on “cleaner” group and “larger” group revealed fewer false-positive clusters and more focused redistribution of the t-scores within the primary cluster in cFE patients when using “cleaner” healthy population. More importantly, the “cleaner” group showed strengthened separation between healthy controls and cFE patients, which is clinically more meaningful. Thus, in this case “quality” seems to be more effective than “quantity”.

As mentioned earlier, some of the false-positive clusters are possibly caused by individual variability and this might include gender differences as well. Gender differences have been extensively investigated over the last decade (Sacher et al., 2013) and studies have found many functional and structural dissimilarities. Chapter 5 explains in more detail that using a gender-matched healthy population further reduces the number of false-positive clusters by 17-21.5% without changing the location of the primary cluster, thus improving the specificity of the method.

In summary, quantifying uFTDI in cFE patients proves to be a sensitive, specific and robust method that localizes the EZ reliably in the majority of cases. Improving and optimizing individual steps within the pre-processing and processing pipeline shows to have small effects, but when combined they have considerably reduced false-positive clusters, increased the t-score of the primary cluster and strengthened the separation between healthy population and cFE patients. Thus, improving sensitivity and specificity to a level not achieved by any other diagnostic method to localize the EZ.

## 6.2. CLINICAL APPLICATION

The ufTDI quantification for localization of the epileptogenic zone in cFE is still an experimental method, nonetheless we are already implementing it routinely in the Epilepsy Centre at the University of Munich Hospital. Currently, we quantify ufTDI in all incoming patients with cryptogenic focal epilepsy before the implantation of the intracranial electrodes. This allows the neurologists to include this information in the planning of the electrode placement. In some cases, the ufTDI quantification showed reductions in regions that were not clinically suspected prior to invasive EEG recordings and often the intracranial electrodes later confirmed that these regions were also involved in seizure generation.

So far I performed the quantification using optimized spatial normalization, U-fiber specific mask and gender-matched control group on 67 patients of which 18 had implantation of electrodes and 10 had resective surgery. Many other patients are currently awaiting implantation of electrodes or resections.

Few patients showed widespread bilateral reductions of U-fiber density (see Fig. 5, Chapter 3) and bilateral seizure onset was then confirmed using intracranial electrodes. These patients are not candidates for resective surgery and ufTDI quantification could potentially be used as an exclusion test in the future. This may prevent unnecessary risks of surgery and invasive EEG recordings.

## SUMMARY POINTS

- U-fiber Track Density Images (ufTDI) reflect the number of U-fibers per voxel in an individual brain
- ufTDI reflect different microstructural tissue properties than conventional FA or MD maps
- ufTDI quantification can localize mild architectural changes in cryptogenic epilepsy with higher specificity and sensitivity than FA or MD
- FA and MD quantification shows widespread and unspecific alterations
- 95% of the patients with no structural lesion in conventional 3T MRI showed reductions in ufTDI
- 75% of all clusters observed in cFE patients correlated with clinical data
- Optimized settings of spatial normalization improve the statistical significance of the ufTDI quantification
- A U-fiber-specific mask reduces the volume of false-positive clusters by 31.6%.
- Both, increasing the size and removing outliers from the healthy population improves the statistical significance of the ufTDI quantification and strengthens the separation of healthy controls and cFE patients
- Using a gender-specific control population reduces the volume of false-positive clusters by 17-21.5%
- Quantification of ufTDI is already routinely used for guidance of electrode implantation in the Epilepsy Centre at the University of Munich Hospital

## REFERENCES

- Anderson, A.W., Ding, Z., 2002. Sub-voxel measurement of fiber orientation using high angular resolution diffusion tensor imaging. Tenth Annu. Meet. Int. Soc. Magn. Reson. Med. Berkeley, CA ISMRM 10, 440.
- Basser, P.J., Mattiello, J., LeBihan, D., 1994. MR diffusion tensor spectroscopy and imaging. *Biophys. J.* 66, 259–67. doi:10.1016/S0006-3495(94)80775-1
- Basser, P.J., Mattiello, J., LeBihan, D., 1994. Estimation of the effective self-diffusion tensor from the NMR spin echo. *J. Magn. Reson. B* 103, 247–254. doi:10.1006/jmrb.1994.1037
- Behrens, T.E.J., Sotiropoulos, S.N., Jbabdi, S., 2009. MR Diffusion Tractography, in: *Diffusion MRI: From Quantitative Measurement to In Vivo Neuroanatomy: First Edition*. Elsevier Inc., pp. 333–351. doi:10.1016/B978-0-12-396460-1.00019-6
- Behrens, T.E.J., Woolrich, M.W., Jenkinson, M., Johansen-Berg, H., Nunes, R.G., Clare, S., Matthews, P.M., Brady, J.M., Smith, S.M., 2003. Characterization and Propagation of Uncertainty in Diffusion-Weighted MR Imaging. *Magn. Reson. Med.* 50, 1077–1088. doi:10.1002/mrm.10609
- Besson, P., Andermann, F., Dubeau, F., Bernasconi, A., 2008. Small focal cortical dysplasia lesions are located at the bottom of a deep sulcus. *Brain* 131, 3246–3255. doi:10.1093/brain/awn224
- Blümcke, I., Thom, M., Aronica, E., Armstrong, D.D., Vinters, H. V, Palmini, A., Jacques, T.S., Avanzini, G., Barkovich, a J., Battaglia, G., Becker, A., Cepeda, C., Cendes, F., Colombo, N., Crino, P., Cross, J.H., Delalande, O., Dubeau, F., Duncan, J., Guerrini, R., Kahane, P.,

- Mathern, G., Najm, I., Ozkara, C., Raybaud, C., Represa, A., Roper, S.N., Salamon, N., Schulze-Bonhage, A., Tassi, L., Vezzani, A., Spreafico, R., 2011. The clinicopathologic spectrum of focal cortical dysplasias: a consensus classification proposed by an ad hoc Task Force of the ILAE Diagnostic Methods Commission. *Epilepsia* 52, 158–74. doi:10.1111/j.1528-1167.2010.02777.x
- Calamante, F., Tournier, J.-D., Jackson, G.D., Connelly, A., 2010. Track-density imaging (TDI): super-resolution white matter imaging using whole-brain track-density mapping. *Neuroimage* 53, 1233–43. doi:10.1016/j.neuroimage.2010.07.024
- Chamberlain, W.A., Cohen, M.L., Gyure, K.A., Kleinschmidt-DeMasters, B.K., Perry, A., Powell, S.Z., Qian, J., Staugaitis, S.M., Prayson, R.A., 2009. Interobserver and intraobserver reproducibility in focal cortical dysplasia (malformations of cortical development). *Epilepsia* 50, 2593–2598. doi:10.1111/j.1528-1167.2009.02344.x
- Dumas de la Roque, A., Oppenheim, C., Chassoux, F., Rodrigo, S., Beuvon, F., Daumas-Duport, C., Devaux, B., Meder, J.-F., 2005. Diffusion tensor imaging of partial intractable epilepsy. *Eur. Radiol.* 15, 279–85. doi:10.1007/s00330-004-2578-8
- Eriksson, S.H., Rugg-Gunn, F.J., Symms, M.R., Barker, G.J., Duncan, J.S., 2001. Diffusion tensor imaging in patients with epilepsy and malformations of cortical development. *Brain* 124, 617–626. doi:10.1093/brain/124.3.617
- Focke, N.K., Bonelli, S.B., Yogarajah, M., Scott, C., Symms, M.R., Duncan, J.S., 2009. Automated normalized FLAIR imaging in MRI-negative patients with refractory focal epilepsy. *Epilepsia* 50, 1484–1490. doi:10.1111/j.1528-1167.2009.02022.x

- Henson, R., 2006. Comparing a single patient versus a group of controls (and SPM) 1–5.
- Huppertz, H.-J., Grimm, C., Fauser, S., Kassubek, J., Mader, I., Hochmuth, A., Spreer, J., Schulze-Bonhage, A., 2005. Enhanced visualization of blurred grey–white matter junctions in focal cortical dysplasia by voxel-based 3D MRI analysis. *Epilepsy Res.* 67, 35–50. doi:10.1016/j.eplepsyres.2005.07.009
- Le Bihan, D., 2014. Diffusion MRI: What water tells us about the brain. *EMBO Mol. Med.* 6, 569–573. doi:10.1002/emmm.201404055
- Lerner, J.T., Salamon, N., Hauptman, J.S., Velasco, T.R., Hemb, M., Wu, J.Y., Sankar, R., Donald Shields, W., Engel, J., Fried, I., Cepeda, C., Andre, V.M., Levine, M.S., Miyata, H., Yong, W.H., Vinters, H. V., Mathern, G.W., 2009. Assessment and surgical outcomes for mild type I and severe type II cortical dysplasia: A critical review and the UCLA experience. *Epilepsia* 50, 1310–1335. doi:10.1111/j.1528-1167.2008.01998.x
- Lüders, H., 2008. *Textbook of Epilepsy Surgery*. Informa Healthcare. doi:10.1017/CBO9781107415324.004
- Lüders, H.O., Acharya, J., Baumgartner, C., Benbadis, S.R., Bleasel, A., Burgess, R., Dinner, D.S., Ebner, A., Foldvary, N., Geller, E.B., Hamer, H., Holthausen, H., Kotagal, P., Morris, H., Meencke, H.J., Noachtar, S., Rosenow, F., Sakamoto, A., Steinhoff, B.J., Tuxhorn, I., Wyllie, E., 1999. A new epileptic seizure classification based exclusively on ictal semiology. *Acta Neurol. Scand.* 99, 137–141.
- McIntosh, A.M., Averill, C.A., Kalnins, R.M., Mitchell, L.A., Fabinyi, G.C.A., Jackson, G.D., Berkovic, S.F., 2012. Long-term seizure outcome and risk factors for recurrence after

- extratemporal epilepsy surgery. *Epilepsia* 53, 970–978. doi:10.1111/j.1528-1167.2012.03430.x
- O'Brien, T.J., So, E.L., Mullan, B.P., Hauser, M.F., Brinkmann, B.H., Bohnen, N.I., Hanson, D., Cascino, G.D., Jack, C.R., Sharbrough, F.W., 1998. Subtraction ictal SPECT co-registered to MRI improves clinical usefulness of SPECT in localizing the surgical seizure focus. *Neurology* 50, 445–54.
- Ramey, W.L., Martirosyan, N.L., Lieu, C.M., Hasham, H.A., Lemole, G.M., Weinand, M.E., 2013. Current management and surgical outcomes of medically intractable epilepsy. *Clin. Neurol. Neurosurg.* 115, 2411–2418. doi:10.1016/j.clineuro.2013.09.035
- Rosenow, F., Lüders, H., 2001. Presurgical evaluation of epilepsy. *Brain* 124, 1683–700. doi:10.4103/1817-1745.40593
- Rugg-Gunn, F.J., Eriksson, S.H., Symms, M.R., Barker, G.J., Duncan, J.S., 2001. Diffusion tensor imaging of cryptogenic and acquired partial epilepsies. *Brain* 124, 627–636. doi:10.1093/brain/124.3.627
- Sacher, J., Neumann, J., Okon-Singer, H., Gotowiec, S., Villringer, A., 2013. Sexual dimorphism in the human brain: Evidence from neuroimaging. *Magn. Reson. Imaging* 31, 366–375. doi:10.1016/j.mri.2012.06.007
- Stejskal, E.O., Tanner, J.E., 1965. Spin diffusion measurements: spin echoes in the presence of a time-dependant field gradient. *J. Chem. Phys.* 42, 288–292. doi:10.1063/1.1695690
- Thivard, L., Adam, C., Hasboun, D., Clemenceau, S., Dezamis, E., Lehericy, S., Dormont, D., Chiras, J., Baulac, M., Dupont, S., 2006. Interictal diffusion MRI in partial epilepsies

- explored with intracerebral electrodes. *Brain* 129, 375–385.  
doi:10.1093/brain/awh709
- Thivard, L., Bouilleret, V., Chassoux, F., Adam, C., Dormont, D., Baulac, M., Semah, F., Dupont, S., 2011. Diffusion tensor imaging can localize the epileptogenic zone in nonlesional extra-temporal refractory epilepsies when [(18)F]FDG-PET is not contributive. *Epilepsy Res.* 97, 170–82. doi:10.1016/j.eplepsyres.2011.08.005
- Thom, M., 2011. Neuropathology of epilepsy., in: *Epilepsy 2011 From Science to Society, A Practical Guide to Epilepsy*. International League Against Epilepsy (UK Chapter) and Epilepsy Society, pp. 39–67. doi:10.1097/00005072-199903000-00015
- Tuch, D.S., 2004. Q-ball imaging. *Magn. Reson. Med.* 52, 1358–1372.  
doi:10.1002/mrm.20279
- Tuch, D.S., Reese, T.G., Wiegell, M.R., Makris, N., Belliveau, J.W., Van Wedeen, J., 2002. High angular resolution diffusion imaging reveals intravoxel white matter fiber heterogeneity. *Magn. Reson. Med.* 48, 577–582. doi:10.1002/mrm.10268
- Tufenkjian, K., Lüders, H.O., 2012. Seizure semiology: Its value and limitations in localizing the epileptogenic zone. *J. Clin. Neurol.* 8, 243–250. doi:10.3988/jcn.2012.8.4.243
- Van Paesschen, W., 2004. Ictal SPECT. *Epilepsia* 45 Suppl 4, 35–40. doi:10.1111/j.0013-9580.2004.04008.x
- Vollmar, C., Diehl, B., 2011. Diffusion tensor tractography in extratemporal lobe epilepsy, in: *Extratemporal Lobe Epilepsy Surgery*. pp. 197–205.
- Winston, G.P., 2015. The potential role of novel diffusion imaging techniques in the

understanding and treatment of epilepsy. *Quant. Imaging Med. Surg.* 5, 279–287.

doi:10.3978/j.issn.2223-4292.2015.02.03

Zhang, J., Liu, W., Chen, H., Xia, H., Zhou, Z., Mei, S., Liu, Q., Li, Y., 2014. Multimodal neuroimaging in presurgical evaluation of drug-resistant epilepsy. *NeuroImage Clin.* 4, 35–44. doi:10.1016/j.nicl.2013.10.017

## ACKNOWLEDGMENTS

First and foremost, I would like to thank my supervisor Dr. Christian Vollmar for his never-ending support, patience and guidance throughout my PhD. Thank you for our many scientific (and not only) discussions, your help and for all that you have taught me and most of all for inspiring and motivating me during this process.

Furthermore, I am grateful to Prof Soheyl Noachtar who encouraged and supported me every step of the way. I am very grateful to be part of the Epilepsy Group who are wonderful. I have been very lucky to have met some of my closest friends there. I am very thankful to Dr. Elisabeth Hartl and Katharina Ernst for being there for me.

I would also like to thank Prof Stefan Glasauer and Dr. Afra Wohlschläger for their helpful discussions and guidance during TAC meetings. I was most fortunate to have such a great committee!

I would not be able to find this great project if it wasn't for Graduate School of Systemic Neurosciences (GSN) and for this I will be forever grateful. GSN has been incredibly supportive, especially during the difficult moments.

I would like to express my sincere gratitude to my family who have been so incredibly encouraging and always showed interest in my project.

Last but definitely not least, my special thanks go to my fiancé Jan Bartkiewicz for everything that he has done to show his support, understanding and love. He consoled me and listened to me every time I needed him. So thank you!

Thank you all that have been involved in this wonderful process. I honestly cannot imagine a more enjoyable and exciting PhD project!

## CURRICULUM VITAE

### Education

---

- Oct. 2012 – Current                      PhD candidate in Clinical Neuroscience at Graduate School of Systemic Neurosciences Ludwig-Maximilians-University Munich, Germany
- Sept. 2011 – Jul. 2012                      MSc in Clinical Neuroscience at University College London, UK
- Sept. 2008 – Jul. 2011                      BSc in Biomedical Science at King’s College London, UK

### Research Experience

---

- Oct. 2013 – Current                      Researcher for doctoral degree (PhD)  
Epilepsy Centre at University Hospital Munich  
LMU Munich, Germany  
Supervisor: Dr. Christian Vollmar  
Dissertation title: “Establishing a novel diagnostic method to localize the epileptogenic zone in cryptogenic focal epilepsy”
- Oct. 2012 – Oct. 2013                      Researcher  
Institute of Pharmacology, Toxicology and Pharmacy  
LMU Munich, Germany  
Supervisor: Prof. Heidrun Potschka
- Dec. 2011 – June 2012                      Researcher for MSc degree  
Dept. of Neuropathology, UCL Institute of Neurology  
Supervisor: Prof. Sanjay Sisodiya and Prof. Maria Thom  
Dissertation title: “Study of cellular reactions around electrode tracks in patients with drug-resistant focal epilepsy”
- Summer 2010                                  Research Intern  
Dept. of Craniofacial Development and Stem Cell Biology  
King’s College London, UK  
Supervisor: Dr. Albert Basson

---

## Honors

---

GSN Scholarship Allowance (Sept. 2013 – Feb. 2014)

1<sup>st</sup> Place Poster Award at 114<sup>th</sup> Meeting of the British Neuropathology Society, London, UK (March 2013)

---

## Poster Presentations

---

- **Goc, J.**, Hartl, E., Noachtar, S., Vollmar, C. (2016). DTI Analysis of U-fiber density images localizes the epileptogenic zone better than FA or MD. *22<sup>nd</sup> Annual Meeting of the Organization for Human Brain Mapping, Genève, Switzerland*
- **Goc, J.**, Hartl, E., Noachtar, S., Vollmar, C. (2016). U-fiber density imaging identifies specific microstructural alteration in the epileptogenic zone in individual patients with cryptogenic focal epilepsy. *60<sup>th</sup> Scientific Annual Meeting of the German Society for Clinical Neurophysiology and Functional Imaging, Düsseldorf, Germany*
- Ernst, K., Hartl, E., **Goc, J.**, Noachtar, S., Vollmar, C. (2016). Increased coherence to the midline in interictal EEG predicts generalized seizures in focal epilepsy. *60<sup>th</sup> Scientific Annual Meeting of the German Society for Clinical Neurophysiology and Functional Imaging, Düsseldorf, Germany*
- **Goc, J.**, Khalilieh, N., Hartl, E., Noachtar, S., Vollmar, C. (2015). The effects of preprocessing on statistical DTI fiber quantification in cryptogenic focal epilepsy. *21<sup>st</sup> Annual Meeting of the Organization for Human Brain Mapping, Honolulu, Hawaii*
- **Goc, J.**, Noachtar, S., Vollmar, C. (2014). Case Report: Diffusion Tensor Imaging and Tractography identify structural changes in 14 year old male with cryptogenic focal epilepsy (2014). *88 Kongress der Deutschen Gesellschaft für Neurologie: Neurowoche, Munich, Germany*
- **Goc, J.**, Liu, J., Sisodiya, S., Thom, M. (2013). A study of gliogenesis in the vicinity of depth electrode tracts. *114<sup>th</sup> Meeting of the British Neuropathology Society, London, UK*

## LIST OF PUBLICATIONS

- Hartl, E., Rémi, J., Vollmar, C., **Goc, J.**, Loesch, A.M., Rominger, A., Noachtar, S., 2016. PET imaging in extratemporal epilepsy requires consideration of electroclinical findings. **Epilepsy Res.** 125, 72–76.
- Russmann, V., **Goc, J.**, Boes, K., Ongerth, T., Salvamoser, J.D., Siegl, C., Potschka, H., 2016. Minocycline fails to exert antiepileptogenic effects in a rat status epilepticus model. **Eur. J. Pharmacol.** 771, 29–39. doi:10.1016/j.ejphar.2015.12.002
- Walker, A., Russmann, V., Deeg, C.A., von Toerne, C., Kleinwort, K.J.H., Szober, C., Rettenbeck, M.L., von Rüden, E.-L., **Goc, J.**, Ongerth, T., Boes, K., Salvamoser, J.D., Vezzani, A., Hauck, S.M., Potschka, H., 2016. Proteomic profiling of epileptogenesis in a rat model: Focus on inflammation. **Brain. Behav. Immun.** 53, 138–158. doi:10.1016/j.bbi.2015.12.007
- Goc, J.**, Liu, J.Y.W., Sisodiya, S.M., Thom, M., 2014. A spatiotemporal study of gliosis in relation to depth electrode tracks in drug-resistant epilepsy. **Eur. J. Neurosci.** 39, 2151–2162. doi:10.1111/ejn.12548
- Thom, M., Kensche, M., Maynard, J., Liu, J., Reeves, C., **Goc, J.**, Marsdon, D., Fluegel, D., Foong, J., 2014. Interictal psychosis following temporal lobe surgery: dentate gyrus pathology. **Psychol. Med.** 44, 3037–3049. doi:10.1017/S0033291714000452
- Shepherd, C., Liu, J., **Goc, J.**, Martinian, L., Jacques, T.S., Sisodiya, S.M., Thom, M., 2013. A quantitative study of white matter hypomyelination and oligodendroglial maturation in focal cortical dysplasia type II. **Epilepsia** 1–11. doi:10.1111/epi.12143

**AFFIDAVIT**

Hiermit versichere ich an Eides statt, dass ich die vorliegende Dissertation “**Establishing a novel diagnostic method to localize the epileptogenic zone in cryptogenic focal epilepsy**” selbstständig angefertigt habe, mich außer der angegebenen keiner weiteren Hilfsmittel bedient und alle Erkenntnisse, die aus dem Schrifttum ganz oder annähernd übernommen sind, als solche kenntlich gemacht und nach ihrer Herkunft unter Bezeichnung der Fundstelle einzeln nachgewiesen habe.

I hereby confirm that the dissertation “**Establishing a novel diagnostic method to localize the epileptogenic zone in cryptogenic focal epilepsy**” is the result of my own work and that I have only used sources or materials listed and specified in the dissertation.

Datum/Date:

Unterschrift/signature

München, 4<sup>th</sup> November 2016

**Joanna Irena Goc**

## DECLARATION OF AUTHOR CONTRIBUTIONS

Chapter 2. *Performance of different DTI-based measures to localize the epileptogenic zone in cryptogenic focal epilepsy* was done under the supervision of Dr. Christian Vollmar (CV).

Joanna Goc (JG) and CV designed the research. JG, CV and Dr. Elisabeth Hartl (EH) recruited and scanned participants. JG designed the method and carried out the research and analysis and together with CV discussed the results. JG wrote the article.

Chapter 3. *Looking at the Dark Side of Diffusion Tensor Imaging Data – U-Fiber Track Density Imaging Identifies Specific Structural Changes in Non-lesional Focal Epilepsy*, where the author of this doctoral thesis, Joanna Goc (JG), contributed to the study by scanning the patients and controls with Dr. Christian Vollmar (CV). JG also contributed by carrying out the research and analysis and together with CV discussed the results. CV wrote the article.

Chapter 4. *The effects of pre-processing pipeline steps on statistical DTI tract quantification in cryptogenic focal epilepsy* was done under the supervision of Dr. Christian Vollmar (CV). CV developed the initial hypothesis and together with Joanna Goc (JG) designed the research. JG, CV and Dr. Elisabeth Hartl (EH) recruited and scanned participants. JG developed the method and Nadia Khalilieh (NK) optimized spatial normalization procedures that JG later used in the study. JG carried out the research and analysis and together with CV discussed the results. JG wrote the article.

Chapter 5. *Careful control selection improves the quantification of fiber density images in cryptogenic focal epilepsy* was done under the supervision of Dr. Christian Vollmar (CV). Joanna Goc (JG) developed the initial hypothesis and designed the research. JG and Dr.

Elisabeth Hartl (EH) recruited and scanned additional healthy controls. JG adjusted the previously mentioned method in Chapters 3 and 4. JG carried out the research and analysis and together with CV discussed the results. JG wrote the article.

Munich, 4<sup>th</sup> November 2016

Joanna Goc

Dr. Christian Vollmar